NO. UMTA-MA-06-0031-75-2

# POWER AND PROPULSION CHARACTERISTICS OF THE DULLES TRANSPO® '72 PERSONAL RAPID TRANSIT VEHICLES

Frank L. Raposa
Wendell E. Phillips, Jr.

JULY 1975

FINAL REPORT



Prepared for
U.S. DEPARTMENT OF TRANSPORTATION
URBAN MASS TRANSPORTATION ADMINISTRATION
Office of Research and Development
Washington DC 20590

## NOTICE

This document is disseminated under the sponsorship of the Department of Transportation in the interest of information exchange. The United States Government assumes no liability for its contents or use thereof.

## NOTICE

The United States Government does not endorse products or manufacturers. Trade or manufacturers' names appear herein solely because they are considered essential to the object of this report.

Technical Report Documentation Page

| | | |
|---|---|---|
| 1. Report No. UMTA-MA-06-0031-75-2 | 2. Government Accession No. | 3. Recipient's Catalog No. |
| 4. Title and Subtitle POWER AND PROPULSION CHARACTERISTICS OF THE DULLES TRANSPO '72 PERSONAL RAPID TRANSIT VEHICLES | | 5. Report Date July 1975 |
| | | 6. Performing Organization Code |
| 7. Author(s) Frank L. Raposa, Wendell E. Phillips, Jr.* | | 8. Performing Organization Report No. DOT-TSC-UMTA-74-12 |
| 9. Performing Organization Name and Address U.S. Department of Transportation, Transportation Systems Center, Kendall Square, Cambridge MA 02142 | | 10. Work Unit No. (TRAIS) UM509/R5731 |
| | | 11. Contract or Grant No. |
| 12. Sponsoring Agency Name and Address U.S. Department of Transportation, Urban Mass Transportation Administration, Office of Research and Development, Washington DC 20590 | | 13. Type of Report and Period Covered Final Report October 1973 to June 1974 |
| | | 14. Sponsoring Agency Code |

15. Supplementary Notes *Mr. Phillips is a consulting engineer at:
Alexander Kusko, Inc.
161 Highland Avenue
Needham Heights MA 02194

16. Abstract

The Power and Propulsion Characteristics of the four different PRT vehicles demonstrated at Transpo® '72 are determined by using analytical descriptions, manufacturers' data, and the test data from the Post-Transpo® '72 Test Program. A comparative analysis of the four systems is presented. The performance features necessary to adequately describe each vehicle's power and propulsion characteristics are also discussed.

| | |
|---|---|
| 17. Key Words Electric Power, Propulsion, Thyristor Control | 18. Distribution Statement DOCUMENT IS AVAILABLE TO THE PUBLIC THROUGH THE NATIONAL TECHNICAL INFORMATION SERVICE, SPRINGFIELD, VIRGINIA 22161 |

| 19. Security Classif. (of this report) | 20. Security Classif. (of this page) | 21. No. of Pages | 22. Price |
|---|---|---|---|
| Unclassified | Unclassified | 116 | |

Form DOT F 1700.7 (8-72) Reproduction of completed page authorized

# TABLE OF CONTENTS

## TABLE OF CONTENTS (CONTINUED)

## LIST OF ILLUSTRATIONS

## LIST OF ILLUSTRATIONS (CONTINUED)

## LIST OF ILLUSTRATIONS (CONTINUED)

## LIST OF ILLUSTRATIONS (CONTINUED)

## LIST OF ILLUSTRATIONS (CONTINUED)

# LIST OF ILLUSTRATIONS (CONTINUED)

# ABBREVIATIONS

| | |
|---|---|
| A | amperes |
| APL | applied physics laboratory |
| DC | direct current |
| $E_A$ | armature voltage |
| $E_{LL}$ | rms line to line voltage |
| $e_{LN}$ | instantaneous line to neutral voltage |
| F | Tractive effort (force) |
| fig | figure |
| ft | feet |
| hp | horsepower |
| $I_A$ | Armature Current |
| $I_d$ | DC amperes |
| $I_{L1}$ | rms value of the fundamental frequency component of the AC line current |
| $I_T$ | rms value of total current |
| in. | inches |
| $k_T$ | motor constant |
| $k_v$ | motor constant |
| $k_{v'}$ | motor constant |
| kVA | complex power (kilo-volt-amperes) |
| kVAR | reactive power (Kilo-volt-amperes reactive) |
| KW | real power (killo-watts) |
| lbs | pounds |

| | |
|---|---|
| LIM | Linear Induction Motor |
| M | the ratio of total complex power to fundamental complex power |
| Max | Maximum |
| Min | Minimum |
| mh | milli henries |
| mph | miles-per-hour |
| N | Motor Speed (rpm) |
| NEMA | National Electrical Manufactures Association |
| PDR | Phase Delay Rectifier |
| pf | power factor |
| PRT | Personal Rapid Transit |
| $R_A$ | Armature Resistance |
| rms | root mean square |
| rpm | revolutions per minute |
| $S_T$ | total system complex power |
| T | torque |
| $T_A$ | net torque producing acceleration |
| $T_B$ | net torque producing deceleration |
| $T_D$ | the torque equivalent of all friction losses |
| $T_M$ | torque produced in the motor |
| TSC | Transportation Systems Center |
| TTI | Transportation Technology Inc. |
| t | time |
| UMTA | Urban Mass Transportation Administration |
| v | volts |

## ABBREVIATIONS (CONT.)

| | |
|---|---|
| $V_d$ | output voltage of rectifier |
| $V_{do}$ | maximum dc output voltage from rectifier |
| $^\circ$ | degrees |
| $\alpha$ | thyristor firing angle delay |
| $\phi$ | angle between fundamental phase voltage and fundamental phase current |
| $\omega$ | angular frequency |
| $\Omega$ | ohms |

# PREFACE

The work described in this report was performed in the Power and Propulsion Branch at the Transportation System Center under the sponsorship of the New Systems Division of the Office of Research, Development and Demonstrations, Urban Mass Transportation Administration.

The objective of this work was to establish the power and propulsion characteristics of each of the Dulles Transpo® '72 PRT vehicles. These characteristics are to be determined by using analytical descriptions, manufacturer's data, and the test data from the Post-Transpo® '72 Test Program.

Mr. Raposa is a member of the Mechanical Engineering Division of the Transportation Systems Center, and Mr. Phillips is a consulting engineer with Alexander Kusko Inc.

# 1. INTRODUCTION

As part of a program for the development of new urban transportation systems, the Urban Mass Transportation Administration (UMTA) initiated a project for the construction and testing of four prototype "Personal Rapid Transit (PRT) Systems" at Dulles International Airport in conjunction with Transpo® '72. These four systems were the Bendix Dashaveyor System, the Ford Motor ACT System, the Rohr Monocab System, and the Transportation Technology TTI System.

Each prototype system consisted of two vehicles with a minimum of 1000 feet of guideway, off-line stations, and fully automatic control. One system (TTI) used air cushions for vertical support and a linear induction motor for propulsion. The other systems used rubber tires, two being supported from a roadway and the other (Monocab) suspended from an overhead guidebeam. Both scheduled operation and demand-actuated operation were demonstrated.

These systems were designed as demonstration systems and, therefore, did not incorporate all of the technological features that would be necessary for operation in an urban environment. Nevertheless, the four systems were hardware embodiments of state-of-the-art design and, thus, afforded a unique opportunity to collect heretofore unmeasured data on those aspects of the systems that were representative of an urban system design and that could be measured and evaluated in a straightforward manner.

The systems were operated during Transpo® '72 and were subject to intensive testing in the period from 1 August to 11 November 1972. The testing was a joint effort of UMTA and the Transportation Systems Center (TSC) of the Department of Transportation, the Applied Physics Laboratory (APL), MITRE Corporation, and the four contractors. The objectives of these tests were:

1. To obtain a data base on those system characteristics that could be tested in the Dulles configurations for use in formulating specifications, evaluating systems, developing analytical models, and identifying component development requirements.
2. To determine the capabilities and limitations of these systems and to assess the current state of the art.
3. To determine the adequacy of specific subsystem and component designs.

The purpose of this report is to establish the power and propulsion characteristics of each of the vehicles. These characteristics are to be determined by using analytical descriptions, manufacturer's data and the test data from the Post-Transpo® '72 Test Program.

In the sections that follow, the propulsion and power characteristics are established for each of the four vehicles. The final section provides some comparative analysis in select areas in propulsion and power. This analysis has as its primary objective the identification of those performance features necessary to adequately describe the power and propulsion characteristics of each of the vehicles.

# 2. BENDIX DASHAVEYOR SYSTEM

## 2.1 SYSTEM DESCRIPTION

The vehicle propulsion system consists of two single-axle bogies with rubber-tired wheels, each driven by an electric motor. Power for the vehicle is obtained from three-phase power rails providing 480 V line-to-line, and power collectors are located on both sides of the vehicle. A block diagram of the electrical system is shown in Figure 2-1.

The motor providing propulsion power in each bogie is a dc series motor. The two motors are connected in parallel, and each motor is connected to the drive axle through a speed reduction ratio of 5.12:1. The motor is a special design by General Electric, their type MD-606 AE, with a nameplate rating of 25 hp, 575 rpm at 230 V. DC-propulsion power is provided by a three-phase thyristor, six-pulse rectifier operating directly from the 480-V ac line. A smoothing reactor is used on the output of the rectifier. The auxiliary equipment operates from the three-phase 480-V bus. Vehicle braking is mechanical.

The specifications of the vehicle pertinent to the propulsion system are:

<u>Capacity</u>

| | |
|---|---|
| Curb Weight | 18,200 lbs |
| Gross Weight | 23,500 lbs |
| Number of Passengers | |
| Seated | 12 |
| Standing | 20 |

<u>Dimensions</u>

| | |
|---|---|
| Wheelbase | 198.0 in. |
| Overall Length | 282.0 in. |
| Height | 130.5 in. |
| Width | 85.5 in. |
| Tread | 58.0 in. |

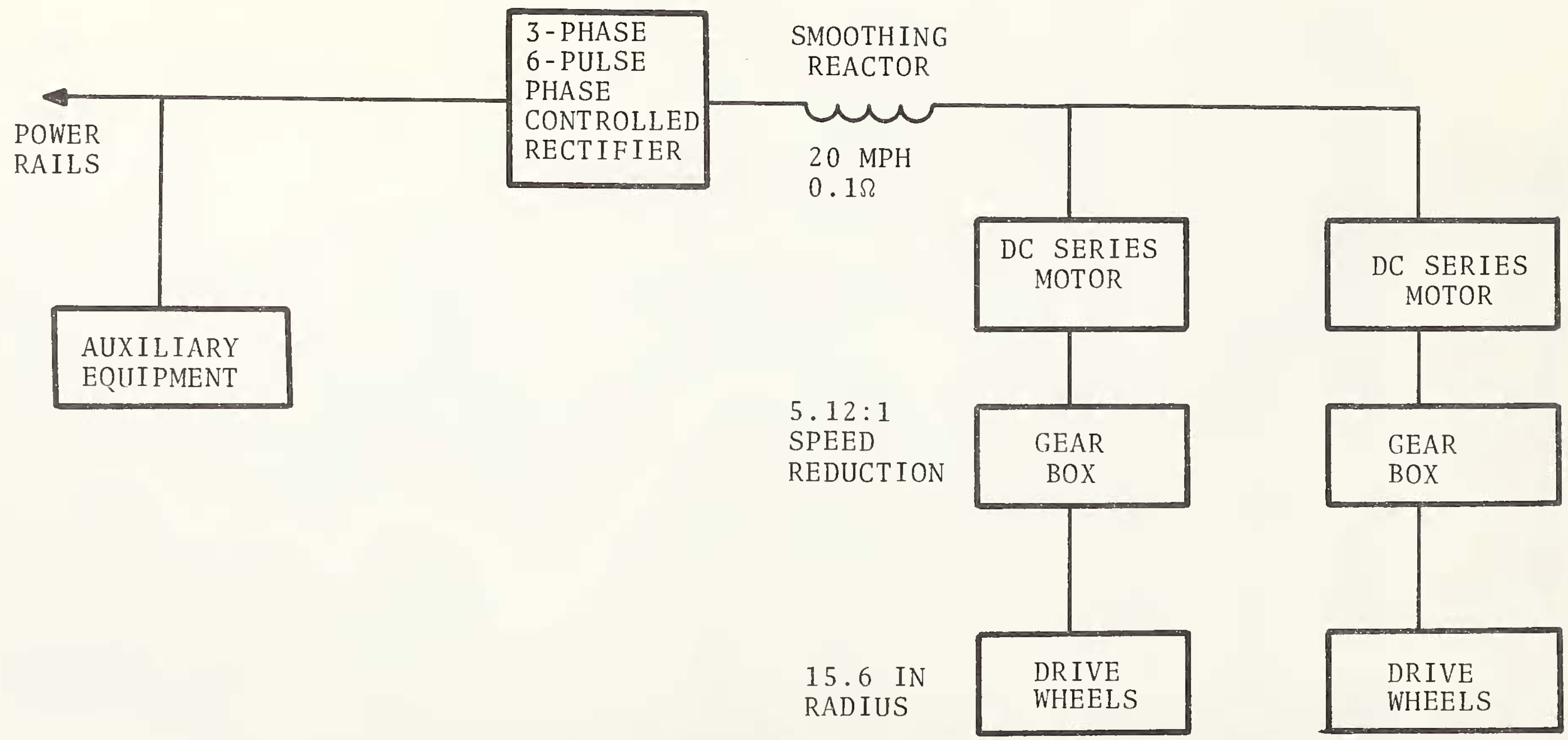


Figure 2-1 Bendix Dashaveyor Vehicle Block Diagram

## 2.2 PROPULSION SYSTEM ANALYSIS

In a three-phase, six-pulse rectifier maximum dc output voltage occurs when there is no delay in the firing angle. The average direct voltage is found by integrating the instantaneous voltages over a period of the wave. This results in

$$V_{do} = \frac{3\sqrt{2}}{\pi} E_{LL} = 1.35\ E_{LL} \qquad \text{(Reference 1)}$$

where $V_{do}$ = the maximum dc output voltage from the rectifier
and $E_{LL}$ = the rms line-to-line voltage on the input to the rectifier.

When there is a delay introduced in the firing angle, it can be shown that the output $V_d$ is given by

$$V_d = V_{do} \cos \alpha \qquad \text{(Reference 1)}$$

where $\alpha$ is the firing angle delay.

The relationship between the rectifier output voltage and the delay angle is shown in Figure 2-2, (Reference 1).

When a constant current flows in the dc load with no firing angle delay, the line current on the input to the rectifier has the wave shape shown in Figure 2-3, consisting of positive and negative rectangular pulses of height $I_d$, the direct current, and width $2\pi/3$ radians. If $I_{L1}$ is the rms value of the fundamental-frequency component of the alternating line current, a Fourier analysis of the waveform yields

$$\sqrt{2}\ I_{L1} = \frac{2}{\pi}\int_{-\pi/3}^{+\pi/3} I_d \cos \omega t \ d(\omega t)$$

or

$$I_{L1} = \frac{\sqrt{6}}{\pi} I_d = 0.780\ I_d$$

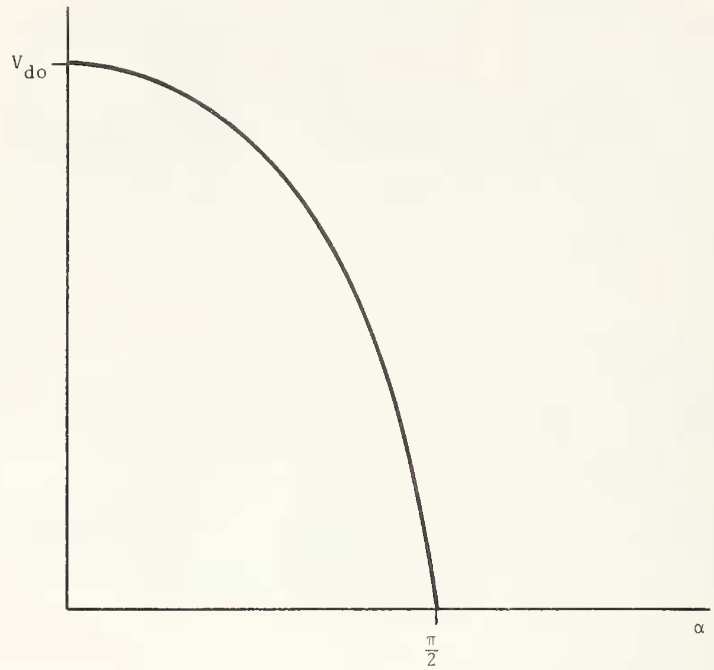


Figure 2-2 Rectifier Output vs. Firing Angle

This is independent of $\alpha$ as long as there is no overlap angle in the rectifier. With losses in the rectifier neglected, the ac power must equal the dc power; that is

$$3\, E_{LN} I_{L1} \cos \phi = I_d V_d = I_d V_{do} \cos \alpha$$

where $\phi$ = the angle between the fundamental phase voltage and the fundamental phase current, $I_{L1}$. Thus $\cos \phi = \cos \alpha$. The above relations must be considered as approximations only, in that they ignore the effects of rectifier conduction overlap and harmonic distortion.

The speed of a series motor varies considerably with changes in load because there is no constant value of flux. The armature current, which is a function of load, determines the strength of the field, having a major influence on the speed. The basic motor relationships are:

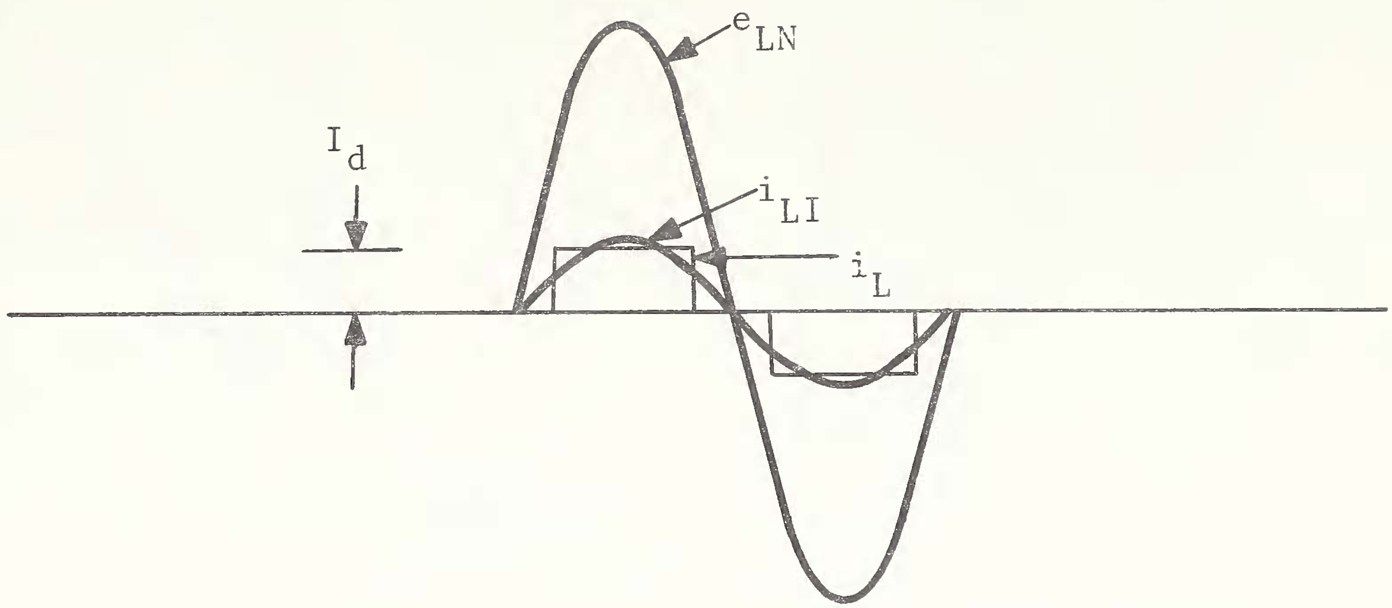


Figure 2-3. Line Currents for Rectifier, $\alpha = 0$

$$N = \frac{V_A - I_A R_A}{k_1 \phi} \qquad \text{(Reference 2)}$$

and

$$T = k_2 I_A \phi \qquad \text{(Reference 2)}$$

where N is the motor speed and T the motor torque. Typical series motor curves are shown in Figure 2-4 (Reference 3). As shown, the same torque may be obtained at different speeds by changing the voltage applied to the motor.

Although the flux is created by the armature current, saturation effects must be considered which affect the above relations. For these reasons, when evaluating a series motor, motor performance curves are required to define the various conditions of load current, voltage, torque and speed. The motor performance curves for the Bendix Dashaveyor motor are shown in Figure 2-5 (Reference 4).

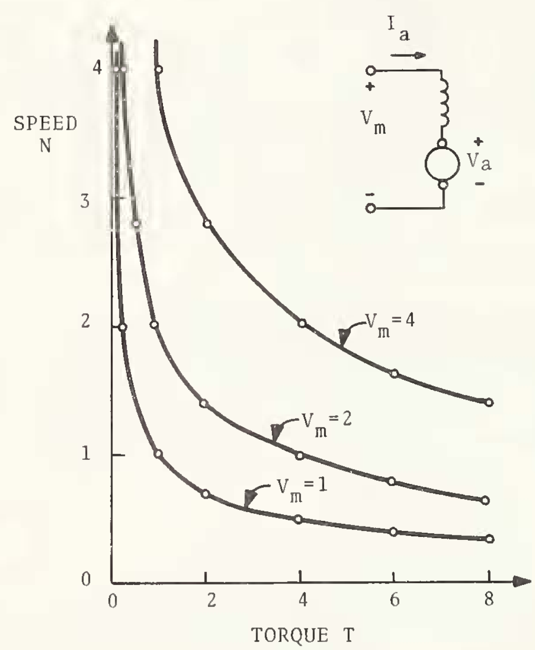


Figure 2-4 Speed-Torque Characteristics of Series Motor Under Voltage Control

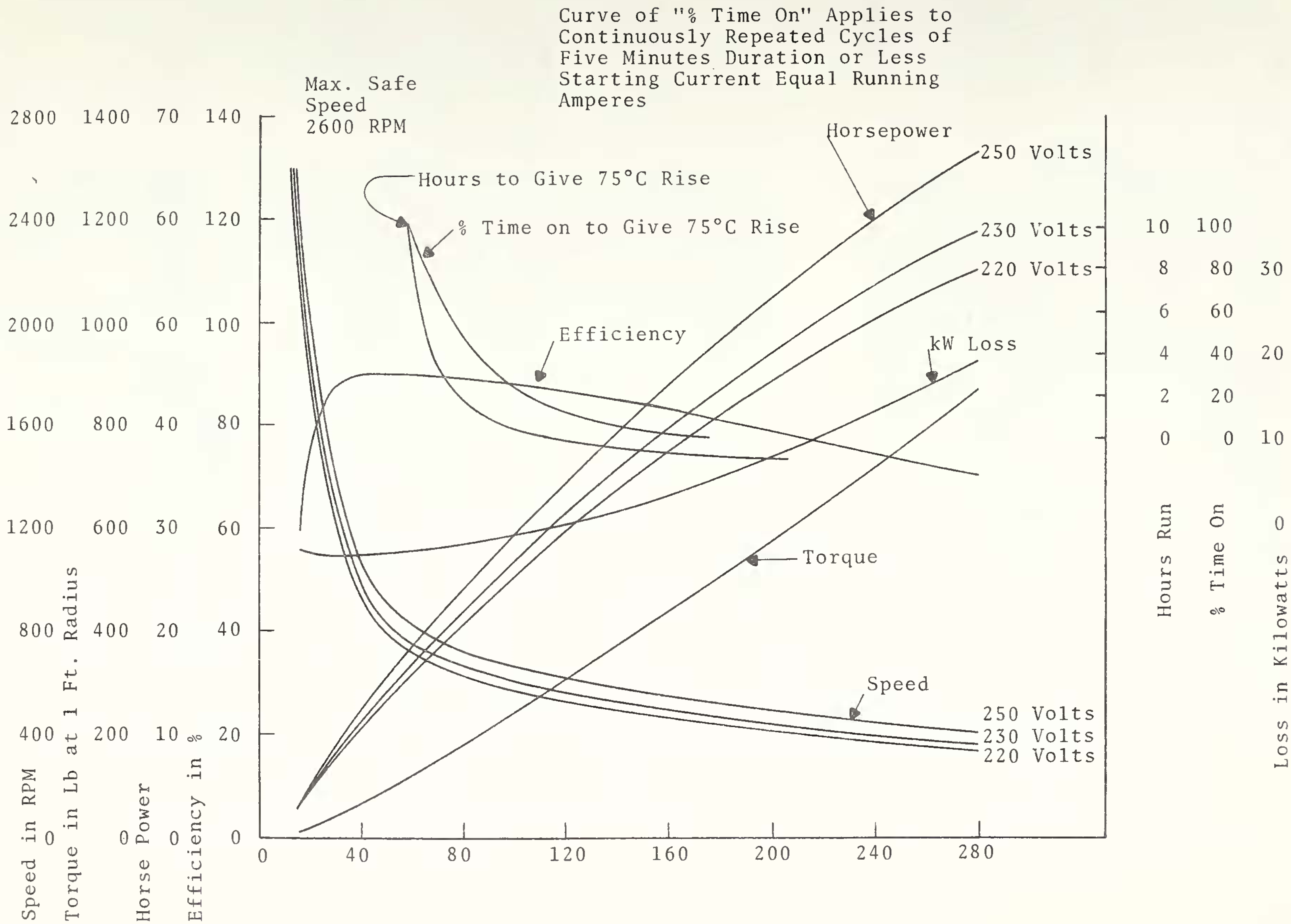


Figure 2-5 Dashaveyor Motor Performance Curves (From Bendix)

The basic test data from which the performance curves are derived comes from magnetic tape 33603 on which vehicle performance parameters were recorded during tests run on October 11, 1972 with the vehicle loaded to 23,500 lbs gross weight. The data reviewed in the preparation of this report was taken during runs 193 to 242 inclusive. Each run consisted of accelerating the vehicle to one of the programmed speeds, cruising for a short time at that speed, and then applying the brakes. All even numbered runs were northbound on the guideway. A comparison of northbound and southbound runs indicates the vehicle performance is the same in either direction. The test data used is displayed on a chart recorded at approximately one inch per second. Data was taken from the tracks showing velocity, motor armature current and motor armature voltage.

## 2.3 PROPULSION SYSTEM PERFORMANCE

Using the data described above the performance of each motor for operation at five programmed speeds is shown in Figures 2-6 through 2-10 inclusive. For each speed the curves show the performance of one motor during acceleration, cruise at the programmed speed, and braking to a stop from the programmed speed.

In these curves armature current and armature voltage came from the test data from the Post-Transpo® '72 Test Program. Motor torque came from the manufacturer's data on motor performance. The firing angle delay in the rectifier was calculated from the ratio of required output voltage to maximum output voltage of the rectifier with 480 V on the rails. In Figures 2-6 to 2-9, it should be noted that the torque was limited during the acceleration period by current limiting of the armature current.

## 2.4 PROPULSION SYSTEM POWER REQUIREMENTS

The formulae for calculating propulsion system fundamental power requirements are:

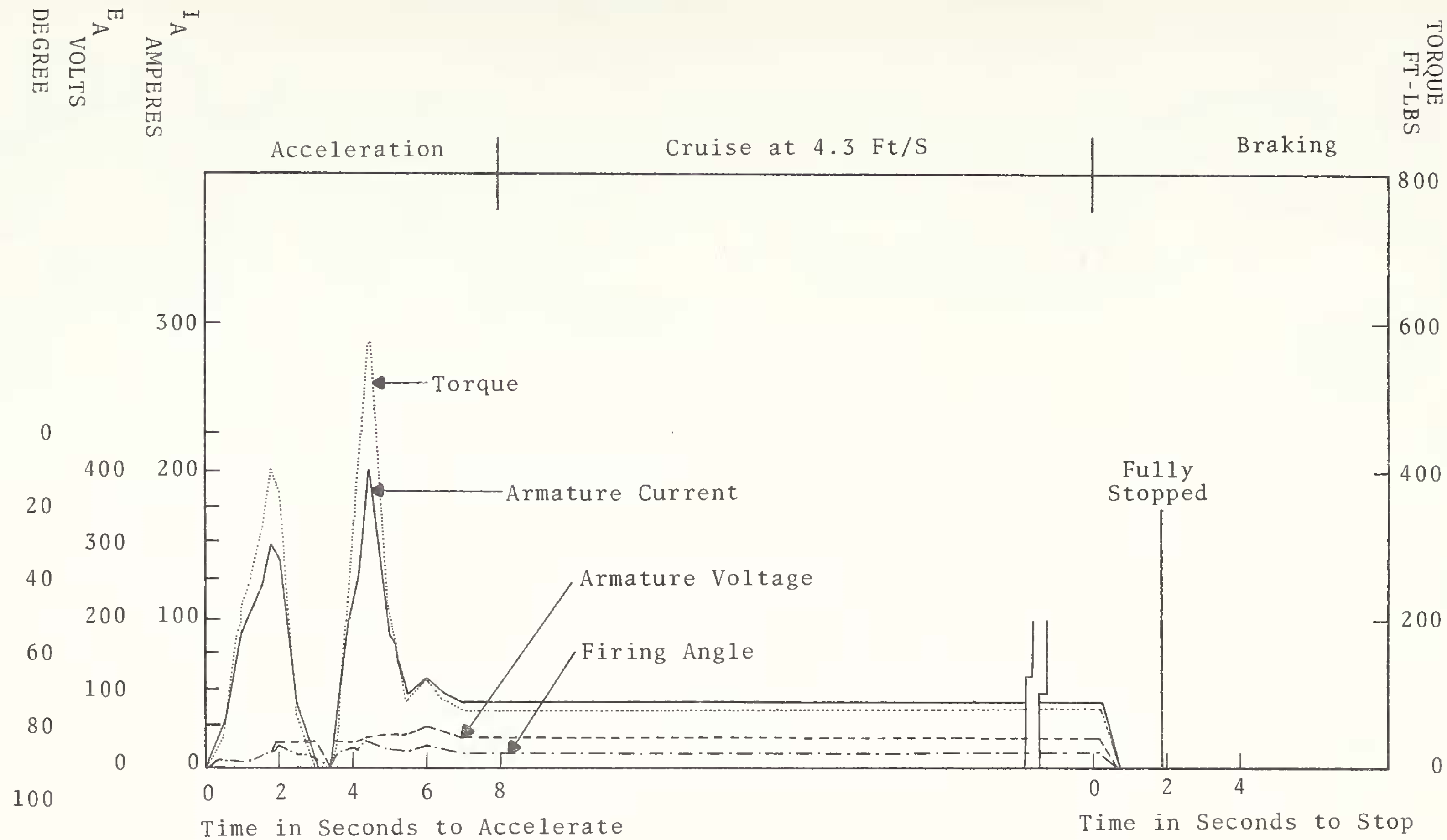


Figure 2-6 Bendix Dashaveyor Vehicle -- Motor Performance for Acceleration, Cruise at 4.3 ft/s and Braking; Vehicle Weight - 23,500 lbs; Level Rail; No Wind; 480 V L-L on Rails

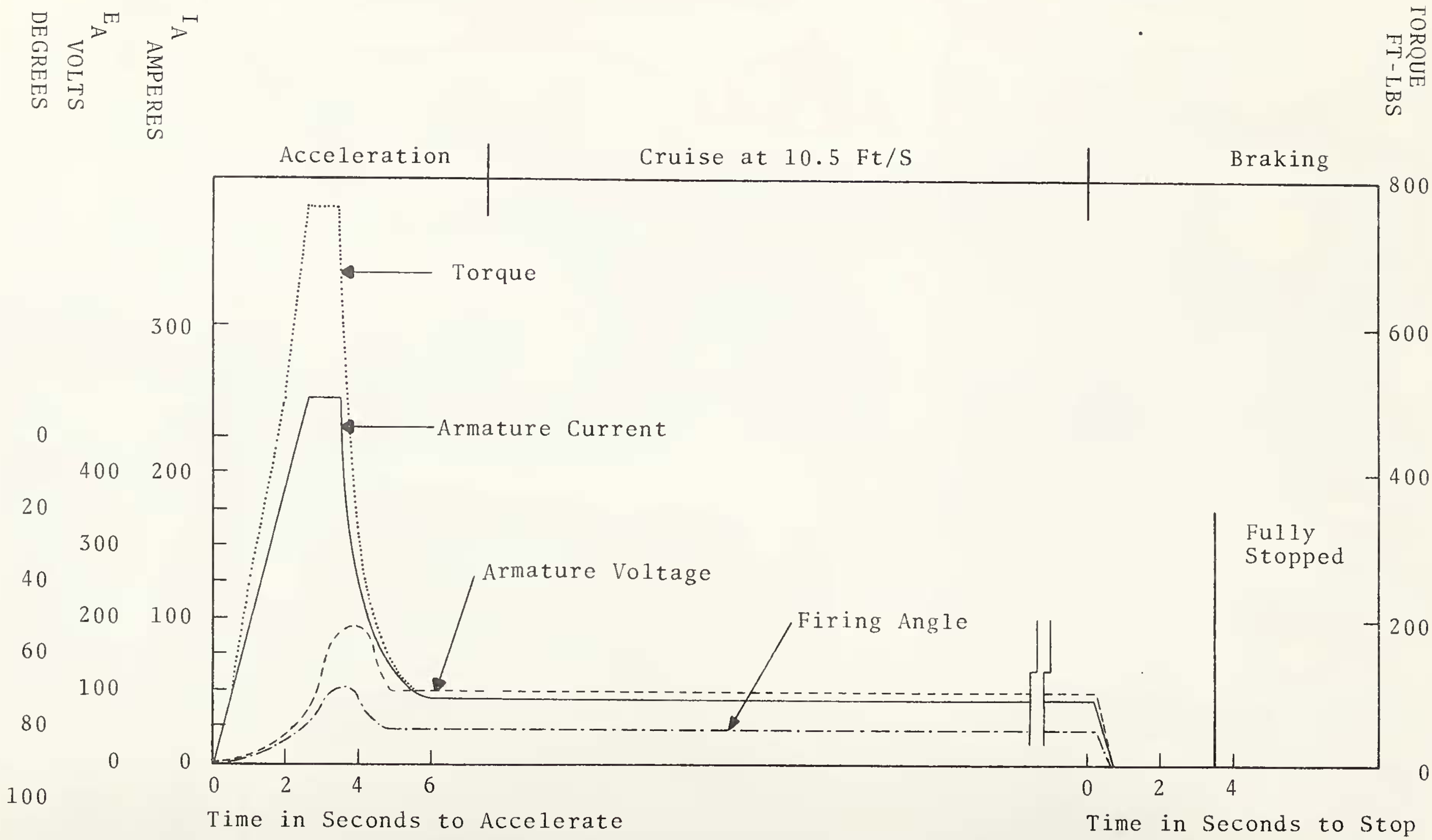


Figure 2-7 Bendix Dashaveyor Vehicle -- Motor Performance for Acceleration, Cruise at 10.5 ft/s and Braking; Vehicle Weight 23,500 lbs; Level Rail; No Wind; 480 V L-L on Rails

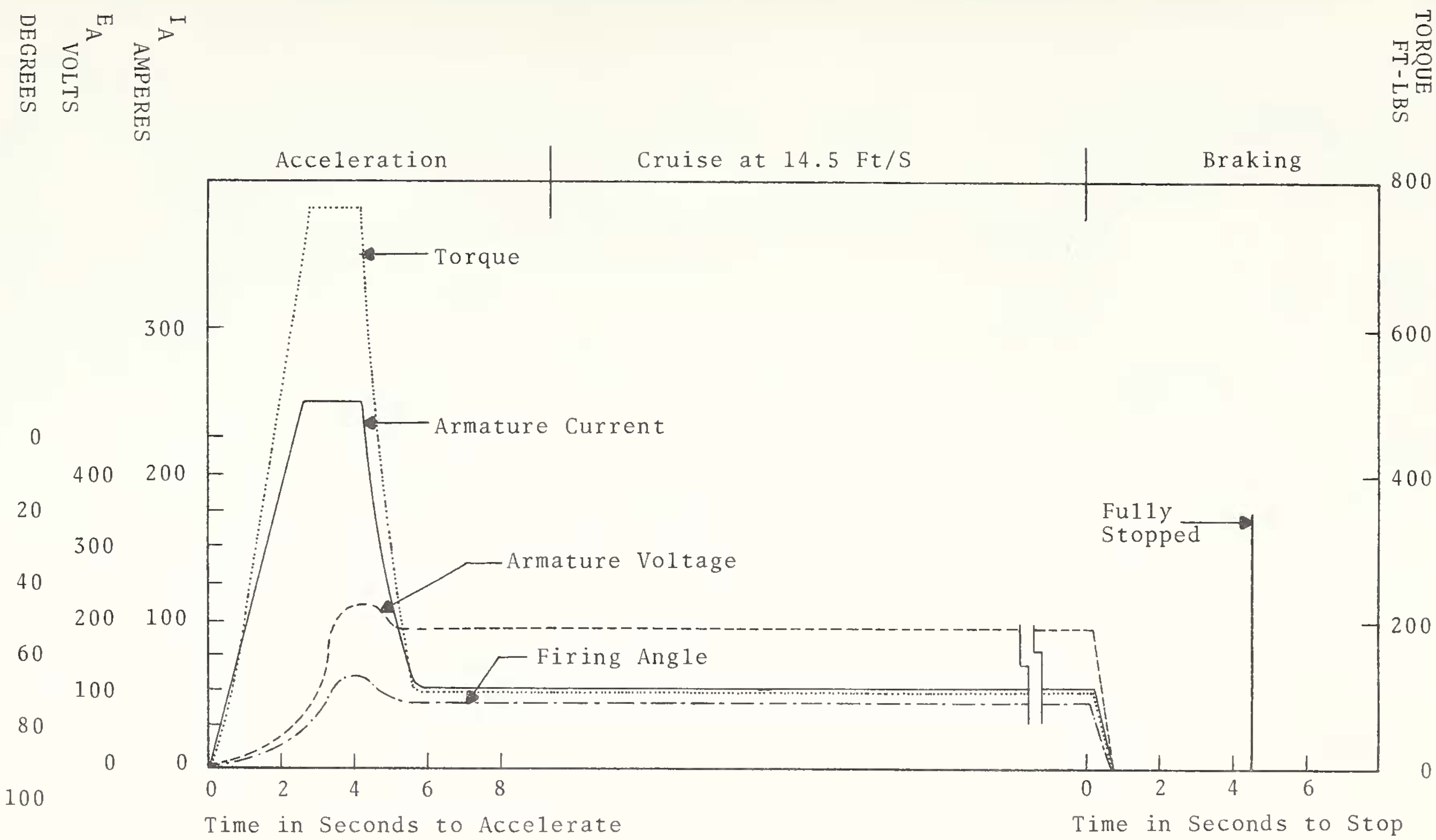


Figure 2-8 Bendix Dashaveyor Vehicle -- Motor Performance for Acceleration, Cruise at 14.5 ft/s and Braking; Vehicle Weight 23,500 lbs; Level Rail; No Wind; 480 V L-L on Rails

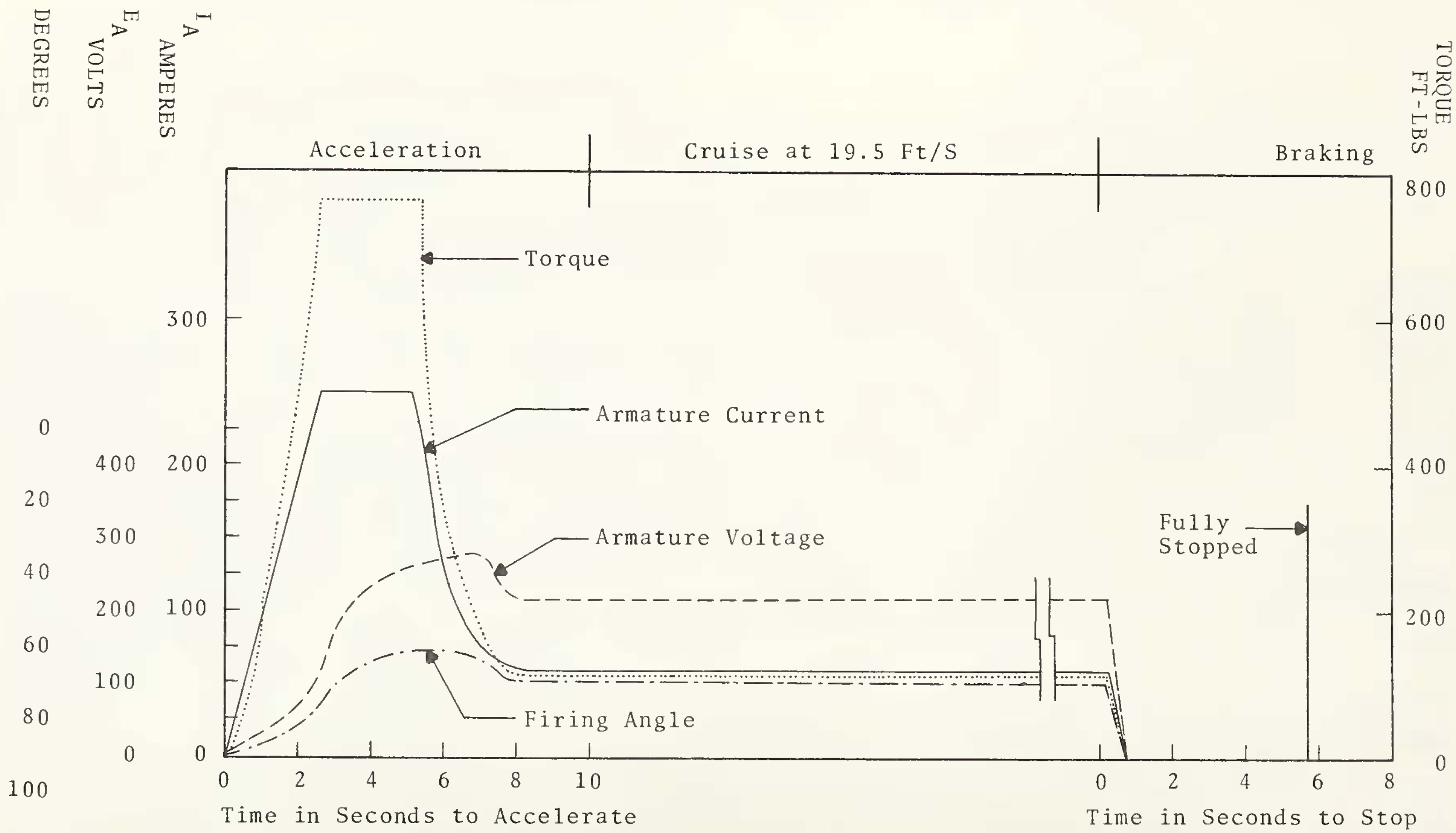


Figure 2-9 Bendix Dashaveyor Vehicle -- Motor Performance for Acceleration; Cruise at 19.5 ft/s and Braking; Vehicle Weight 23,500 lbs; Level Rail; No Wind; 480 V L-L on Rails

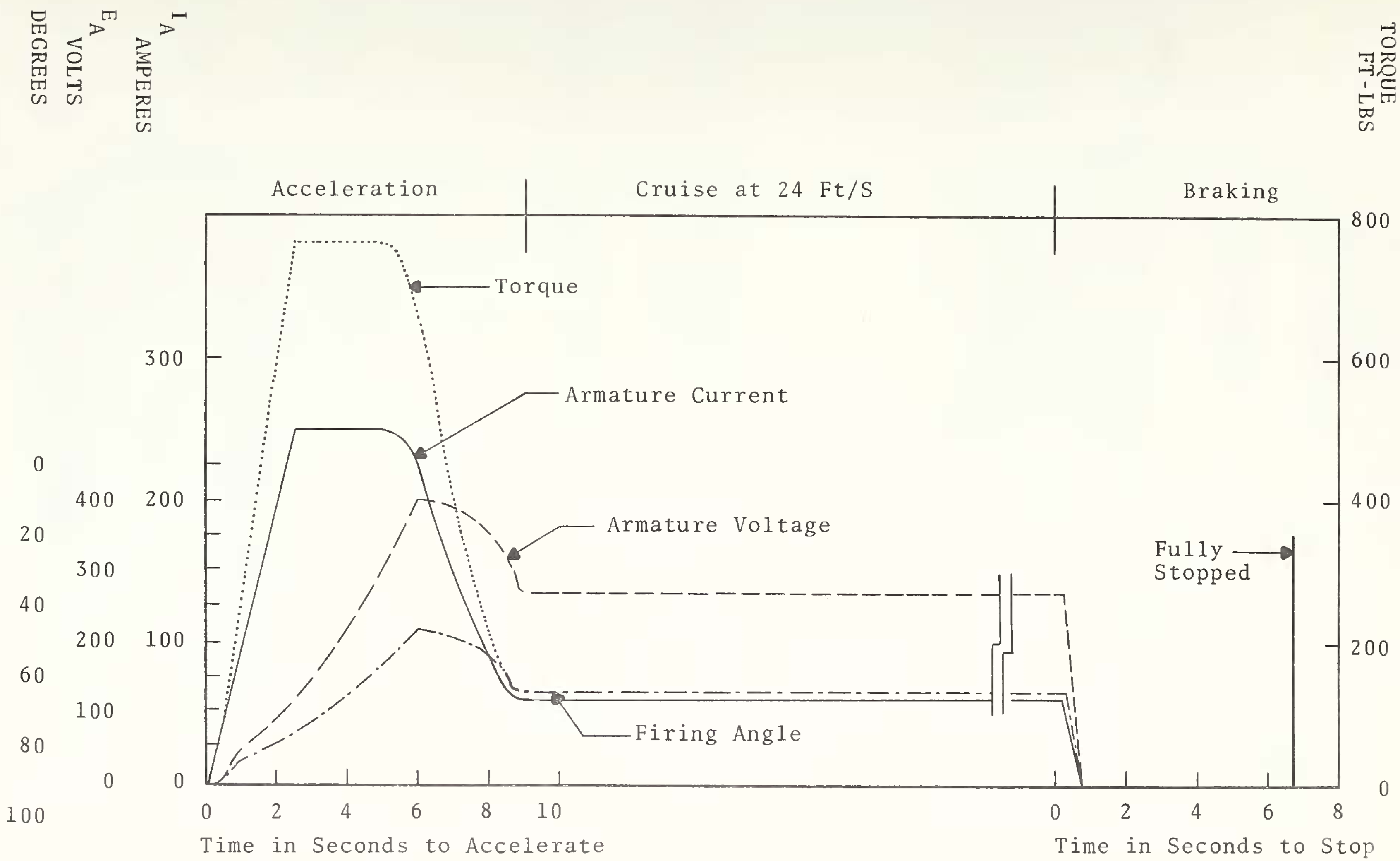


Figure 2-10 Bendix Dashaveyor Vehicle -- Motor Performance for Acceleration, Cruise at 24 ft/s and Braking; Vehicle Weight 23,500 lbs.; Level Rail; No Wind; 480 V L-L on Rails

Fundamental complex power (kVA) $= \frac{\sqrt{3}}{1000} I_{L1}E_{LL}$

Fundamental real power (kW) $= \frac{\sqrt{3}}{1000} I_{L1}E_{LL} \cos\phi$

Displacement reactive power (kvar) $= \frac{\sqrt{3}}{1000} I_{L1}E_{LL} \sin\phi$

The total complex power must take into account the presence of distortion currents caused by the rectifier, and the total complex power. The harmonic currents produced in phase-delay rectifiers have been evaluated by Wlodyka, Abbas and Ploetz, (Reference 5). They have shown that the ratio of each harmonic current amplitude to the fundamental current amplitude depends on the firing angle delay. Thus it is possible to define

$$M = \frac{I_T}{I_{L1}}$$

where $I_T$ = the rms value of the total current, and the value of M will depend on the firing angle delay. The calculation of M is explained in detail in Appendix A.

Thus, the total complex power for the propulsion system, $S_T$, is given by

$$S_T = MS_1$$

where $S_T$ is the fundamental complex power.

The propulsion system power characteristics were calculated for the five programmed speeds using the above formulae. The power characteristics are shown in Figures 2-11 through 2-15 inclusive. For each speed, the propulsion system produces maximum distortion power early in the acceleration. After reaching cruising speed, when less torque is required, the firing angle delay is increased to reduce voltage on the motors, resulting in displacement complex power and total complex power appreciably higher than the real power.

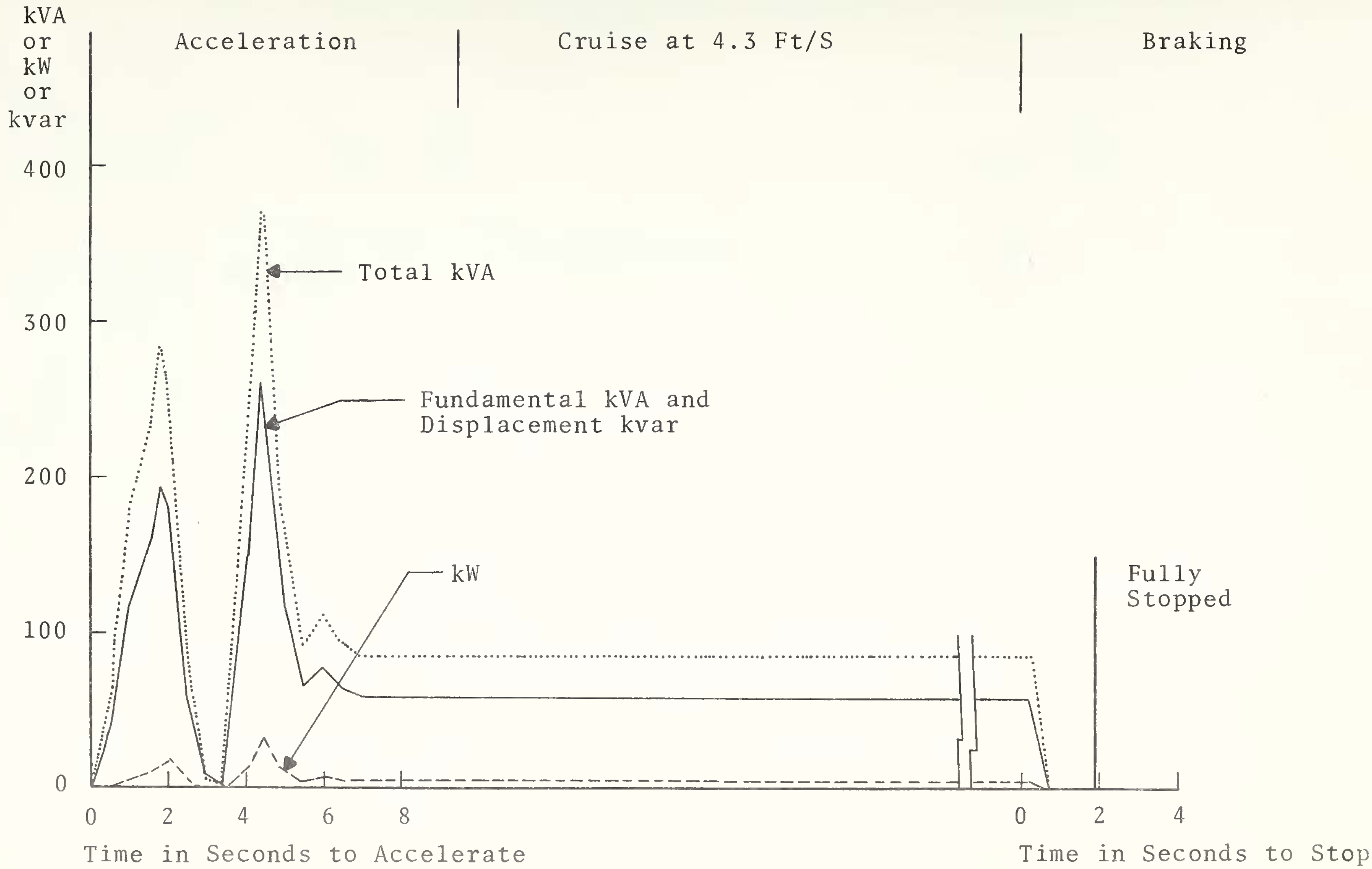


Figure 2-11 Bendix Dashaveyor Vehicle -- Propulsion Power for Acceleration, Cruise at 4.3 ft/s and Braking; Vehicle Weight 23,500 lbs; Level Rail; No Wind; 480 V L-L on Rails

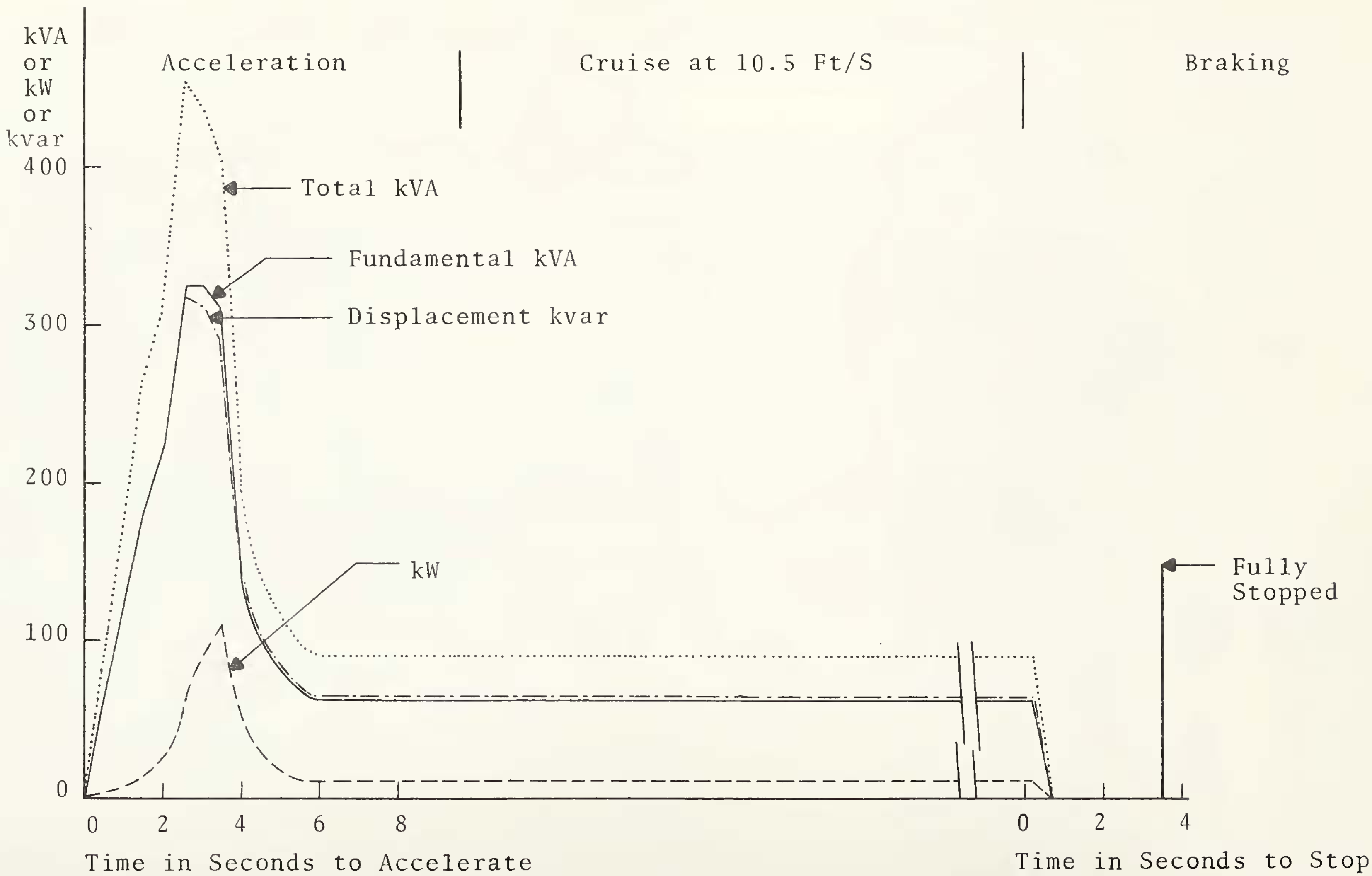


Figure 2-12 Bendix Dashaveyor Vehicle -- Propulsion Power for Acceleration, Cruise at 10.5 ft/s and Braking; Vehicle Weight 23,500 lbs; Level Rail; No Wind; 480 V L-L on Rails

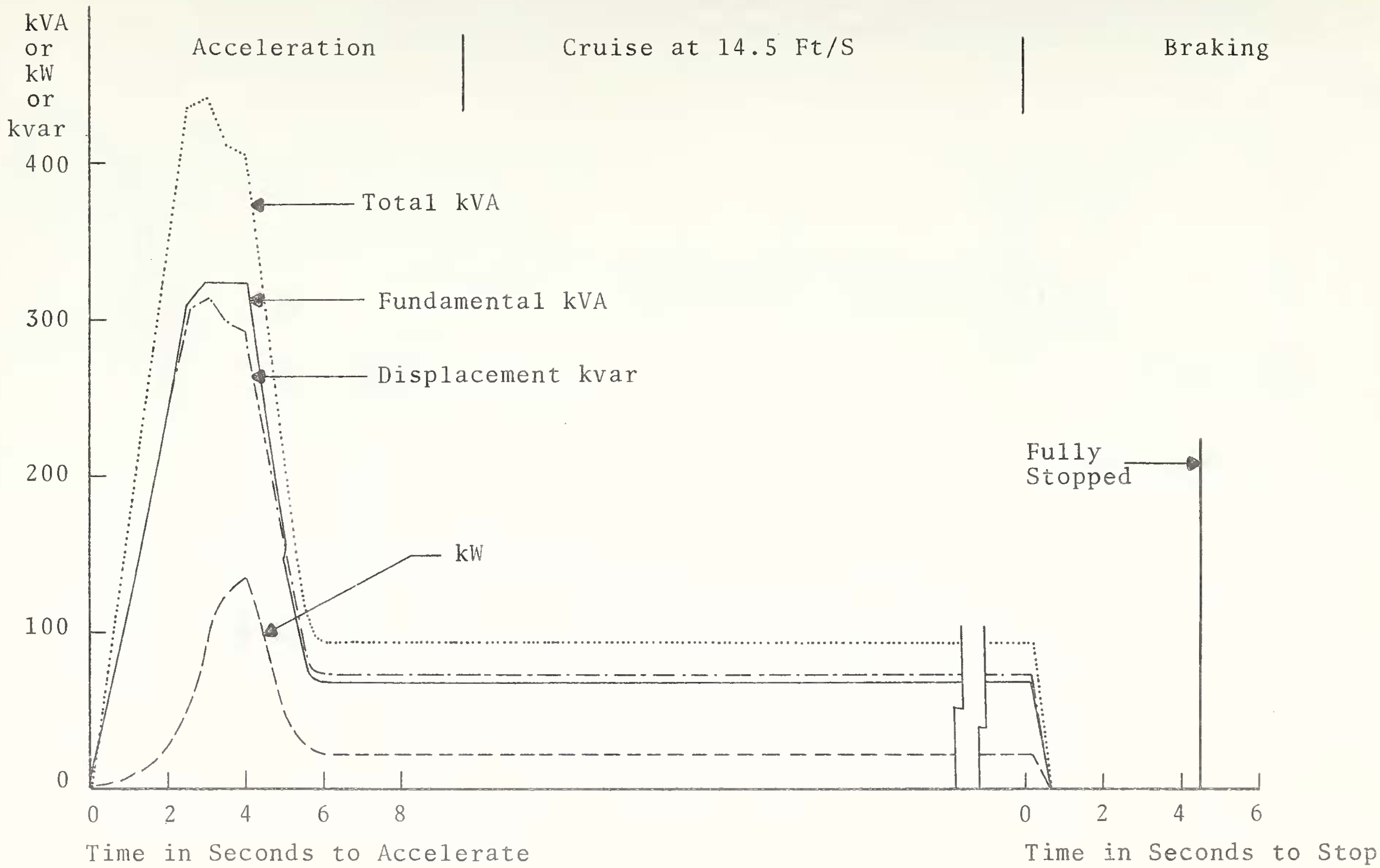


Figure 2-13 Bendix Dashaveyor Vehicle -- Propulsion Power for Acceleration, Cruise at 14.5 ft/s and Braking; Vehicle Weight 23,500 lbs; Level Rail; No Wind; 480 V L-L on Rails

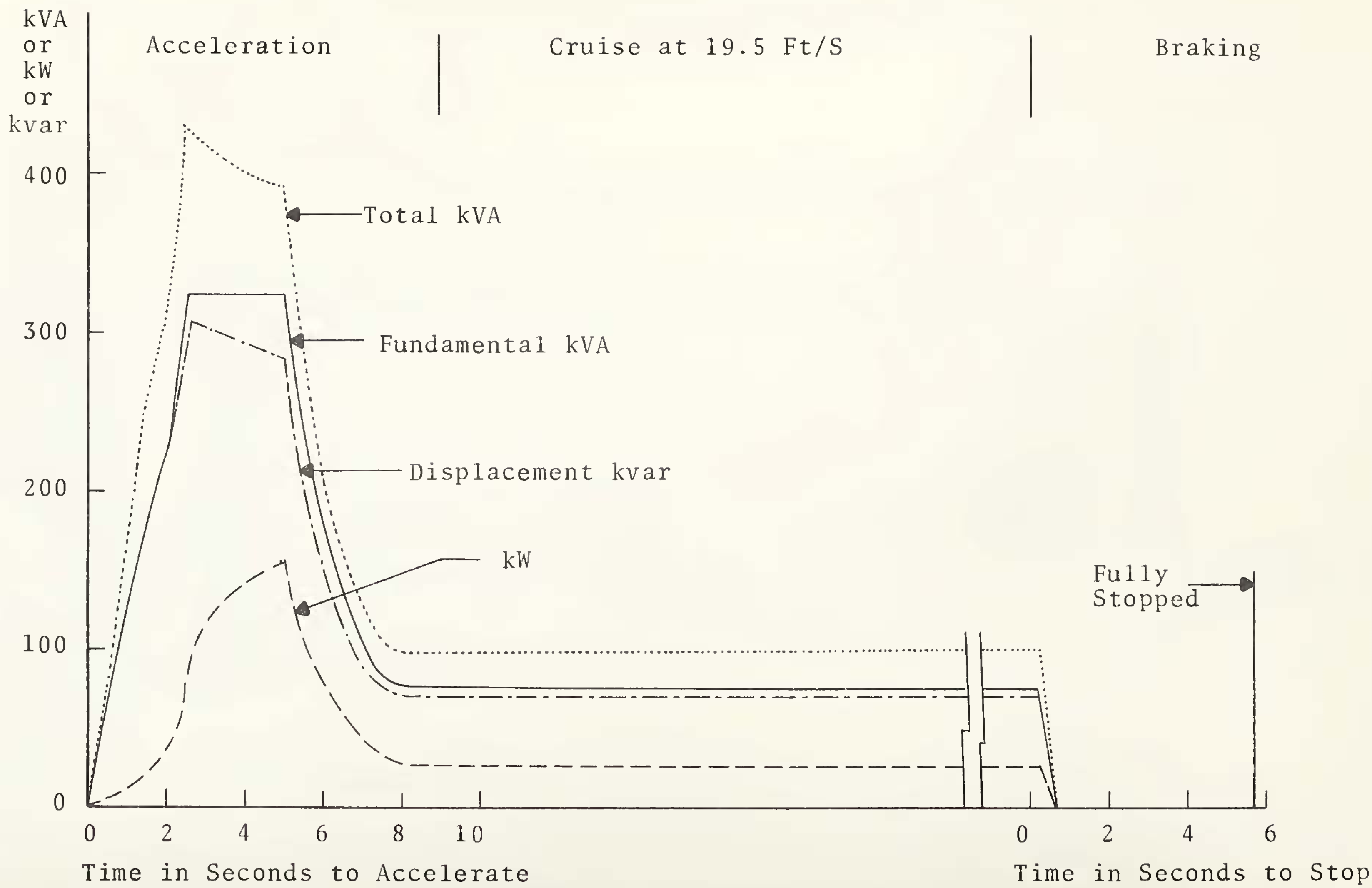


Figure 2-14 Bendix Dashaveyor Vehicle -- Propulsion Power for Acceleration, Cruise at 19.5 ft/s and Braking; Vehicle Weight 23,500 lbs; Level Rail; No Wind; 480 V L-L on Rails

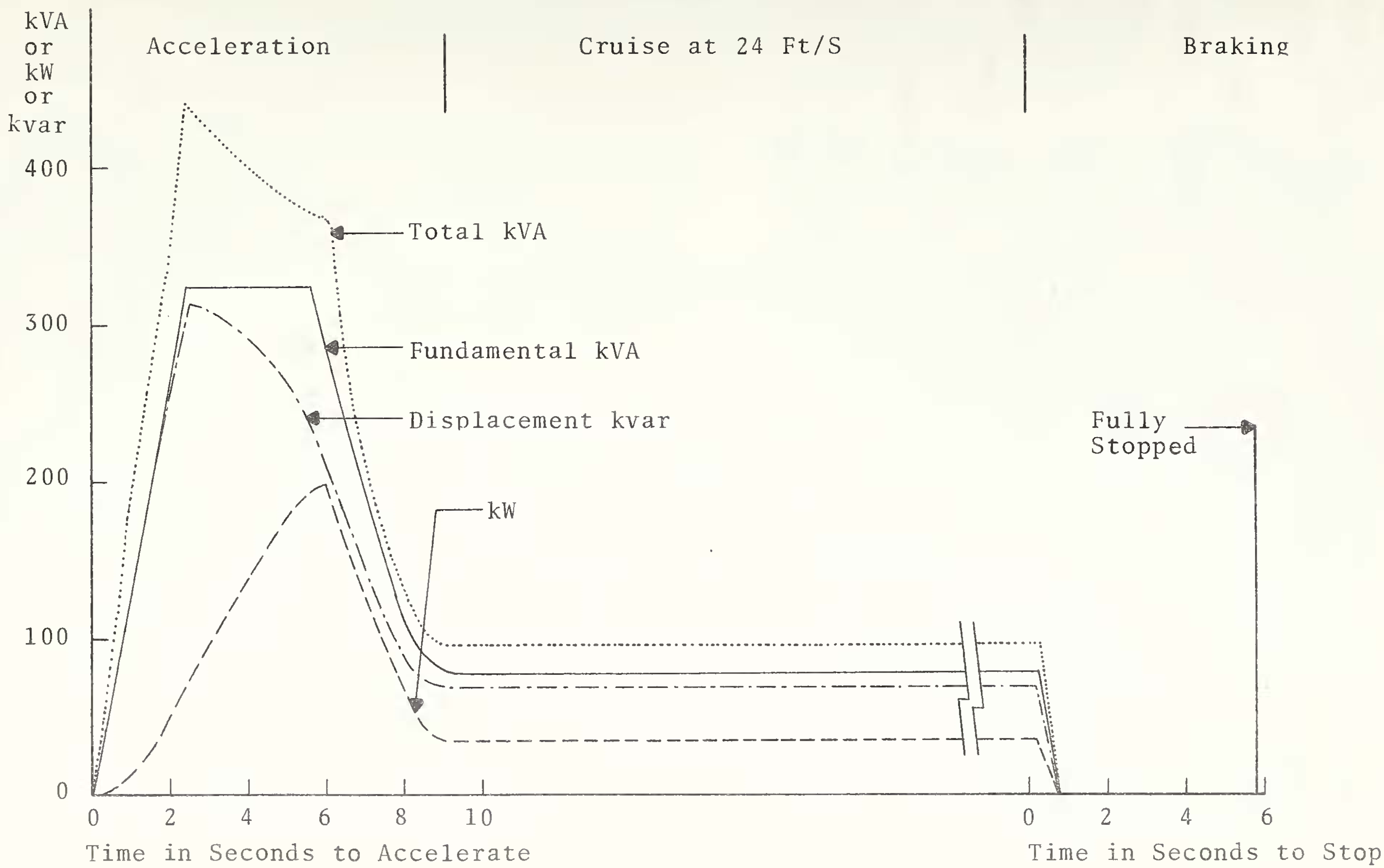


Figure 2-15 Bendix Dashaveyor Vehicle -- Propulsion Power for Acceleration, Cruise at 24 ft/s and Braking; Vehicle Weight 23,500 lbs; Level Rail; No Wind; 480 V L-L on Rails

## 2.5 VEHICLE POWER REQUIREMENTS

In addition to power for propulsion, the vehicle requires power for the operation of auxiliary equipment. We have assumed that the auxiliary equipment produces a constant balanced load on the three phases. The load was assumed to be 6.3 kW with 1.7 kvar displacement power and with a lagging power factor. It was assumed the auxiliary equipment did not require distortion power.

The power characteristics of the entire vehicle were calculated by adding the components of the auxiliary power to the corresponding components of propulsion power. The curves on Figures 2-16 through 2-20 inclusive show the vehicle power for the five programmed speeds. Because the vehicle propulsion system is programmed to provide the same acceleration, independent of final speed, the charts of Figures 2-16 through 2-20 show the peak fundamental complex power during acceleration being independent of the final speed. The peak value of total complex power should be the same but shows small differences which are attributed to small differences in interpreting the charts.

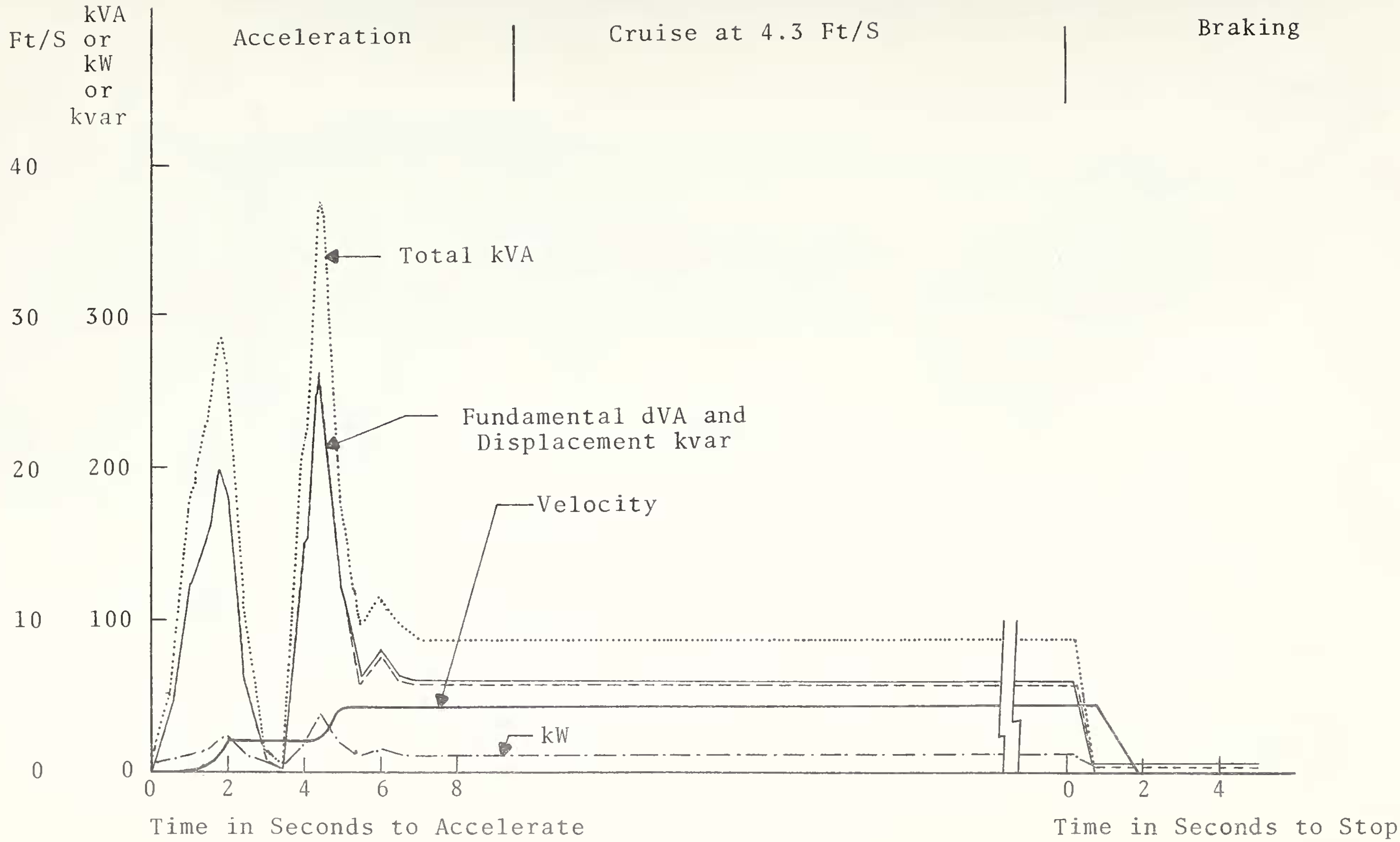


Figure 2-16 Bendix Dasheveyor Vehicle -- Vehicle Power for Acceleration, Cruise at 4.3 ft/s and Braking; Vehicle Weight 23,500 lbs; Level Rail; No Wind; 480 V L-L on Rails

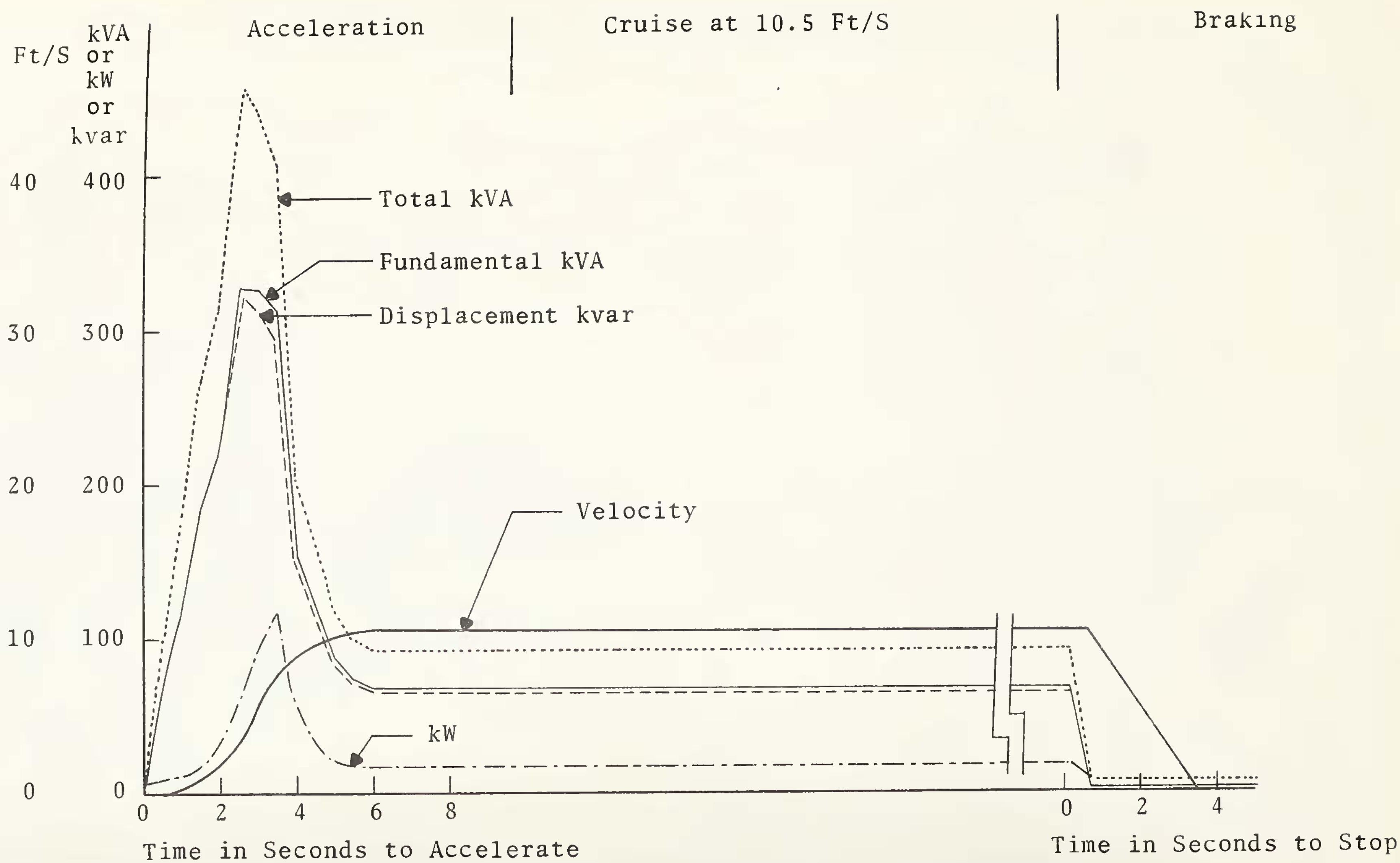


Figure 2-17 Bendix Dashaveyor Vehicle -- Vehicle Power for Acceleration, Cruise at 10.5 ft/s and Braking; Vehicle Weight 23,500 lbs; Level Rail; No Wind; 480 V L-L on Rails

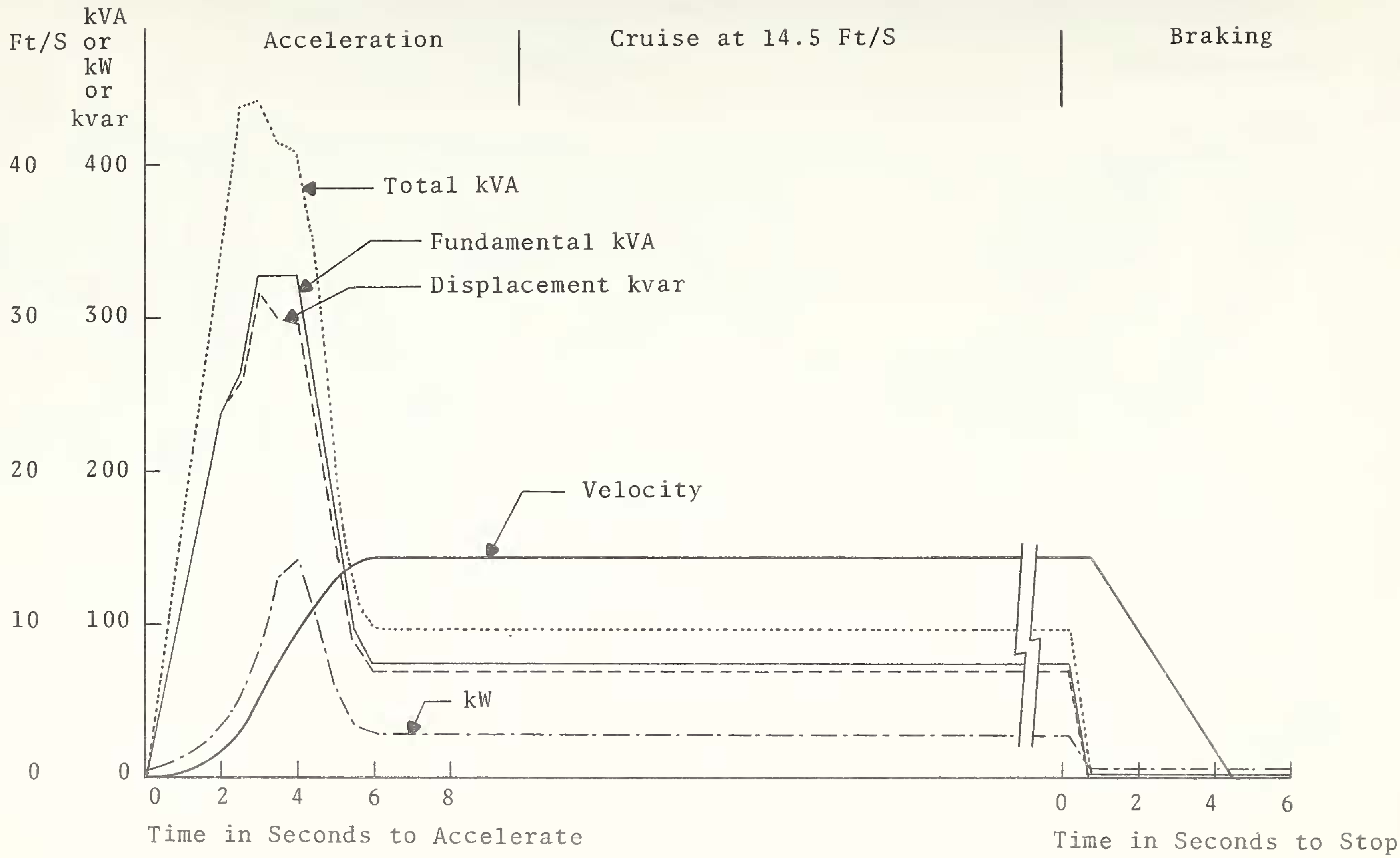


Figure 2-18 Bendix Dashaveyor Vehicle -- Vehicle Power for Acceleration, Cruise at 14.5 ft/s and Braking; Vehicle Weight 23,500 lbs; Level Rail; No Wind; 480 V L-L on Rails

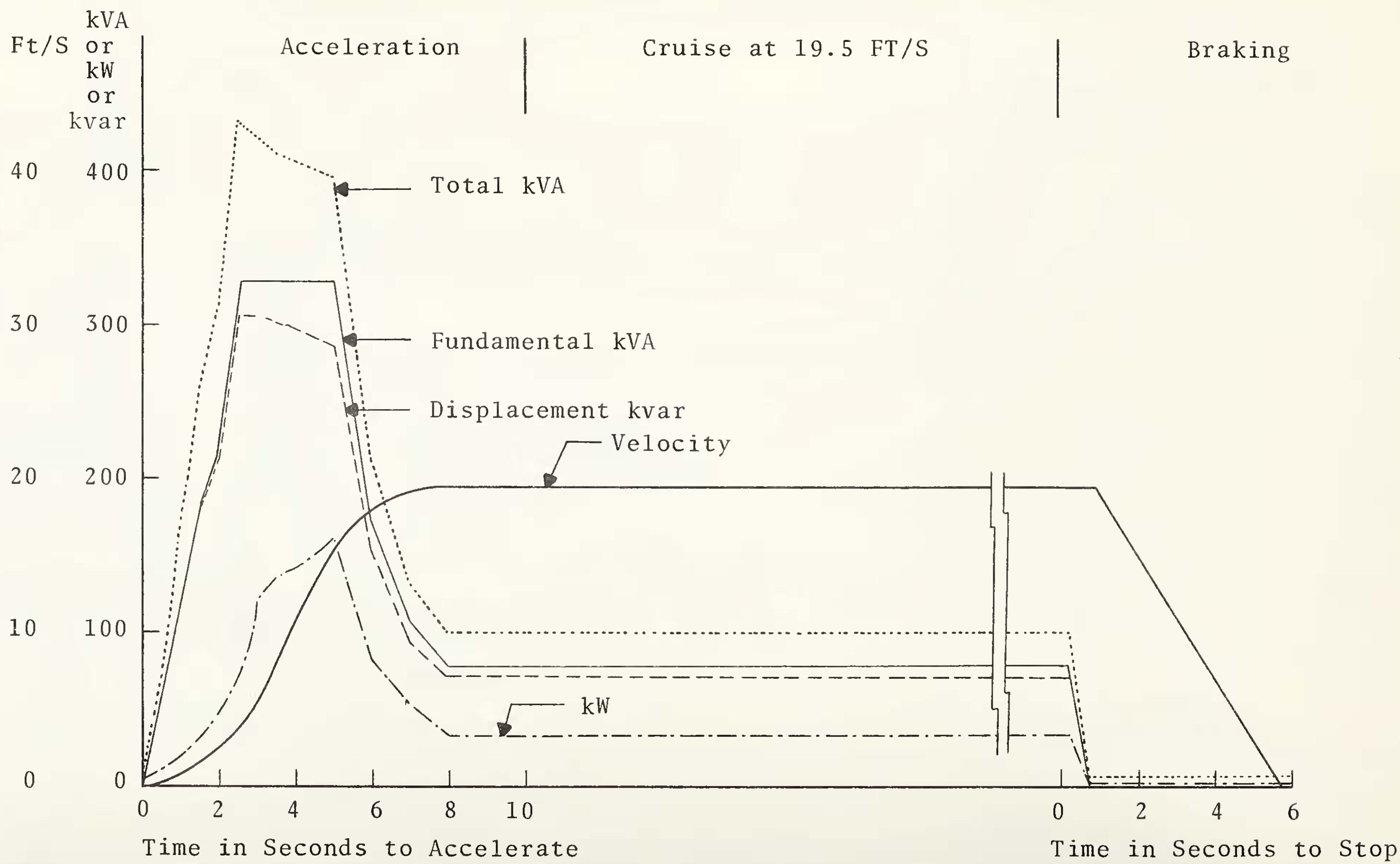


Figure 2-19 Bendix Dashaveyor Vehicle -- Vehicle Power for Acceleration, Cruise at 19.5 ft/s and Braking; Vehicle Weight 23,500 lbs; Level Rail; No Wind; 480 V L-L Rails

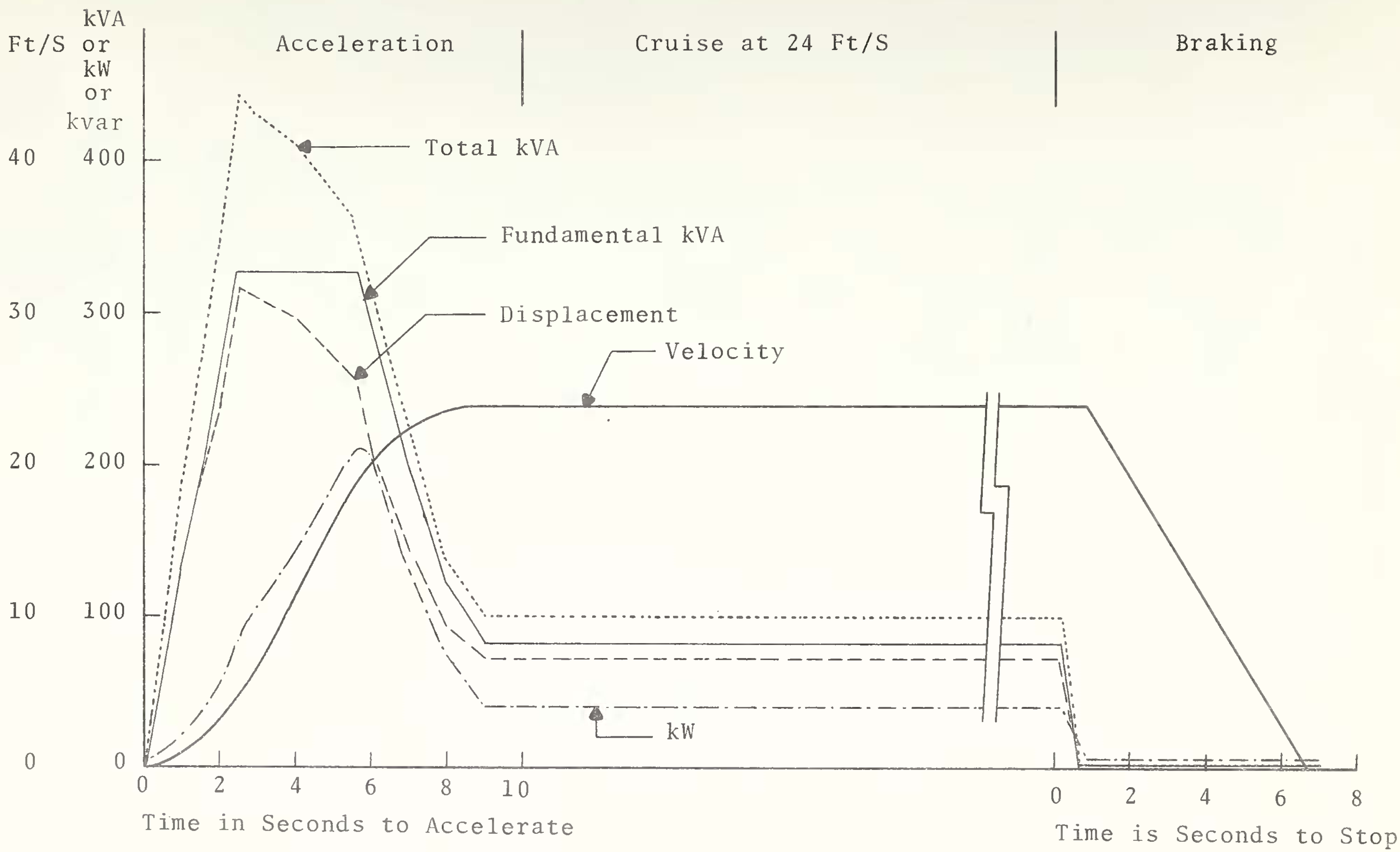


Figure 2-20 Bendix Dashaveyor Vehicle -- Vehicle Power for Acceleration, Cruise at 24 ft/s and Braking; Vehicle Weight 23,500 lbs; Level Rail; No Wind; 480 V L-L on Rails

# 3. FORD ACT VEHICLE

## 3.1 SYSTEM DESCRIPTION

The vehicle propulsion system consists of two identical subsystems symmetrically located at opposite ends of the vehicle. In each subsystem there is a solid driving axle with dual rubber tires, driven by an electric motor. Power for the vehicle is obtained from three-phase power rails providing 480 V line-to-line. A block diagram of the system is shown in Figure 3-1.

A dc shunt motor provides propulsion power in each subsystem. Each motor is connected to its drive axle through a chain drive transfer case with a speed reduction of 1.184:1, a drive shaft, and axle gearing with a speed reduction of 5.87:1. The motors have a nominal rating of 60 hp, 250 rpm at 480 V.

The armature of each motor is provided with dc propulsion power by a three-phase six-pulse thryistor, rectifier, operating directly from the 480-V bus in the vehicle. Each motor also has a separate rectifier to provide field power. Normal braking is obtained by reversing the direction of field current in the motors with armature current maintained in the same direction. Armature current is controlled to establish the braking torque produced in the motors. The dc voltage of the armature rectifier-inverter is controlled as necessary to maintain the desired torque. A system of mechanical brakes can be blended with the electrical braking, or can furnish emergency braking if the electrical system fails. Auxiliary equipment in the vehicle operates from the 480-V bus.

The specifications of the vehicle pertinent to the propulsion system are:

<u>Capacity</u>

| | |
|---|---|
| Curb Weight | 15,330 lbs. |
| Gross Weight | 19,650 lbs. |
| Number of Passengers | |
| Seated | 12 |
| Standing | 12 |

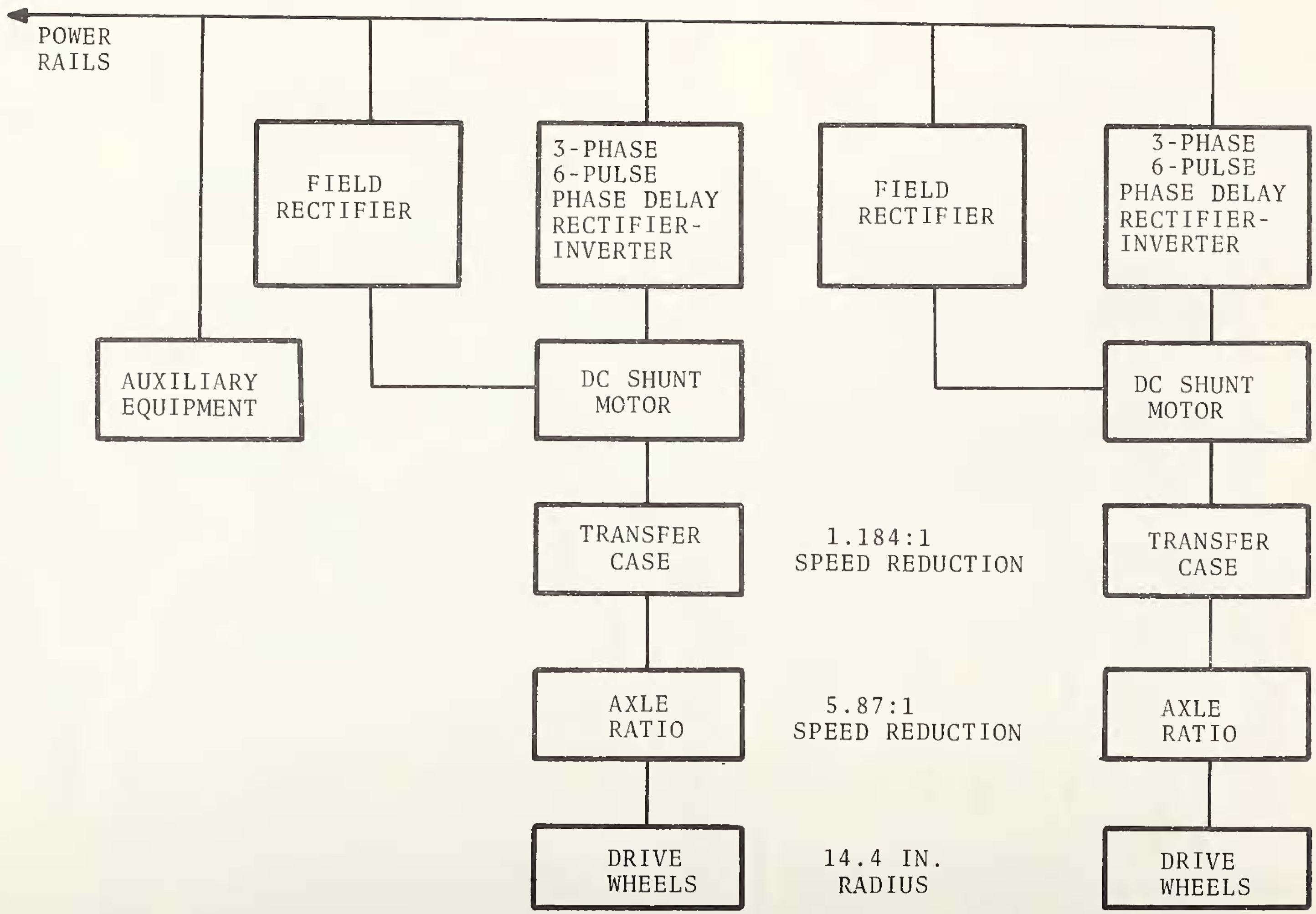


Figure 3-1 Ford ACT Vehicle Block Diagram

Dimensions

| | |
|---|---|
| Wheelbase | 205 in. |
| Overall Length | 316 in. |
| Height | 105 in. |
| Width | 80 in. |
| Tread | 63 in. |

## 3.2 PROPULSION SYSTEM ANALYSIS

During acceleration and cruise the propulsion system uses phase angle control in the rectifier-inverters to establish the correct armature voltages for the motors. This is similar to the phase angle control as discussed for the Bendix vehicle in Section 2 of this report. During braking at high vehicle speeds, the motors operate as generators absorbing the kinetic energy of the vehicle. The rectifier-inverters are operated with a phase angle delay greater than $90^{\circ}$ where they operate as inverters, and the regenerated power is returned to the power rails.

During braking of the vehicle at low speeds, the motors are plugged and power is drawn from the power rails to electrically brake the vehicle. The rectifier relationships developed in the previous section are valid for this vehicle, with the phase delay angle, being allowed to vary from 0 to $\pi$ radians; the rectifier-inverter characteristics are shown in Figure 3-2. This figure is similar to that of Figure 2-2 except that it has been extended to show the inverter region of operation.

In a dc shunt motor operated with constant field current, the torque is proportional to the armature current, and the induced voltage in the armature is proportional to motor speed. This produces a family of motor performance curves as shown in Figure 3-3 (Reference 3). Thus with constant field current performance of the motors can be defined by the following formulas:

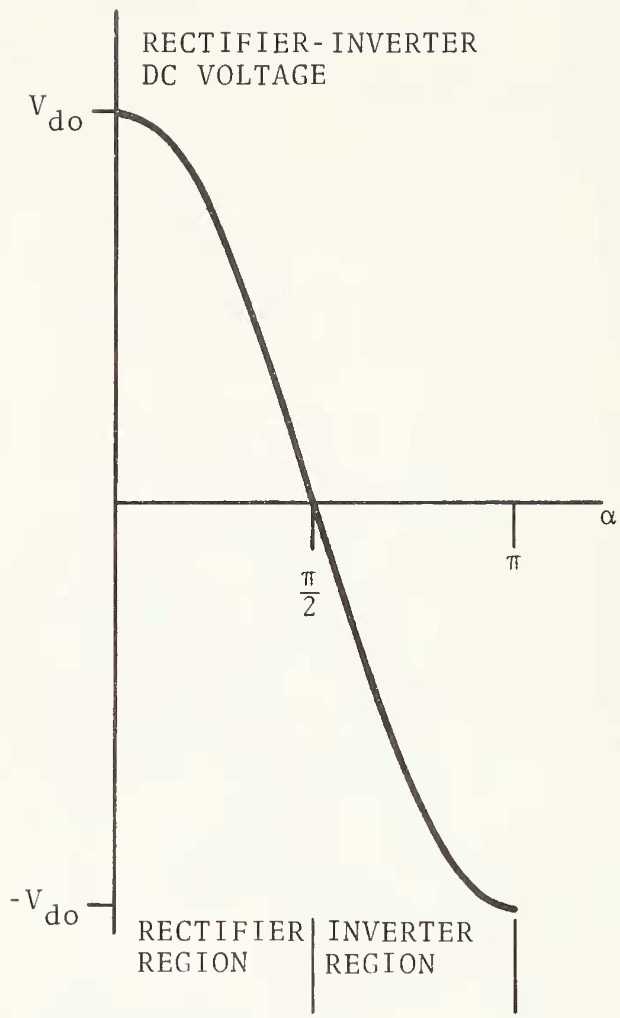


Figure 3-2 Rectifier-Inverter DC Voltage vs. Firing Angle $\alpha$

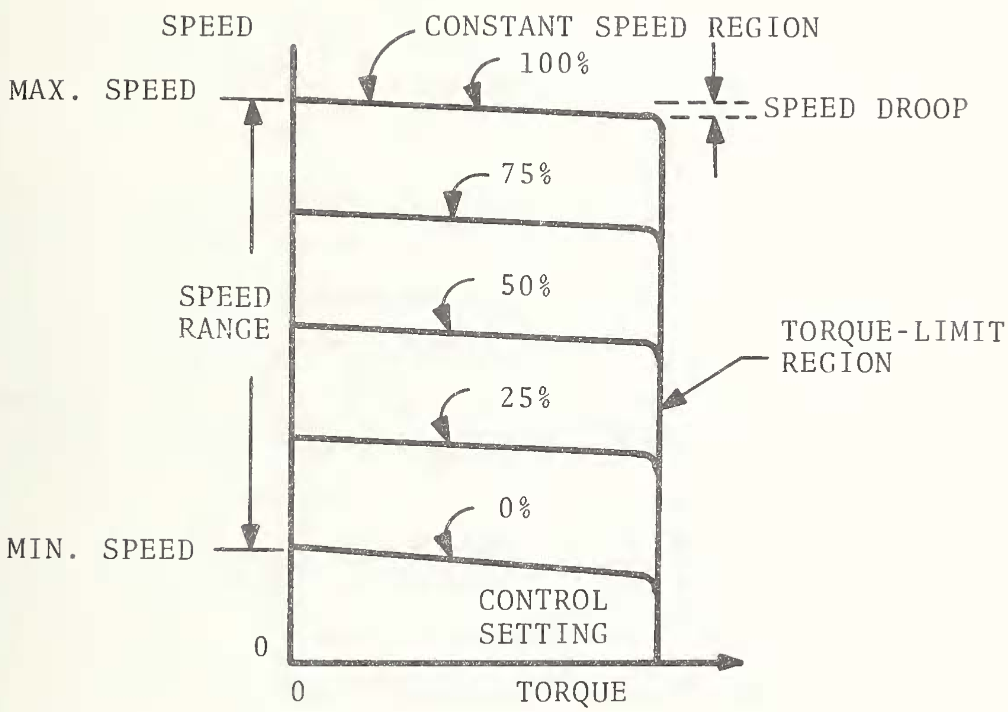


Figure 3-3 Speed-Torque Characteristics of Adjustable Speed Drive

$$T_M = k_T I_A$$

$$\left.\begin{aligned} E_A &= (k_V \text{ x vehicle velocity}) + I_A R_A \text{ or} \\ E_A &= (k_{V'} \text{ x motor rpm}) + I_A R_A \end{aligned}\right\} \text{when motoring}$$

and

$$\left.\begin{aligned} E_A &= (k_V \text{ x vehicle velocity}) - I_A R_A \text{ or} \\ E_A &= (k_{V'} \text{ x motor rpm}) - I_A R_A \end{aligned}\right\} \text{when braking}$$

where

$T_M$ = the torque produced in the motor

$E_A$ = the voltage at the armature terminals

$I_A$ = the armature current

and

$R_A$ = the resistance of the armature circuit

$k_T$, $k_V$, $k_{V'}$ = motor constants

When a vehicle is accelerating, the motors must produce enough torque to accelerate the vehicle, accelerate the rotating parts of the propulsion system, and overcome friction losses such as those in the propulsion system, vehicle rolling friction, drag on the power collector and aerodynamic drag. When the vehicle is decelerating the friction losses assist the motor in stopping the vehicle. Thus:

$$T_A = T_M - T_D \text{ during acceleration}$$

and

$$T_B = T_M + T_D \text{ during braking}$$

where

$T_A$ = the net torque producing acceleration

$T_B$ = the net torque producing deceleration

and

$T_D$ = the torque equivalent of all friction losses

Additionally, we may state

$$T_M = T_D \text{ during constant speed cruise}$$

The test data from the Post-Transpo® '72 Test Program from which this section was prepared were recorded on October 26, 1972 on magnetic tape 33712 during test runs 34 through 46. During these runs the wieght of the vehicle was 16,730 lbs. Each run consisted of two tests, one northbound and one southbound. In each direction the vehicle was accelerated to a planned speed, and stopped using only the electrical braking. No differences in performance in the opposite directions could be detected in the data. At the lowest speed a short period of cruising at the planned speed was possible within the length of guideway available. At higher speeds steady state cruising was not possible. Data was taken from the recorded data tracks showing velocity, motor armature currents, motor armature voltages, and torque command.

## 3.3 PROPULSION SYSTEM PERFORMANCE

Using the data described above, the performance of each motor for operation at three programmed speeds is shown in Figures 3-4, 3-5, and 3-6. For each speed the curves show the performance of one motor during acceleration, cruise at the programmed speed, and braking to a stop without using the mechanical brakes. An expanded time scale has been used in the figures during the braking to show performance of the motors (as generators) more clearly.

The recordings made during the testing show that, typically, the armature current of the motors increases over an interval of about 2.8 seconds before reaching 220 Amperes at which value the current is limited until the vehicle has accelerated to planned speed. The current is then reduced over a period of 2 to 3 seconds and stabilizes at the correct value for cruising. Similar current limiting at 220 Amperes occurs during braking.

Using the formulas as above, the proportion of available torque used for acceleration was determined. The time scale during current limited acceleration was corrected to the value which would be obtained with a full load vehicle weight of 19,650 lbs.

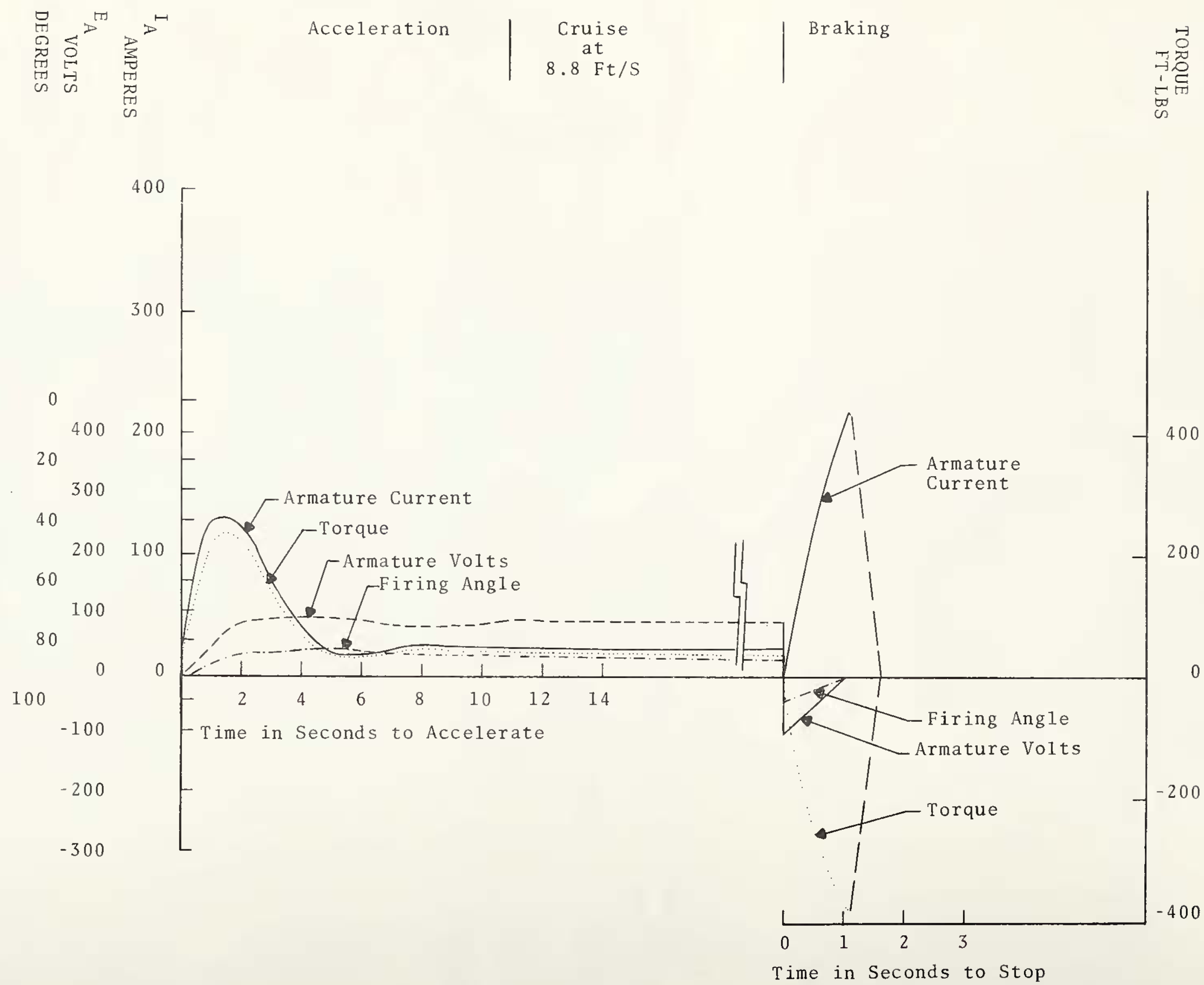


Figure 3-4 Ford ACT Vehicle -- Motor Performance for Acceleration, Cruise at 8.8 ft/s and Braking; Vehicle Weight 19,650 lbs; Level Rail; No Wind; 480 V L-L on Rails

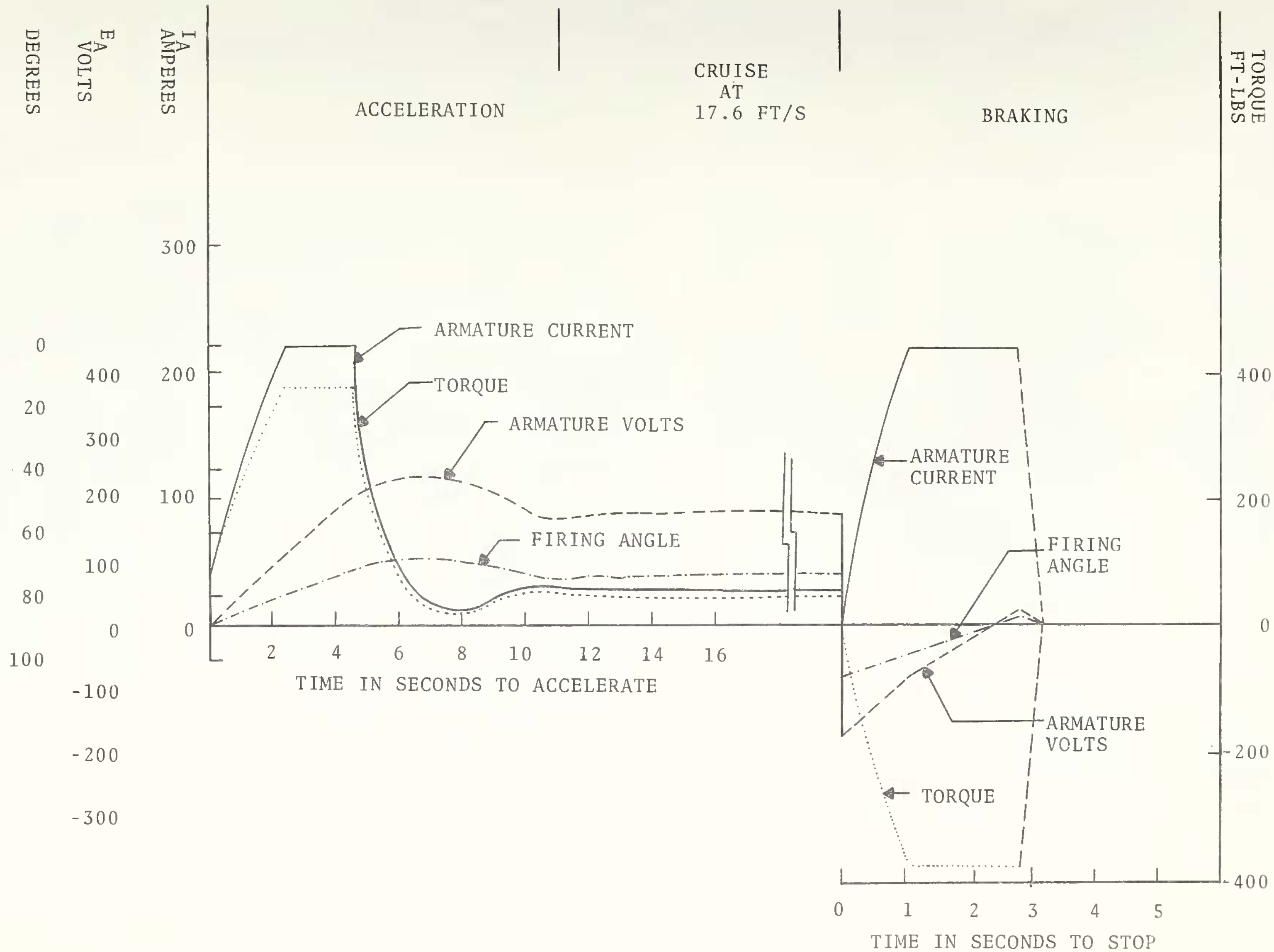


Figure 3-5 Ford ACT Vehicle -- Motor Performance for Acceleration, Cruise at 17.6 ft/s and Braking; Vehicle Weight 19,650 lbs; Level Rail; No Wind; 480 V L-L on Rails

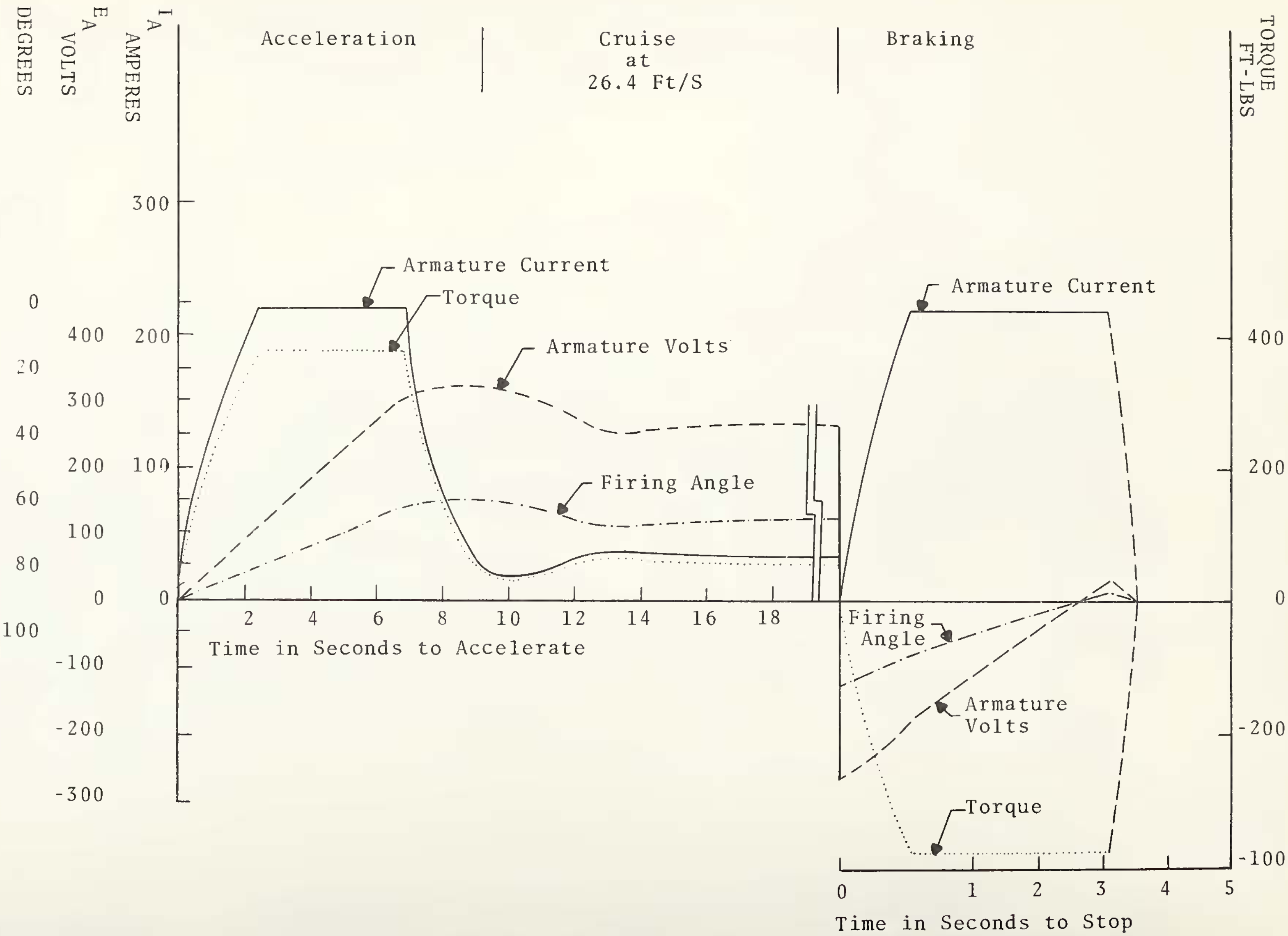


Figure 3-6 Ford ACT Vehicle, Motor Performance for Acceleration, Cruise at 26.4 ft/s and Braking; Vehicle Weight 19,650 lbs; Level Rail; No Wind; 480 V L-L on Rails

The values of $k_T$ and $k_V$ were determined from data on the charts. Motor torque and armature voltage were calculated from the measured values of armature current. The firing angle delay in the rectifier was calculated using the method described for the Dashaveyor Vehicle.

The values of $T_D$ were determined as described above to establish required power during steady state cruise conditions where none was recorded. The complete transient after accelerating to the programmed speed was derived from the tests at the lowest speeds to supplement that part of the transient shown in the recorded data.

During braking each motor is operated as a generator feeding power to the rectifier-inverter, until the vehicle speed is too low to generate a voltage capable of maintaining the armature current. At the lower speeds the motors are plugged, using power from the rectifier-inverter.

## 3.4 PROPULSION SYSTEM POWER REQUIREMENTS

The equations shown for the Dashaveyor vehicle were employed to calculate real power, fundamental reactive power and distortion power for the armature. The real power and fundamental reactive power required for the field circuit were added to the corresponding components to determine propulsion power during acceleration and cruise. During braking the power characteristics on the ac side of the inverter were calculated using the same equations as used for the Dashaveyor vehicle. These are valid for values of firing angle delay greater than $90^{\circ}$ giving a negative value of $\cos \alpha$ indicating a return of power to the ac bus in the vehicle.

The nonsinusoidal currents which flow during inverter operation of the thyristor circuits produce harmonic currents similar to those produced during rectifier operation. No record could be found of a study of the magnitude of the harmonics produced in an inverter. It is noted that for a firing angle delay of $90^{\circ} + \Delta$, the waveshape of current is the mirror image of the waveshape of $90^{\circ} - \Delta$. Since this is so, the ratios of harmonic currents to fundamental current reported by Wlodyka, Abbas and Ploetz (Reference 5) are believed to be valid for delay angles exceeding 90°. The value of $M = I_T/I_1$ discussed in Appendix A has been used to determine total kVA during inverter operation. The power characteristics of the propulsion equipment are shown in Figures 3-7, 3-8 and 3-9.

## 3.5 VEHICLE POWER REQUIREMENTS

The auxiliary loads in the vehicle will have a changing power demand as various equipments operate. For purposes of this section it was assumed the auxiliary equipment produced a constant load of 12.4 kW, 6.3 kvar (lagging) balanced on the three phases. This load was added to the propulsion load during acceleration and cruise. At high speed during braking, the propulsion system generates more power than the auxiliary equipment requires. The excess is returned to the power rails. Figures 3-10, 3-11 and 3-12 show these power requirements for the three programmed speeds.

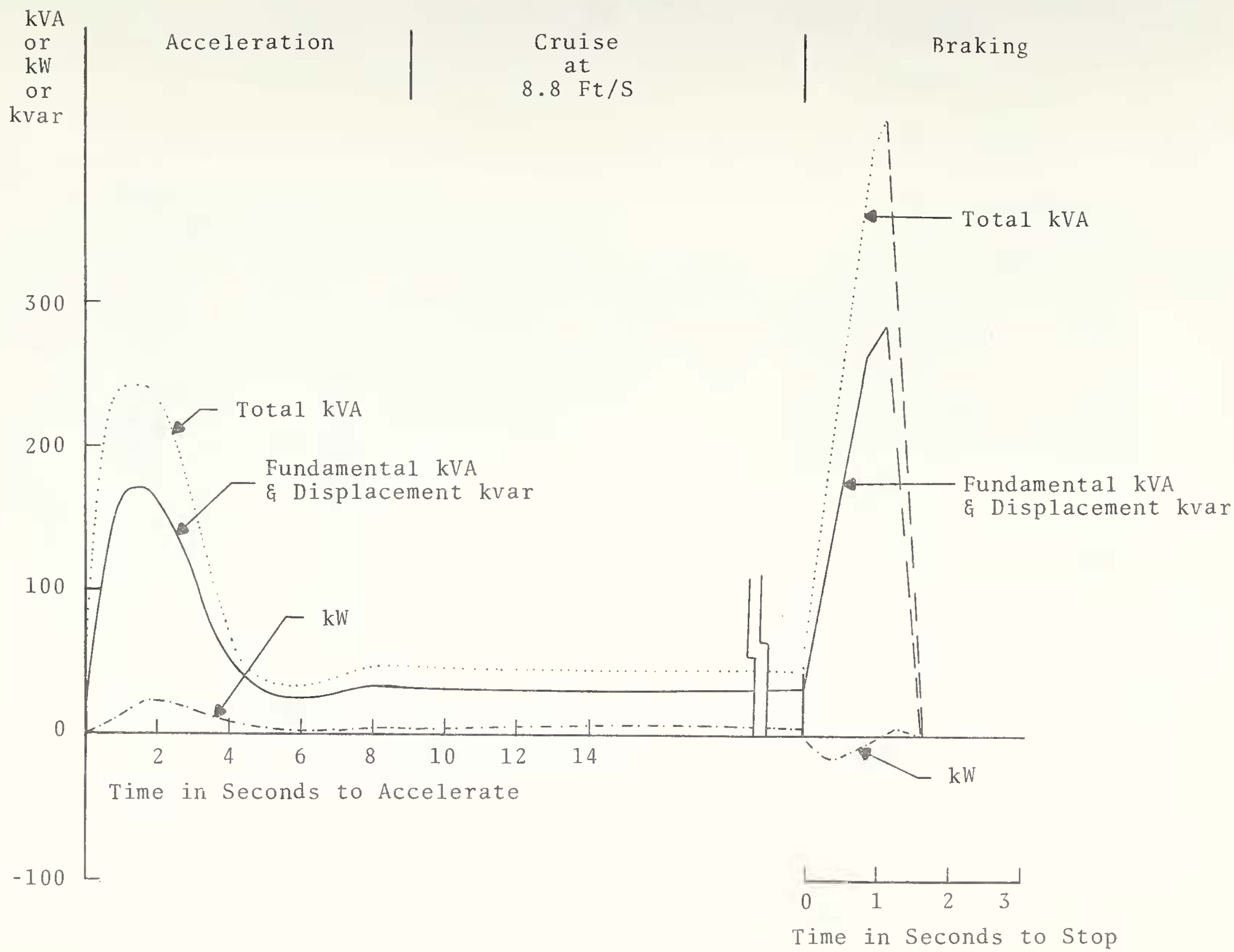


Figure 3-7 Ford ACT Vehicle -- Propulsion Power for Acceleration, Cruise at 8.8 ft/s and Braking; Vehicle Weight 19,650 lbs; Level Rail; No Wind; 480 V L-L on Rails

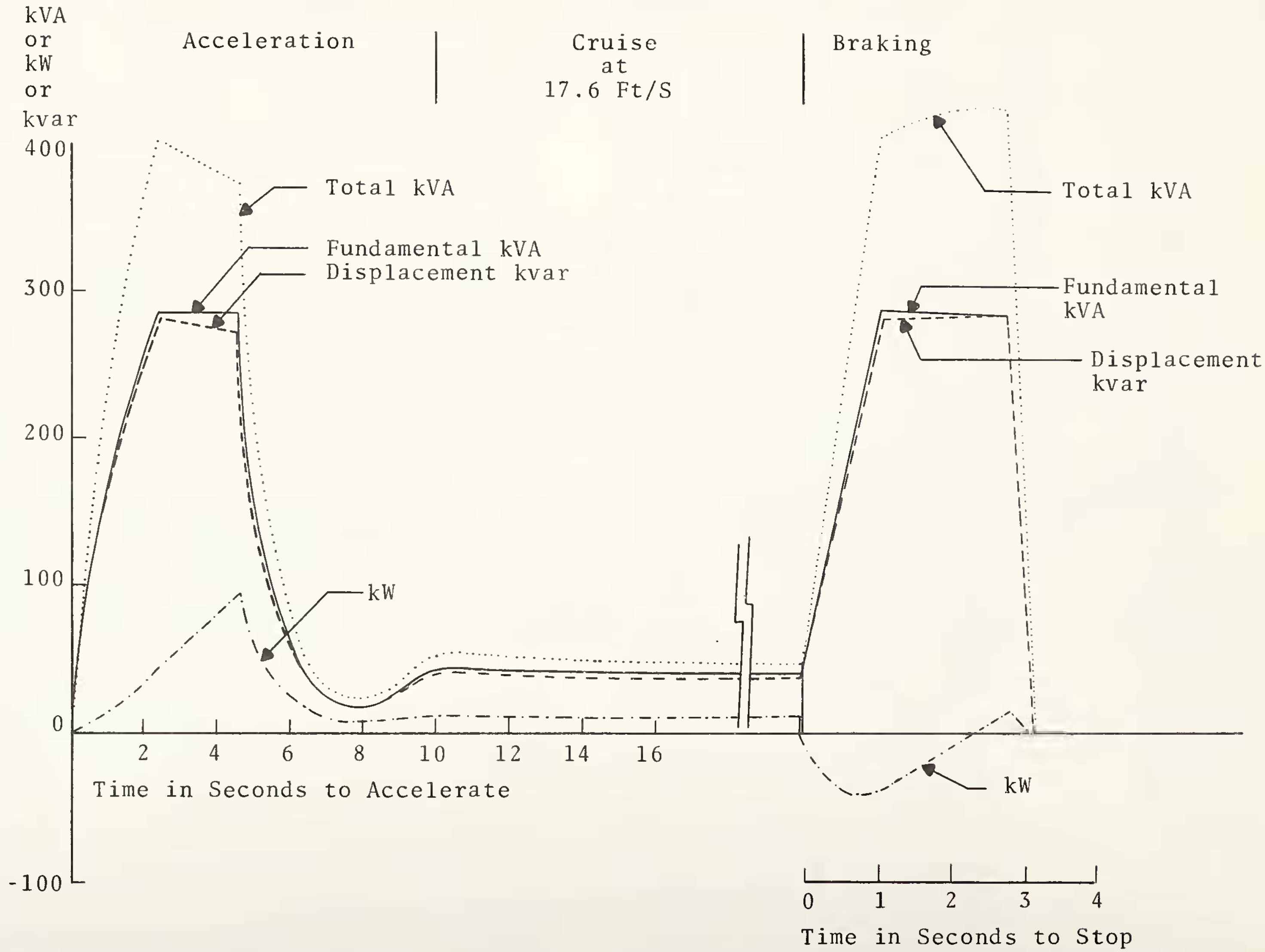


Figure 3-8 Ford ACT Vehicle -- Propulsion Power for Acceleration, Cruise at 17.6 ft/s and Braking; Vehicle Weight 19,650 lbs; Level Rail; No Wind; 480 V L-L on Rails

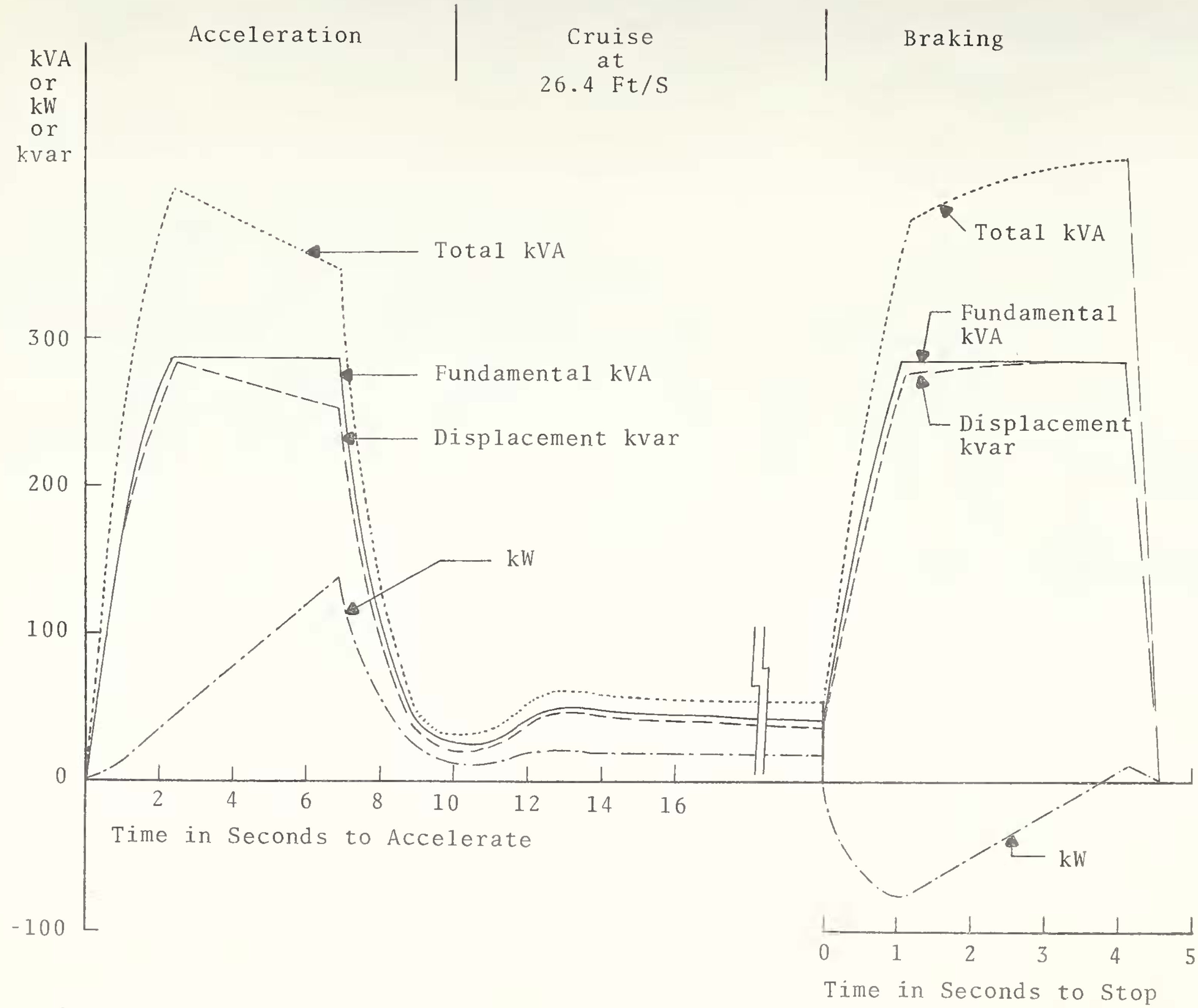


Figure 3-9 Ford ACT Vehicle -- Propulsion Power for Acceleration, Cruise at 26.4 ft/s and Braking; Vehicle Weight 19,650 lbs; Level Rail; No Wind; 480 V L-L on Rails

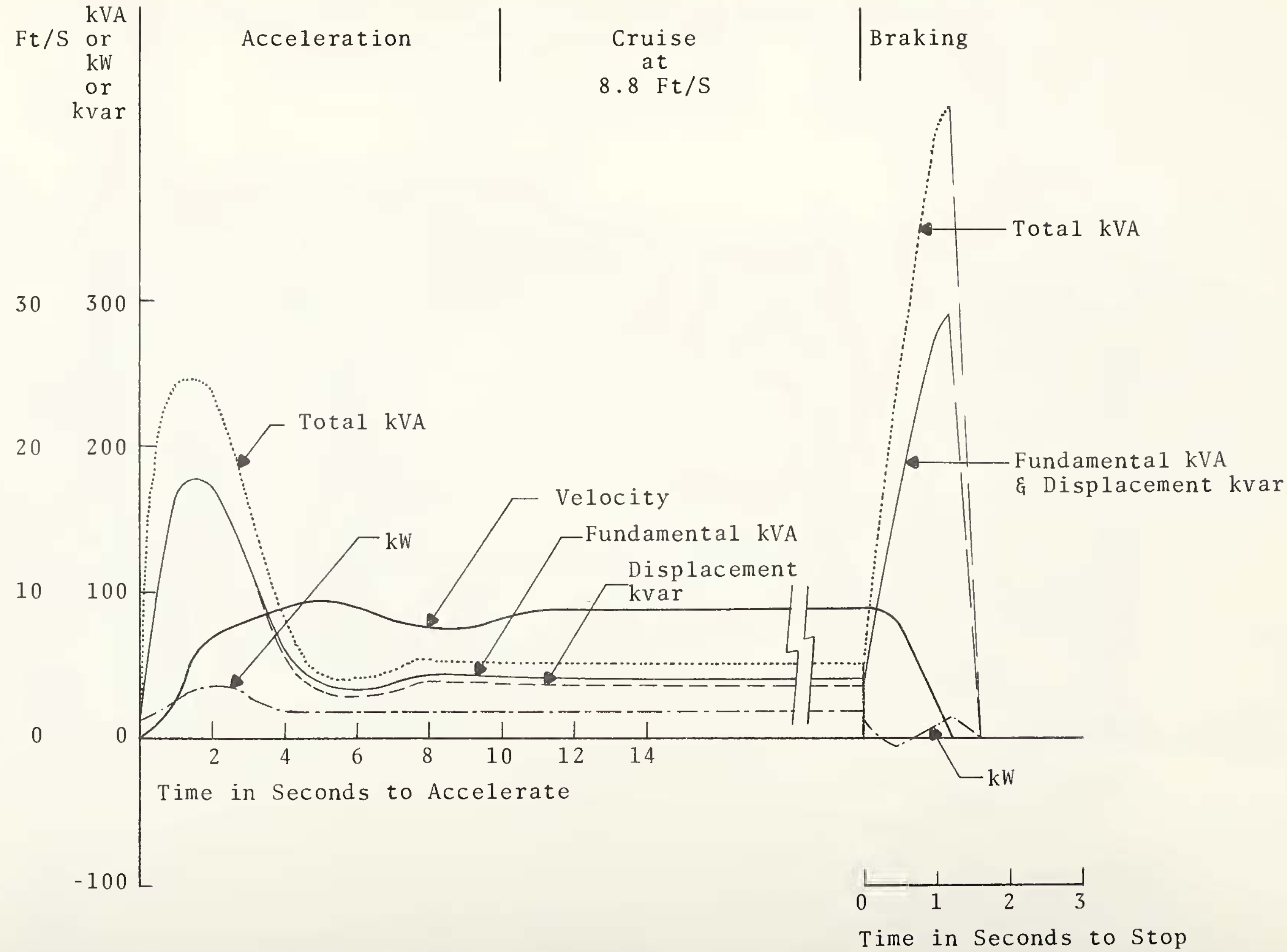


Figure 3-10 Ford ACT Vehicle -- Vehicle Power for Acceleration, Cruise at 8.8 ft/s and Braking; Vehicle Weight 19,650 lbs; Level Rail; No Wind; 480 V L-L on Rails

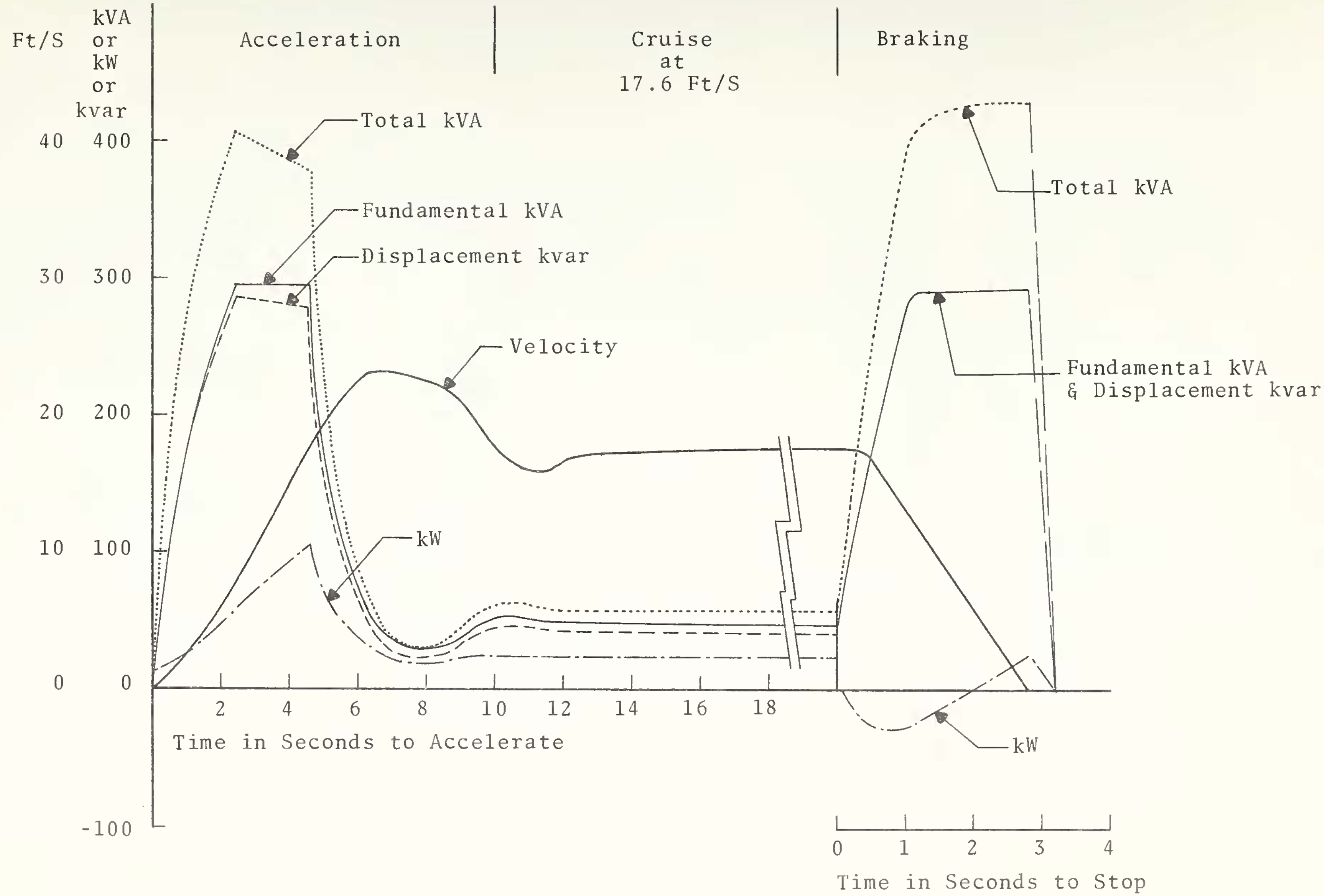


Figure 3-11 Ford ACT Vehicle -- Vehicle Power for Acceleration, Cruise at 17.6 ft/s and Braking; Vehicle Weight 19,650 lbs; Level Rail; No Wind; 480 V L-L on Rails

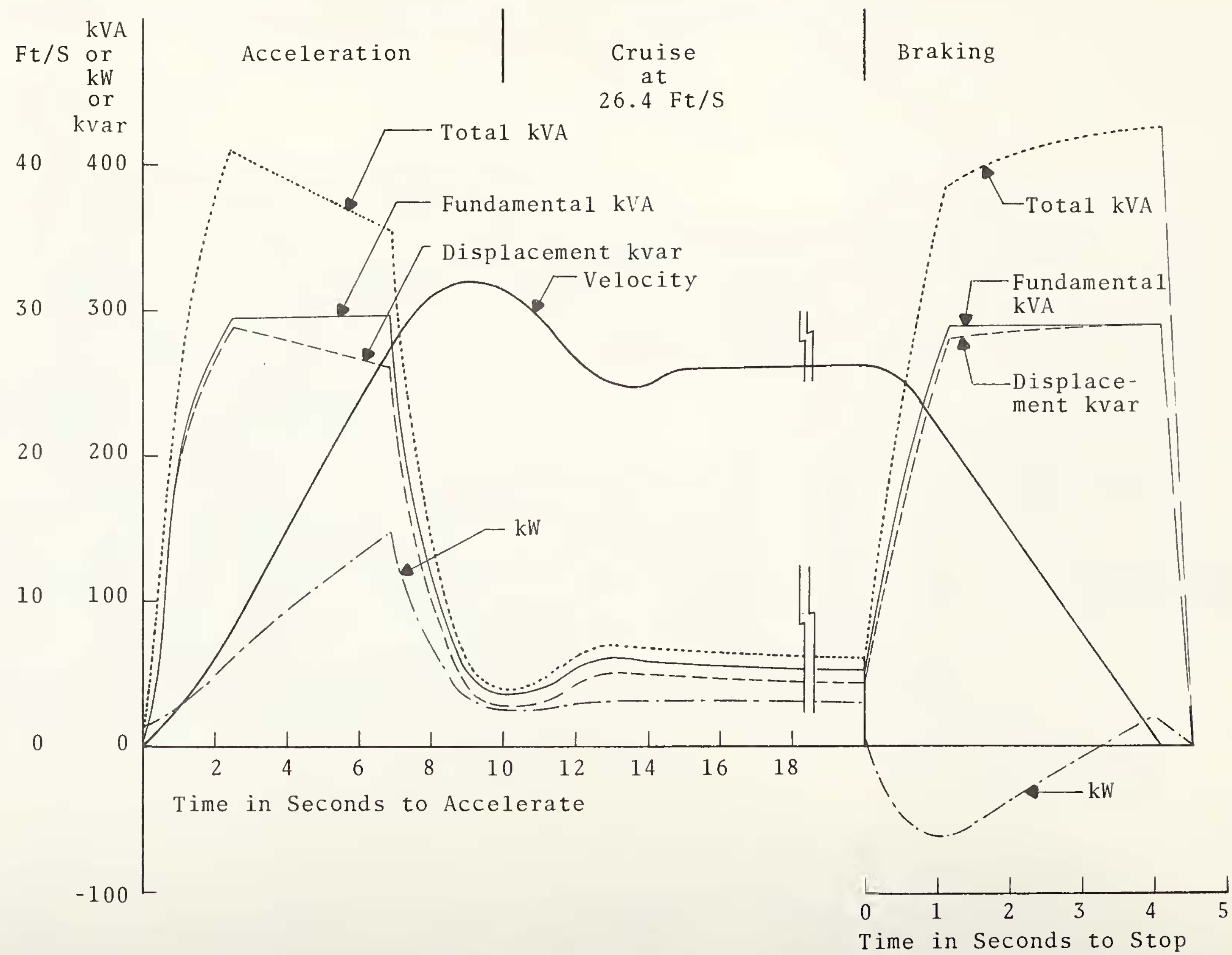


Figure 3-12 Ford ACT Vehicle -- Vehicle Power for Acceleration, Cruise at 26.4 ft/s and Braking; Vehicle Weight 19,650 lbs; Level Rail; No Wind; 480 V L-L on Rails

# 4. MONOCAB VEHICLE

## 4.1 SYSTEM DESCRIPTION

The vehicle is suspended from two single-axle, rubber-tired bogies running within an overhead guideway. One bogie contains a dc motor which propels the vehicle and provides normal braking by operating regeneratively. Power for the vehicle is obtained from three-phase power rails providing 480 V line-to-line. A block diagram of the electrical system is shown in Figure 4-1.

The motor providing propulsion power in the powered bogie is a dc shunt motor with a base rating of 40 hp, 2500 rpm at 500 V dc. The motor is connected to the wheels through a speed reduction ratio of 5.38:1.

A three-phase, thyristor six-pulse rectifier operating directly from the three-phase power rails provides dc armature power. A separate thyristor rectifier provides power for the shunt field coils for the motor which are operated at constant current. Auxiliary equipment in the vehicle operates from the three-phase, 480-V bus.

Normal braking is provided by reversing the connections between the rectifier-inverter and the armature and operating the thyristor rectifier-inverter as an inverter, returning power to the power rails. Mechanical brakes are provided for emergency use on both bogies.

The specifications of the vehicle pertinent to the propulsion system are:

<u>Capacity</u>

| | |
|---|---|
| Empty Weight | 4400 lbs |
| Gross Weight | 5420 lbs |
| Number of Passengers | |
| Seated | 6 |
| Standing | 0 |

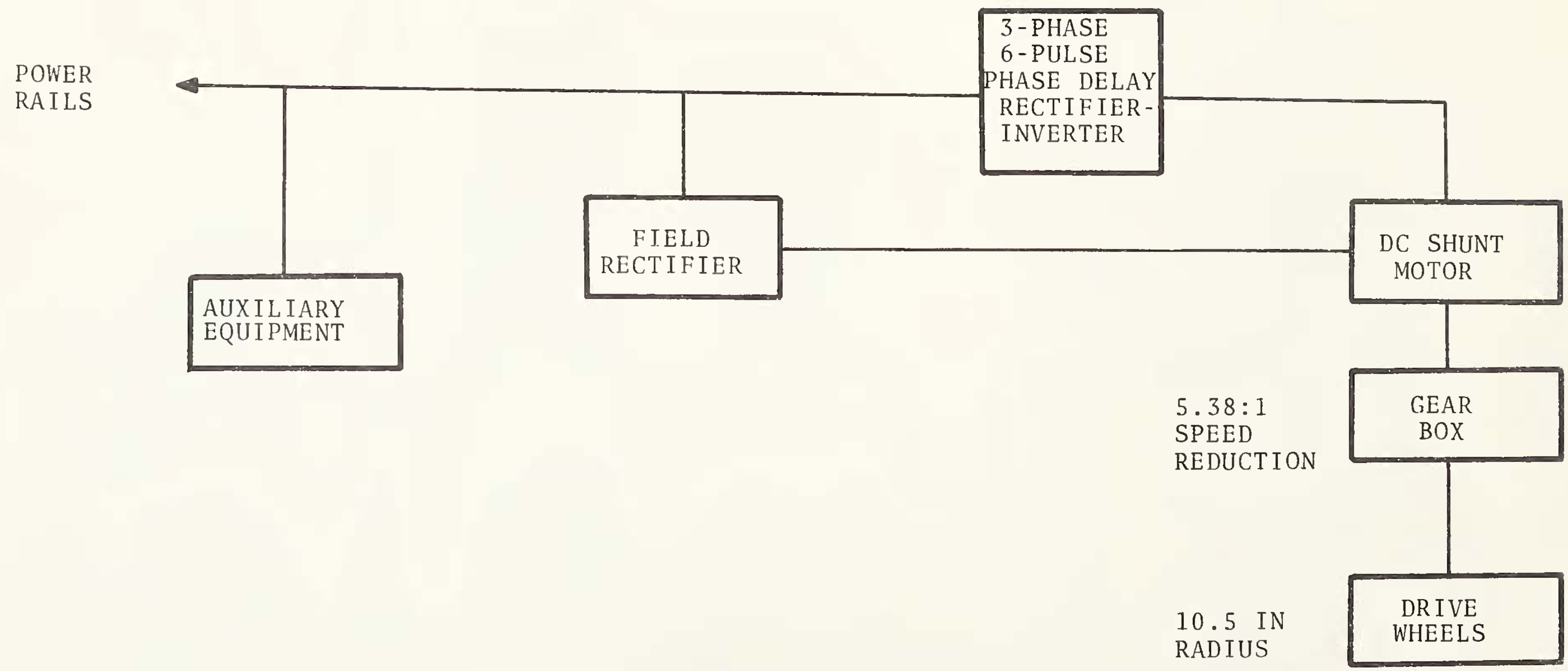


Figure 4-1 Monocab Vehicle Block Diagram

Dimensions

| | |
|---|---|
| Overall Length | 115 in. |
| Height | 80 in. |
| Width | 66 in. |

## 4.2 PROPULSION SYSTEM ANALYSIS

During acceleration and cruise the propulsion system uses phase angle control in the rectifier-inverter to establish the correct armature voltage for the motor. During braking, the motor operates as a generator and the regenerated power is returned to the power rails through the rectifier-inverter. The operation of the rectifier-inverter uses the same principles described in Section 3 for the Ford ACT vehicle.

Operation of the shunt motor is similar to that described in Section 3 for the Ford ACT vehicle. The motor is a NEMA Frame 288 size machine with a base rating of 40 hp, 2500 rpm at 500 Vdc, and an armature current of 64.7 A. The shunt field has a resistance of 55.4 $\Omega$ at 40$^{\circ}$C and draws a current of 3.1 A at base speed. The armature circuit has a total resistance of 0.29 $\Omega$ of which 0.22 $\Omega$ is in the armature and 0.07 $\Omega$ is in the commutating field. The NEMA data for a Frame 288 shunt motor was utilized to determine the torque per ampere of armature current from the base speed operating conditions. Since the motor is operated at constant field current, this value is valid for all operating conditions.

The basic data from which the performance curves are derived comes from magnetic tape 33775 on which vehicle performance parameters were recorded during tests run on November 8, 1972 with the vehicle loaded to 5420 lbs gross weight. The data reviewed in preparation of this section came from Runs 67 through 93 which were conducted primarily to test normal braking. Each run consisted of accelerating to the desired speed, a very short period of cruising at that speed, and application of the normal brakes. Some runs were made in each direction. No differences in performance due to direction are shown in the data. Data were taken from the tracks showing vehicle velocity, armature current and armature voltage.

The method of preparing motor performance curves was similar to that used on the Ford ACT vehicle, i.e., the motor-induced voltage as a function of speed was determined from intervals in the test data during which the vehicle was coasting. This provided data for calculating armature voltage using the velocity and armature current tracks during intervals the recorded data on armature voltage was unusable. The remaining motor performance curves were calculated as described for the Ford ACT vehicle.

## 4.3 PROPULSION SYSTEM PERFORMANCE

Using the data described above, the performance of the propulsion motor is shown in Figures 4-2 through 4-5 inclusive. For each speed the curves show the performance of the motor during acceleration, cruise at the selected speed, and braking to a stop from that speed. The time scale during braking has been expanded to show more detail.

In these curves, armature current came from the test data from the Post-Transpo® '72 Test Program. During acceleration and during braking the armature current is limited at 120 amps. When the vehicle is first started or when braking is first applied the current builds quickly to a value of about 180 amps for about 0.5 seconds before the current limiting becomes effective. This produces high torques and high power demands as shown in the various performance curves.

Armature voltage was calculated from the velocity and armature current data from the test program. Motor torque was calculated from the NEMA motor data at base speed and the armature current data from the test program. The firing angle delay in the rectifier was calculated from the ratio of required output voltage to maximum output voltage of the rectifier with 480 V on the rails.

## 4.4 PROPULSION SYSTEM POWER REQUIREMENTS

The method of calculating propulsion system power requirements was identical to that used to calculate propulsion system power for the Ford ACT vehicle, i.e., calculate real power,

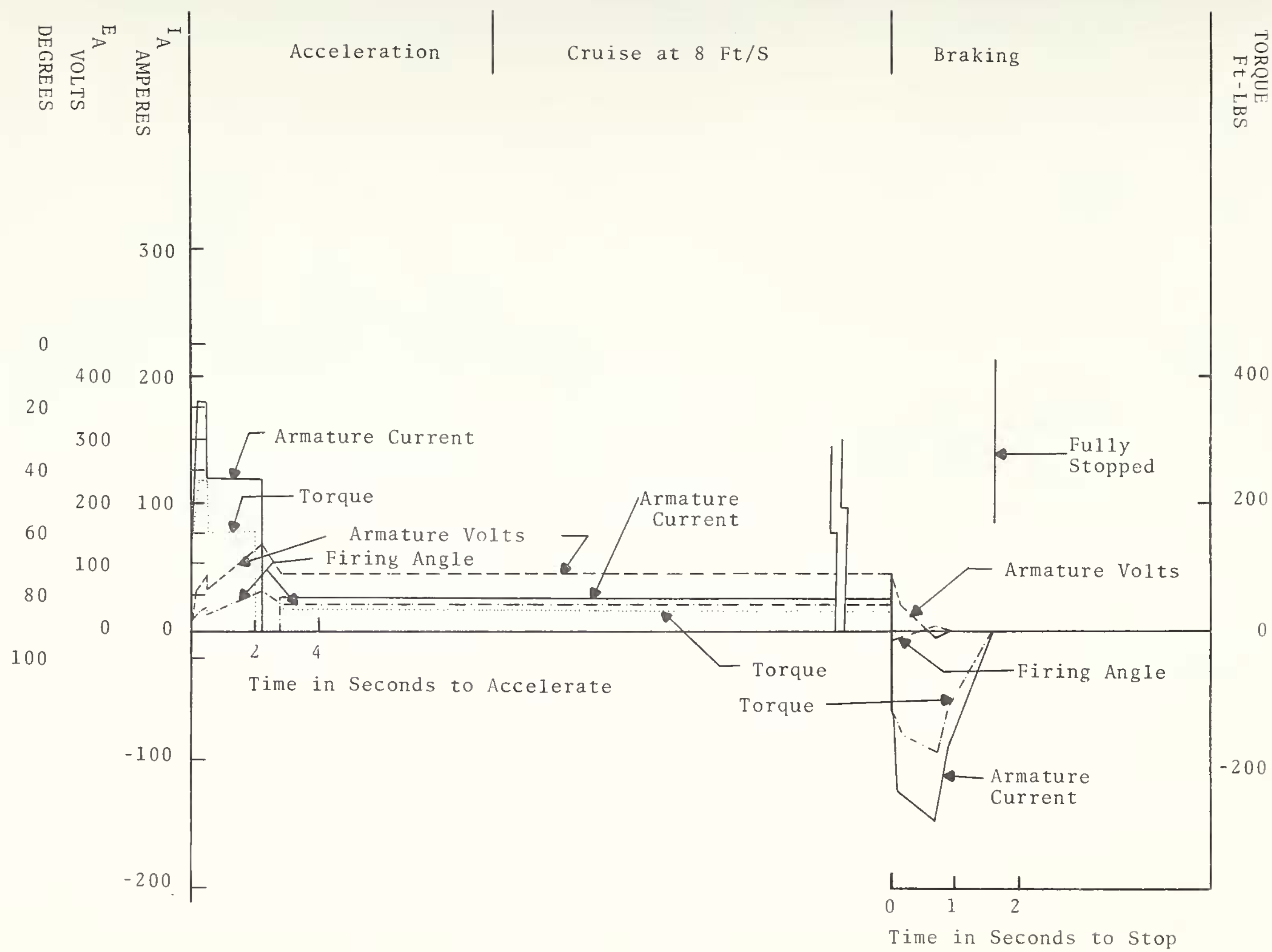


Figure 4-2 Monocab Vehicle -- Motor Performance for Acceleration, Cruise at 8 ft/s and Braking; Vehicle Weight 5,420 lbs; Level Rail; No Wind; 480 V L-L on Rails

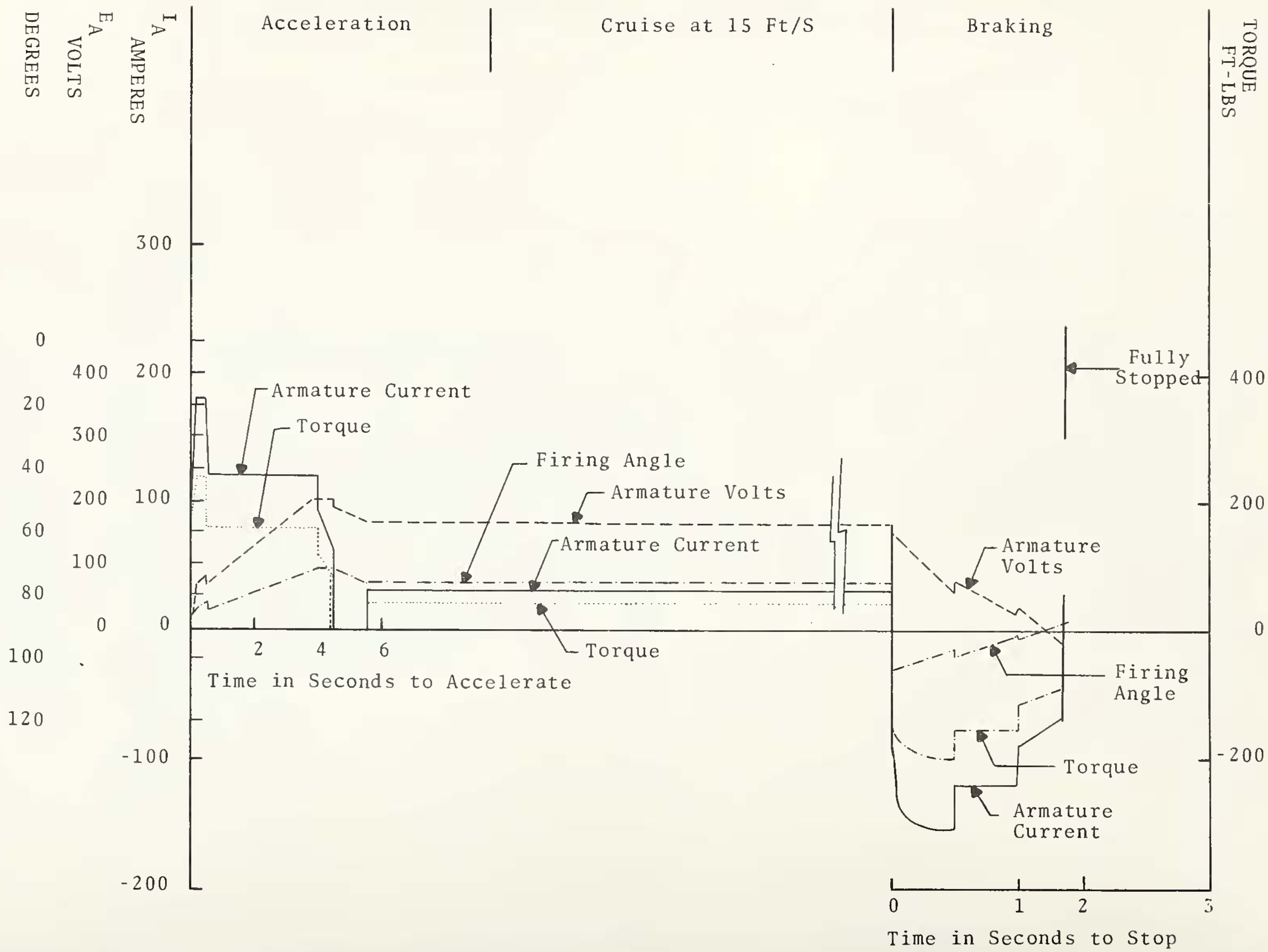


Figure 4-3 Monocab Vehicle -- Motor Performance for Acceleration, Cruise at 15 ft/s and Braking; Vehicle Weight 5,420 lbs; Level Rail; No Wind; 480 V L-L on Rails

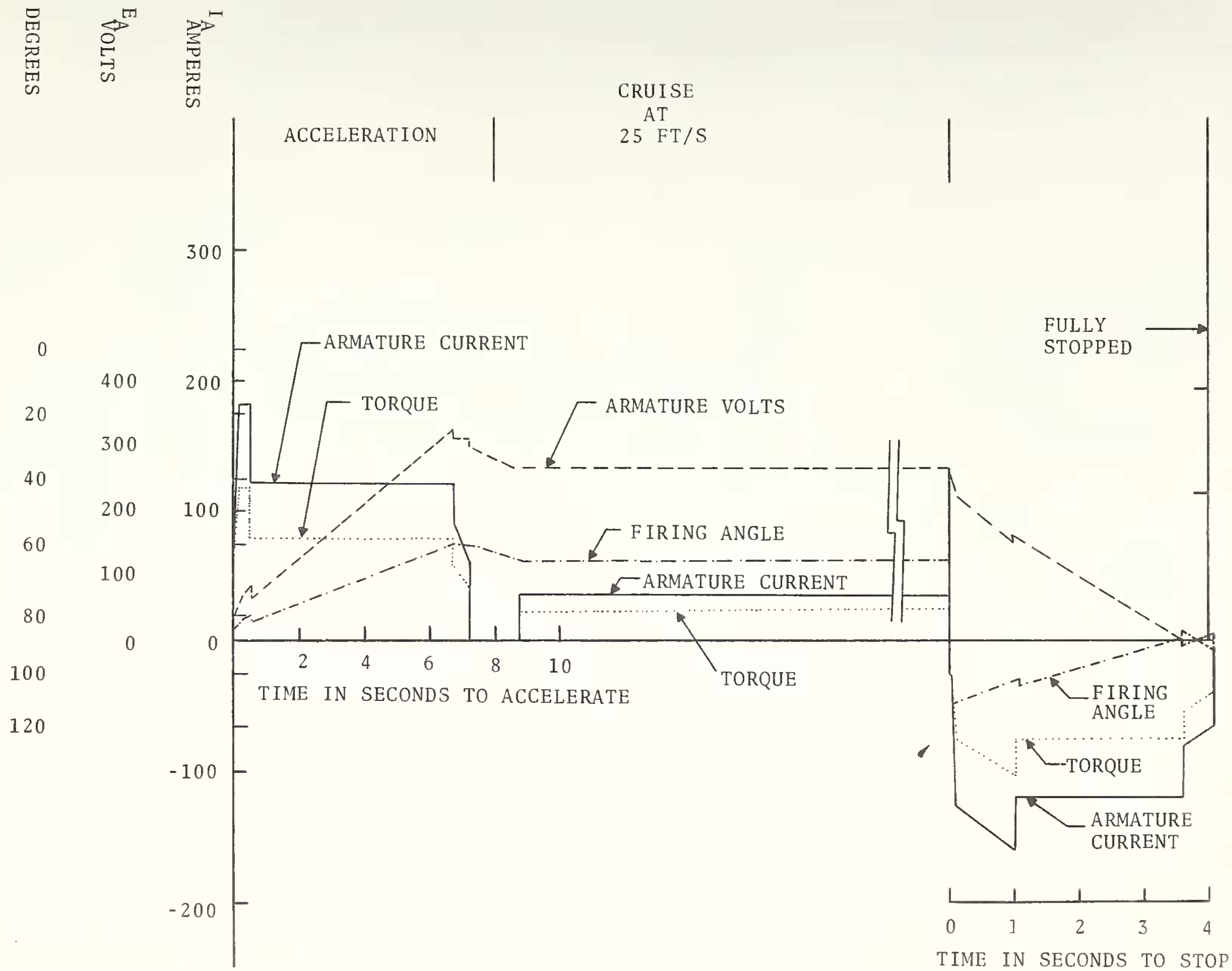


Figure 4-4 Monocab Vehicle -- Motor Performance for Acceleration, Cruise at 25 ft/s and Braking; Vehicle Weight 5,420 lbs; Level Rail; No Wind; 480 V L-L on Rails

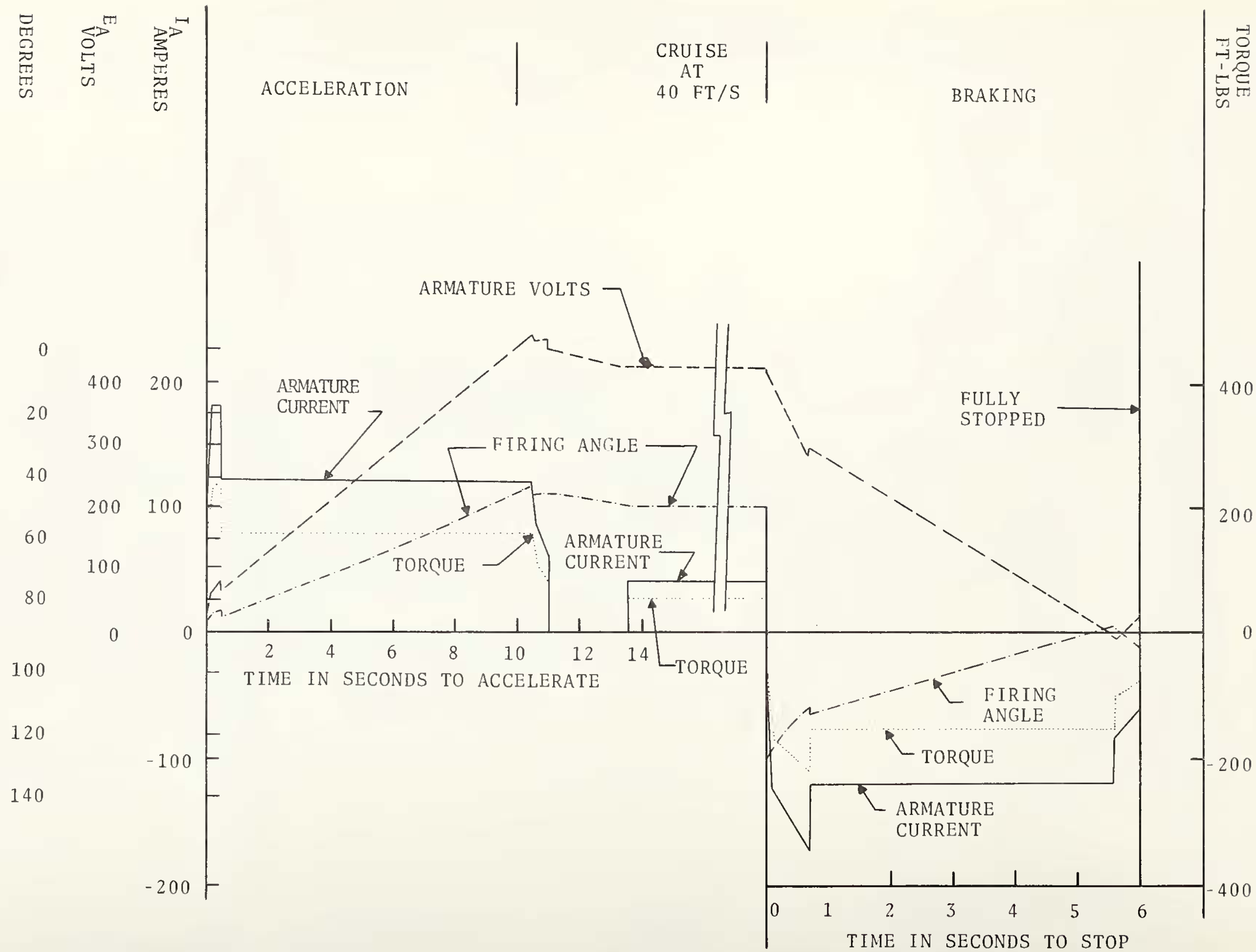


Figure 4-5 Monocab Vehicle -- Motor Performance for Acceleration, Cruise at 40 ft/s and Braking; Vehicle Weight 5,420 lbs; Level Rail; No Wind; 480 V L-L on Rails

displacement reactive power and distortion power for the armature. Real power and displacement reactive power for the field rectifier were added to the corresponding components for the armature to get total propulsion power.

The propulsion system power characteristics were calculated for the four programmed speeds. These power characteristics are shown in Figures 4-6 through 4-9 inclusive. When the braking occurs the motors act as generators and supply power through the rectifier-inverter to the 480-V bus on the vehicle; this generated power is shown in each chart.

## 4.5 VEHICLE POWER REQUIREMENTS

Auxiliary power consisting of 6.4 kW and 3.4 kvar (lagging) evenly divided on the three phases was assumed in calculating total power demand for the vehicle. These calculations were made as described for the Bendix Dashaveyor Vehicle. The results are shown in Figures 4-10 through 4-13 inclusive.

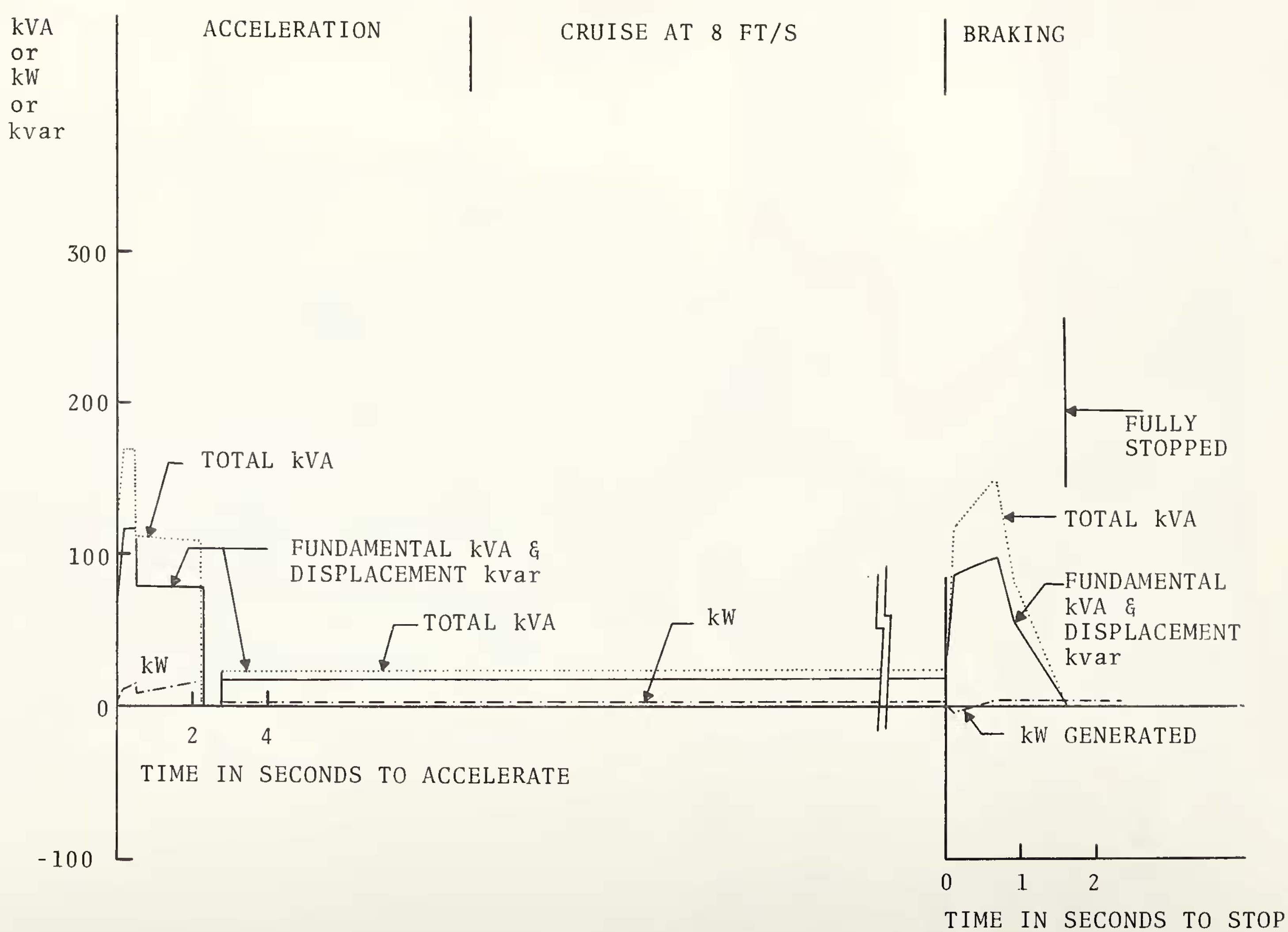


Figure 4-6 Monocab Vehicle -- Propulsion Power for Acceleration, Cruise at 8 ft/s and Braking; Vehicle Weight 5,420 lbs; Level Rail; No Wind; 480 V L-L on Rails

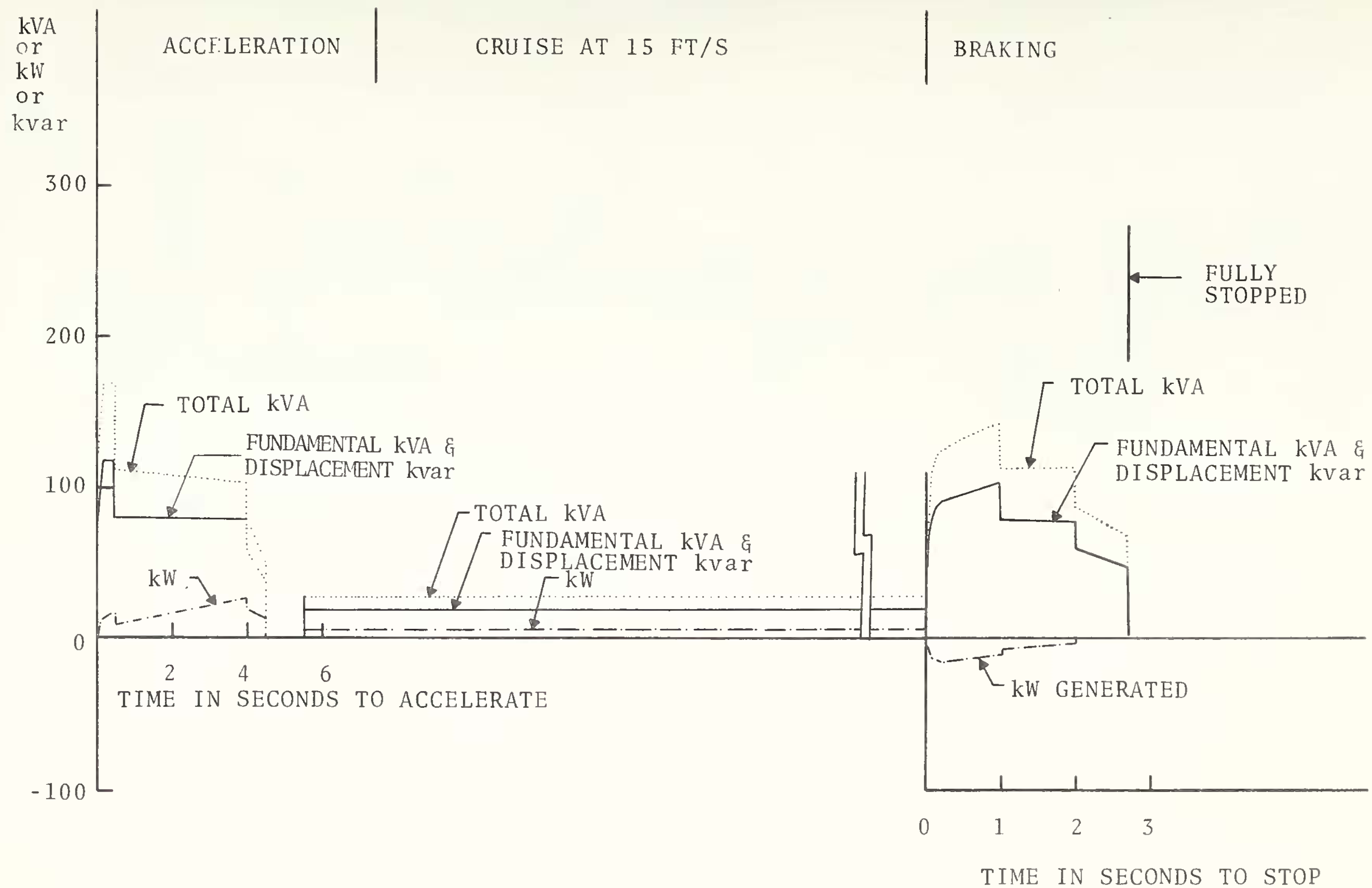


Figure 4-7 Monocab Vehicle -- Propulsion Power for Acceleration, Cruise at 15 ft/s and Braking; Vehicle Weight 5,420 lbs; Level Rail; No Wind; 480 V L-L on Rails

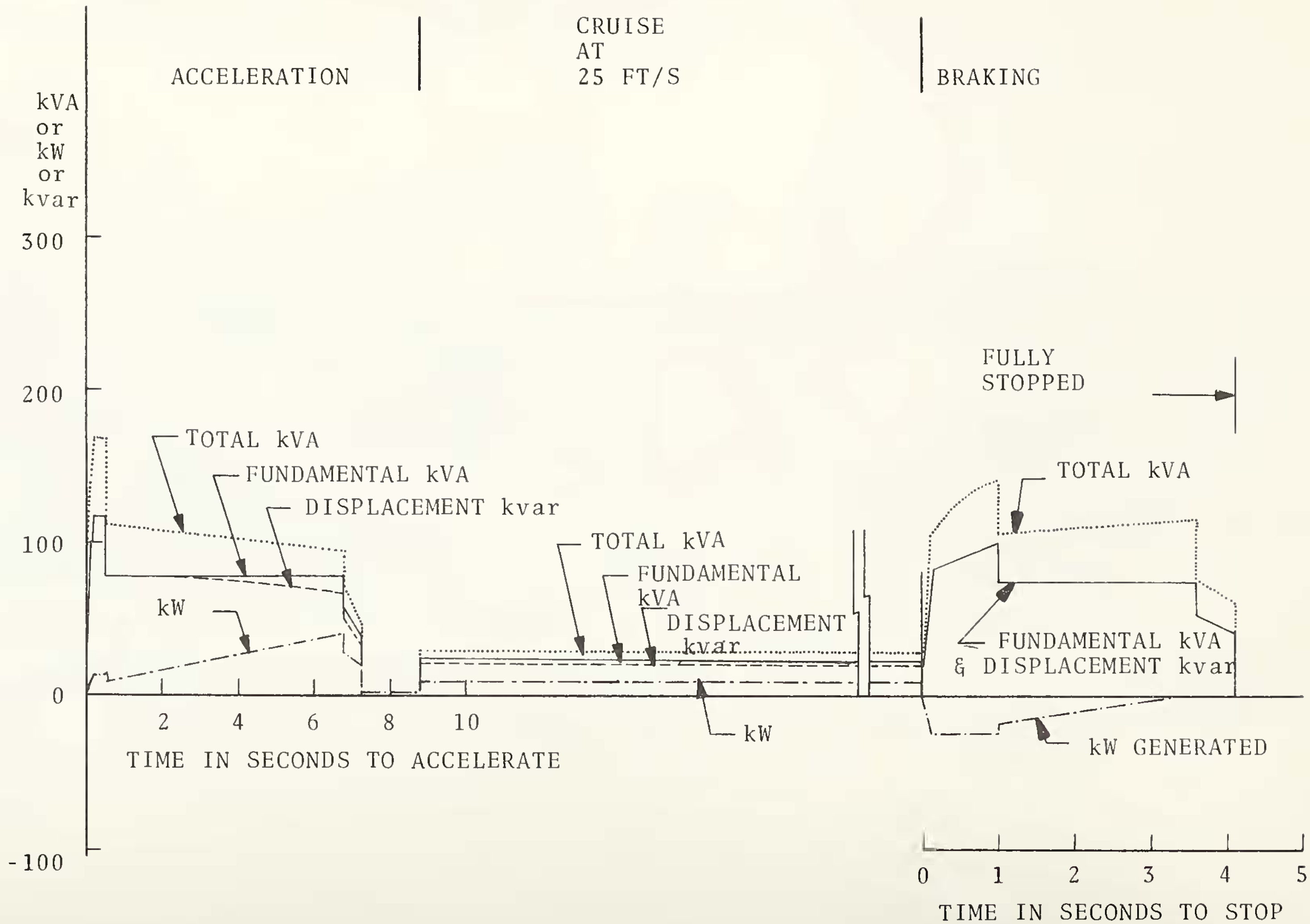


Figure 4-8 Monocab Vehicle -- Propulsion Power for Acceleration, Cruise at 25 ft/s and Braking; Vehicle Weight 5,420 lbs; Level Rail; No Wind; 480 V L-L on Rails

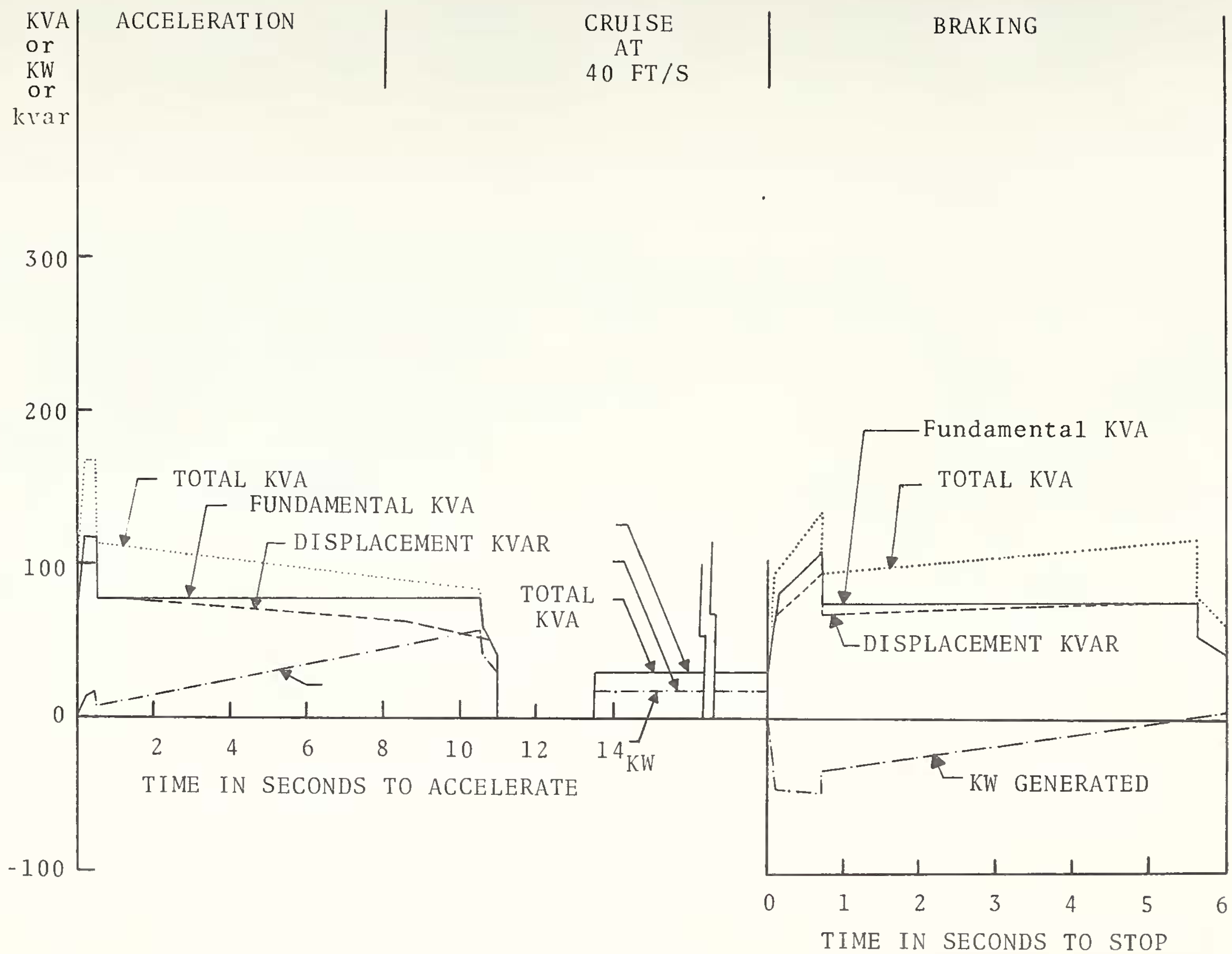


Figure 4-9 Monocab Vehicle -- Propulsion Power for Acceleration, Cruise at 40 ft/s and Braking; Vehicle Weight 5,420 lbs; Level Rail; No Wind; 480 V L-L on Rails

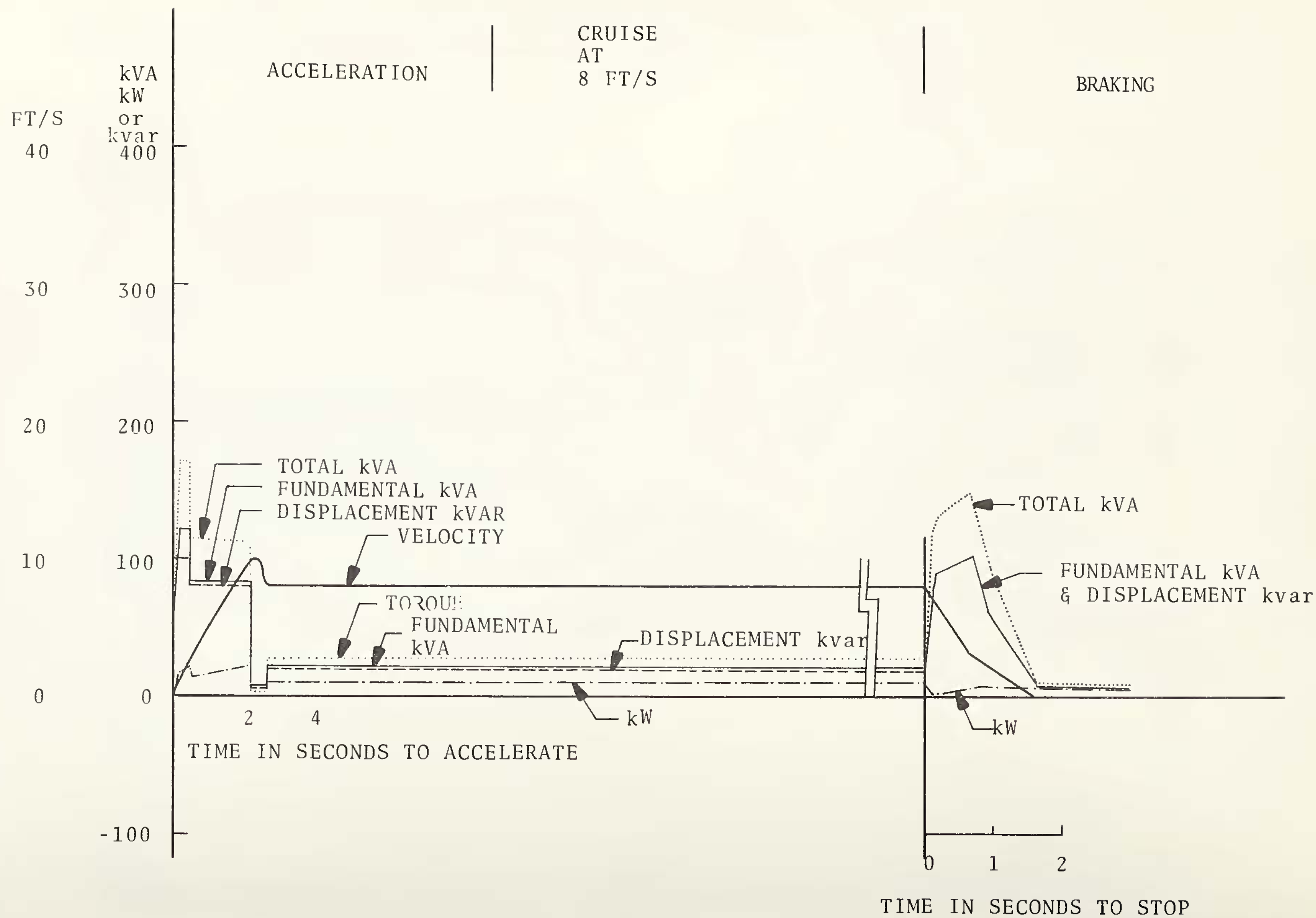


Figure 4-10 Monocab Vehicle -- Vehicle Power for Acceleration, Cruise at 8 ft/s and Braking; Vehicle Weight 5,420 lbs; Level Rail; No Wind; 480 V L-L on Rails

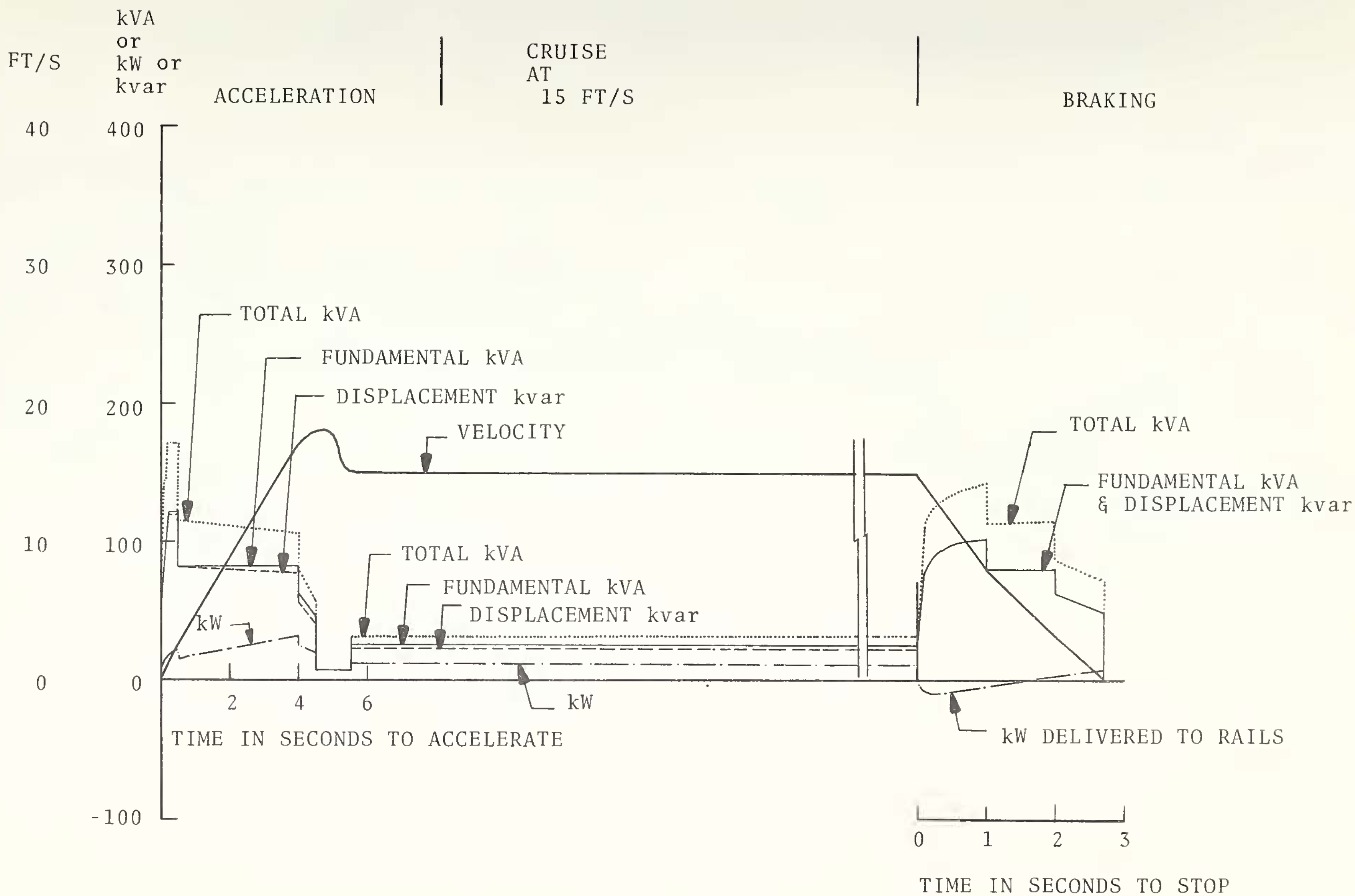


Figure 4-11 Monocab Vehicle -- Vehicle Power for Acceleration, Cruise at 15 ft/s and Braking; Vehicle Weight 5,420 lbs; Level Rail; No Wind; 480 V L-L on Rails

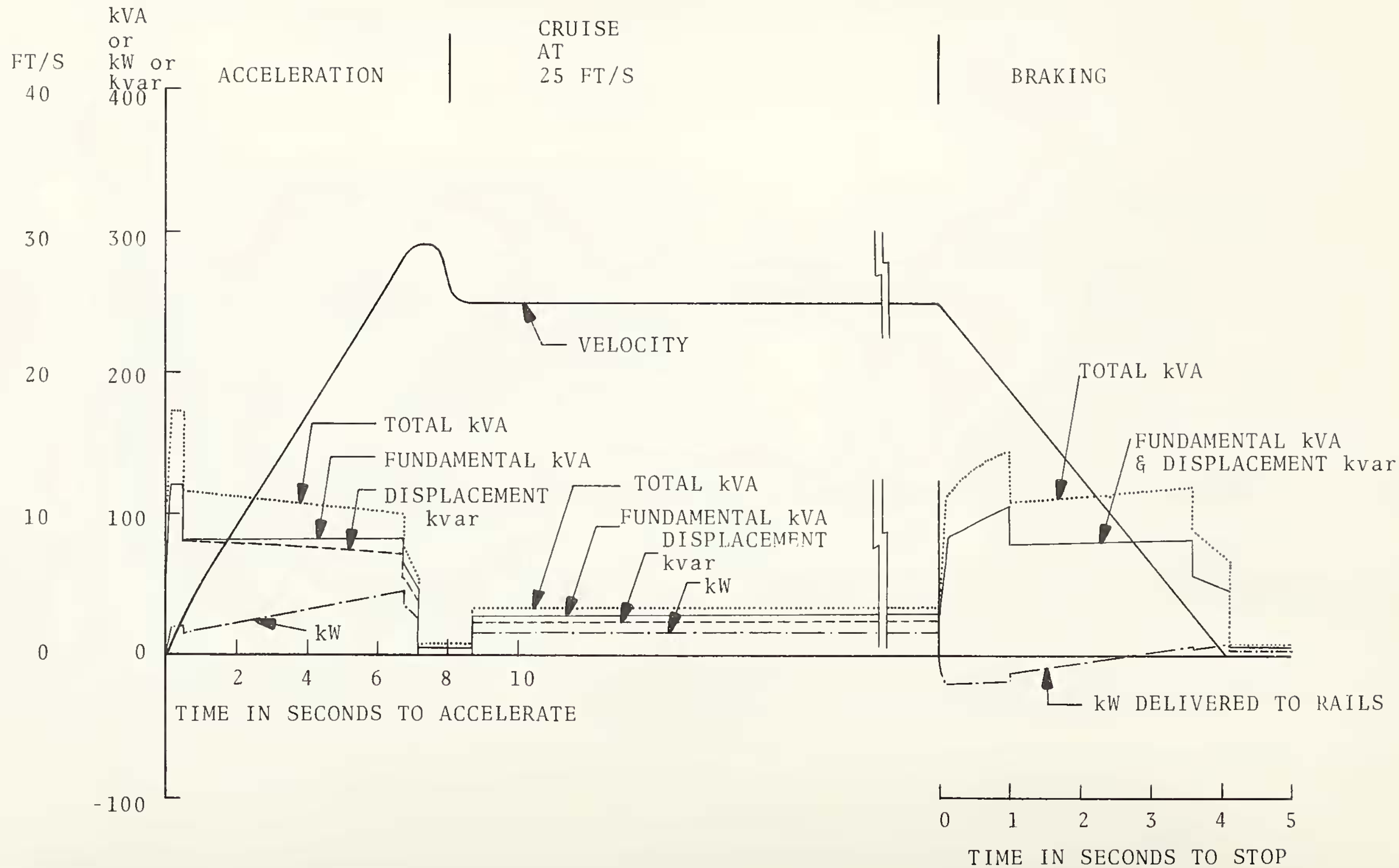


Figure 4-12 Monocab Vehicle -- Vehicle Power for Acceleration, Cruise at 25 ft/s and Braking; Vehicle Weight 5,420 lbs; Level Rail; No Wind; 480 V L-L on Rails

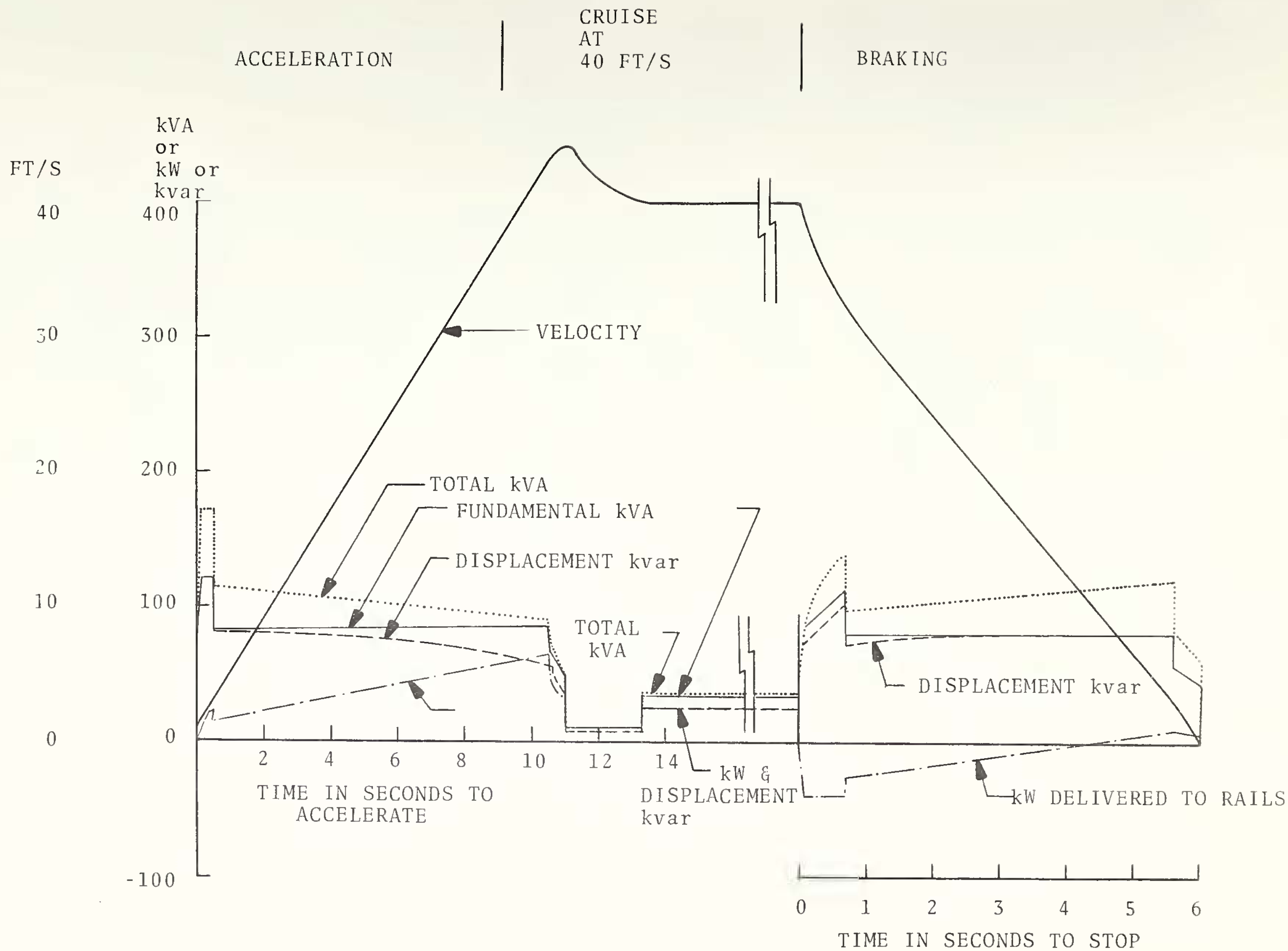


Figure 4-13 Monocab Vehicle -- Vehicle Power for Acceleration, Cruise at 40 ft/s and Braking; Vehicle Weight 5,420 lbs; Level Rail; No Wind; 480 V L-L on Rails

# 5. TTI VEHICLE

## 5.1 SYSTEM DESCRIPTION

The vehicle propulsion system consists of six single-sided linear induction motors (LIM's) mounted in a line beneath the vehicle. The primary circuits for these motors are built into the vehicle. A reaction-rail built into the guideway acts as the secondary for all of the six motors. Power for the vehicles is obtained from three-phase power rails providing 480 V line-to-line. Power collectors are located on both sides of the vehicle; a block diagram of the electrical system is shown in Figure 5-1.

Each motor is either "on" or "off", and the number of motors "on" determines thrust at any time. Braking is accomplished by reversing (plugging) one or more motors. The design of the motors is such that a vehicle speed of 56 ft/s would be synchronous speed.

The auxiliary equipment in the vehicles operates from the 480-V bus. Power for the air-cushion suspension of the vehicles is provided by 480-V induction motors. The specifications of the vehicle pertinent to the propulsion system are:

<u>Capacity</u>

| | |
|---|---|
| Empty weight | 7600 lbs |
| Gross weight | 9400 lbs |
| Number of Passengers | |
| Seated | 10 |
| Standing | 0 |

<u>Dimensions</u>

| | |
|---|---|
| Overall length | 156 in. |
| Height | 72 in. |
| Width | 84 in. |

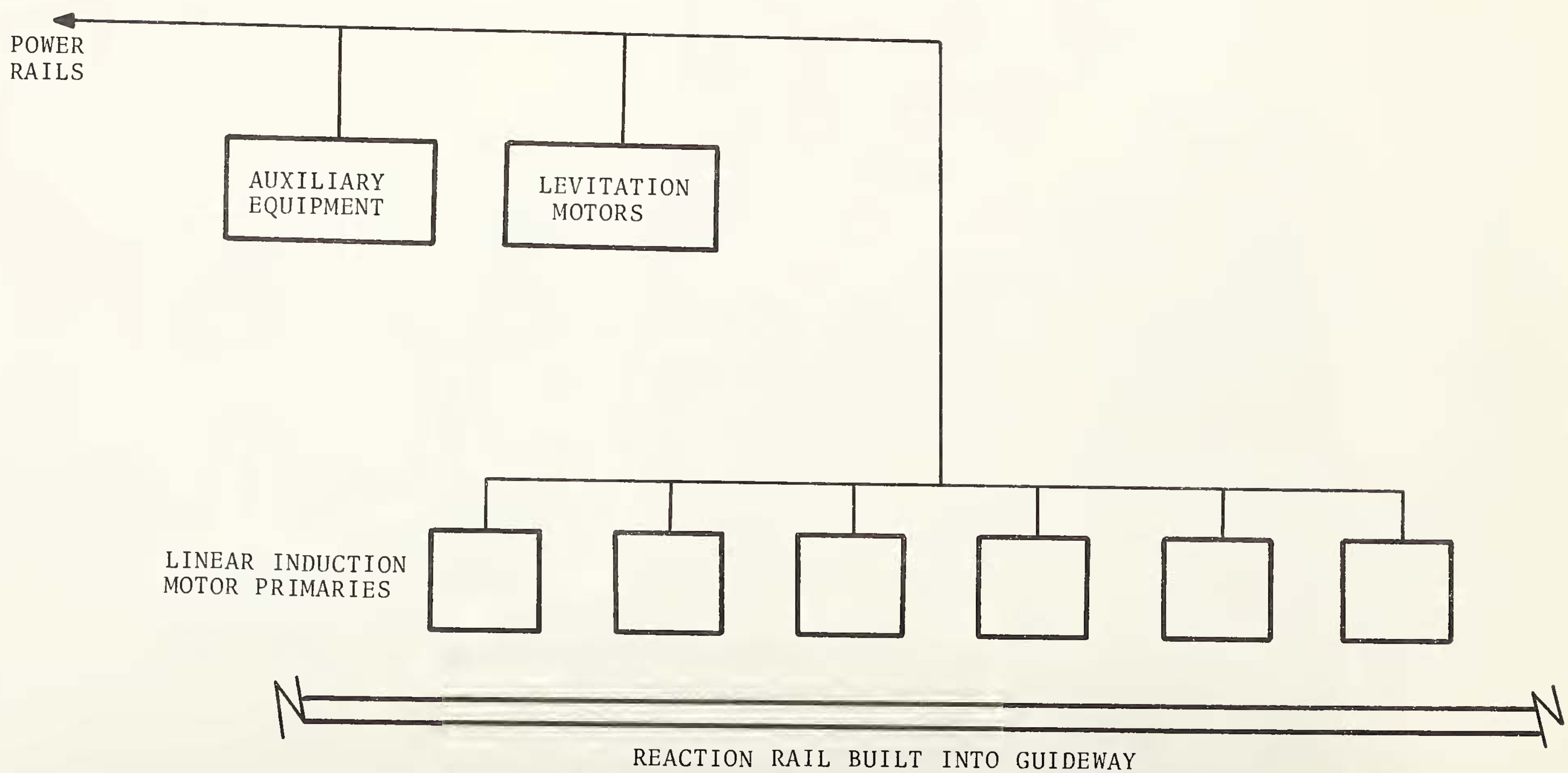


Figure 5-1 TTI Vehicle Block Diagram

## 5.2 PROPULSION SYSTEM ANALYSIS

The performance characteristics of a LIM can be considered similar to those of a rotary induction motor, when such items as end effects and edge effects are appropriately considered (6). Figure 5-2 shows typical performance curves for a LIM which has a high secondary resistance; these performance curves are quite similar to the performance curves of a NEMA Class D rotary induction motor with maximum thrust occurring at a high slip speed. The full load operating point for these motors is usually at a high value of slip where a reasonable compromise can be made between thrust, efficiency and power factor. At each speed, the motor will always produce the thrust shown on the performance curve.

When several identical LIM's are used on a vehicle, each motor will provide the same thrust at any given speed. A typical set of thrust curves for a vehicle with six LIM's is shown in Figure 5-3. Point A in that figure shows the minimum thrust at cruising speed with one motor operating continuously. Additional thrust at cruising speed is available in discrete steps up to Point B showing the thrust available with all six motors running continuously.

If the correct thrust to maintain cruising speed for a particular combination of vehicle drag, grade and headwind does not coincide with one of the discrete values available, a correct average thrust can be achieved by turning one motor on and off at short intervals. If the difference in vehicle accelerations is large as the motor is switched on and off, the passengers may be uncomfortably aware of the pulses of power.

The basic test data from which the performance curves are derived were taken from magnetic tapes 33417 and 33418. These tapes were made simultaneously during Run 8 on October 17, 1972. Run 8 consists of five round trip cycles of TTI Vehicle No. 2 over the experimental section of guideway. The major purpose of these tests was to determine electromagnetic interference created by the vehicle. Each round trip cycle consisted of starting from the

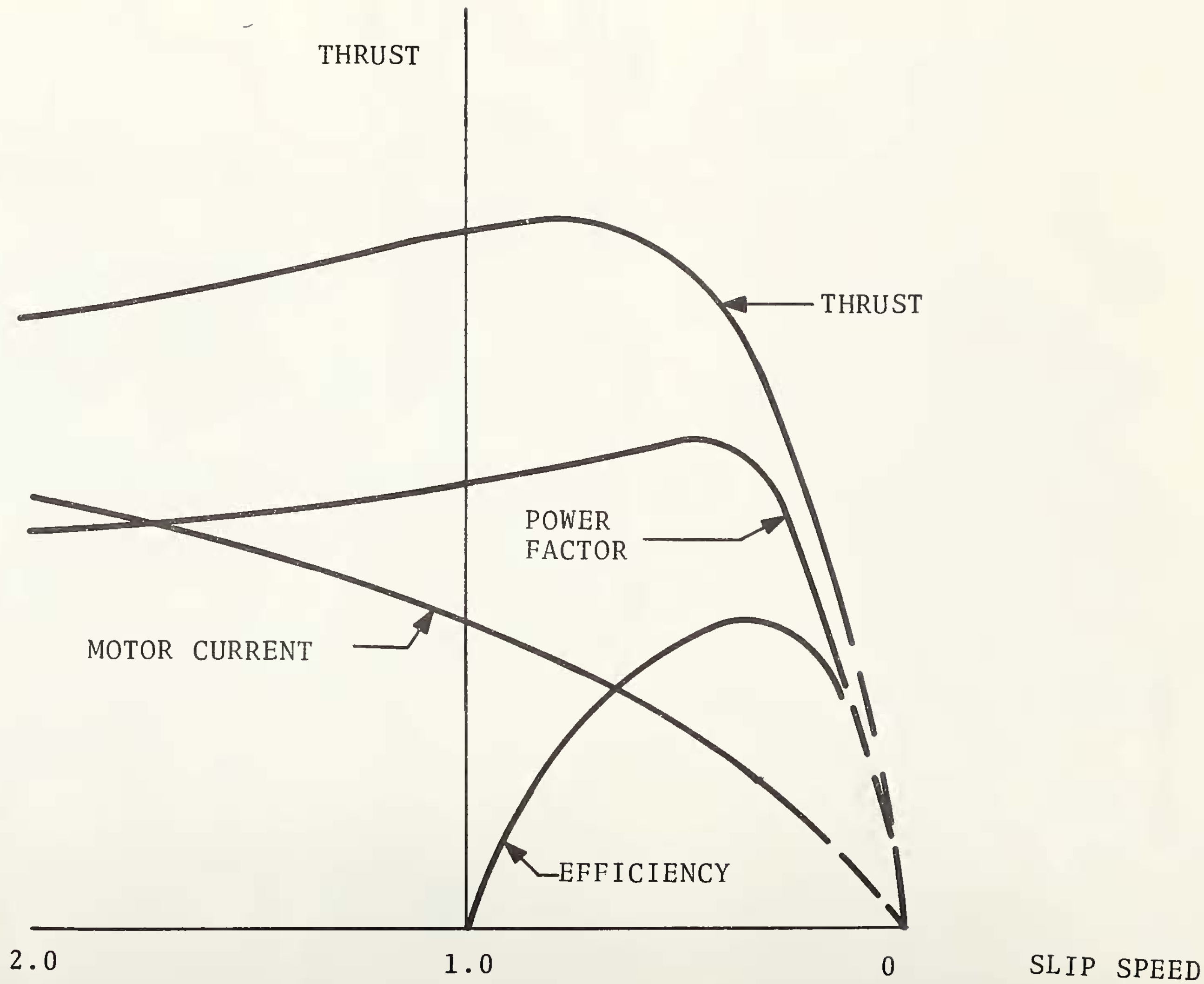


Figure 5-2 Typical LIM Characteristics for Motors with High Resistance Secondaries

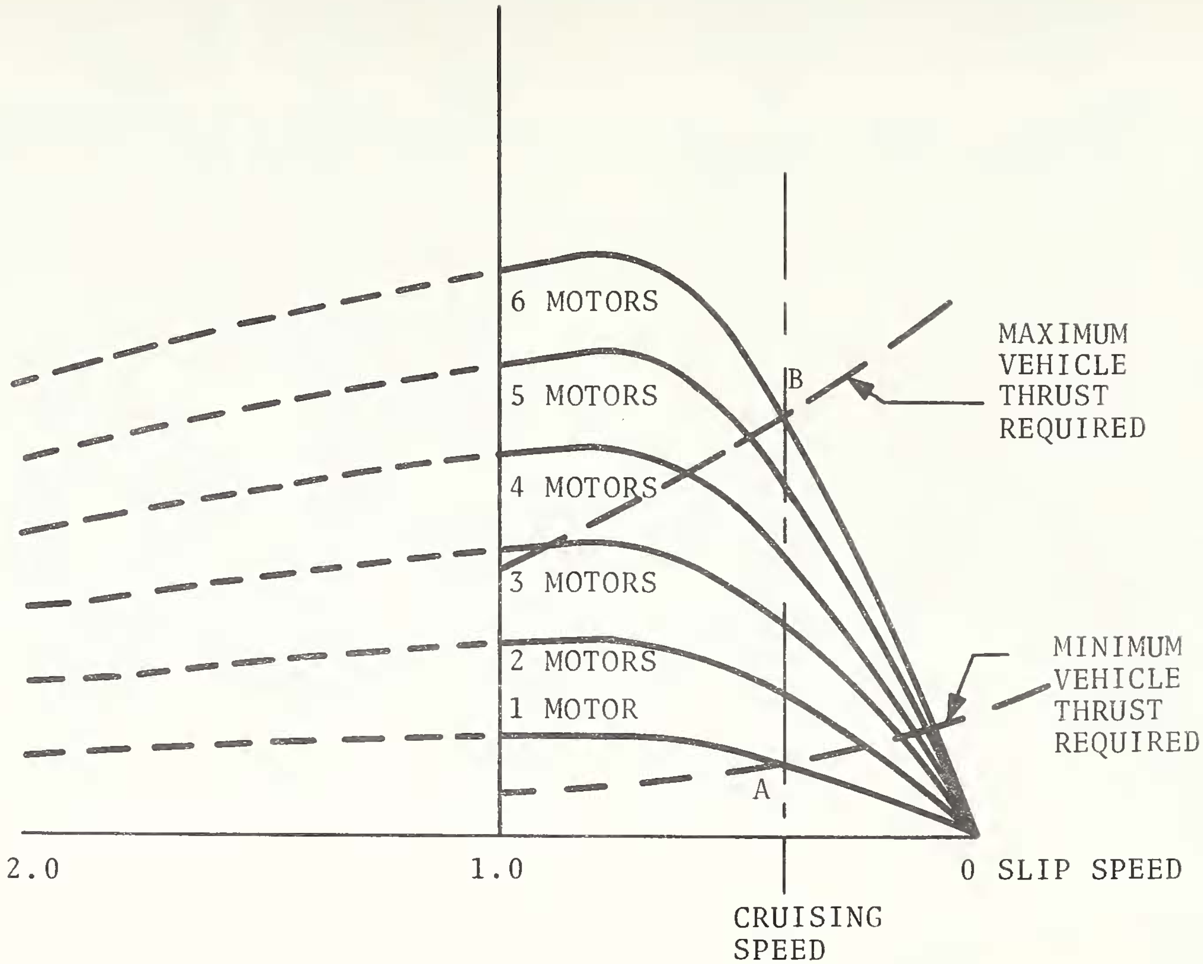


Figure 5-3  Thrust Curves for a Vehicle with 6 LIM's

station, accelerating to a planned speed of 27 ft/s and braking as the end of the guideway was approached. The vehicle was then reversed, and a similar acceleration, cruise and braking took place returning the vehicle to the end of the guideway near the station. After another change of direction the vehicle moved slowly into the station completing the cycle.

Magnetic Tape 33417 contains recordings of wayside test data. The data used is displayed on a chart recorded at approximately one inch per second. Data was taken from three tracks showing the currents fed to each of the power rails, from three tracks showing the line-to-line voltages between the rails, and from a track showing time.

Magnetic Tape 33418 contains recordings of on-board test data. The data used is displayed on a chart recorded at approximately 0.1 inch per second. Data was taken from tracks showing vehicle velocity, acceleration and time.

## 5.3 PROPULSION SYSTEM PERFORMANCE

During the tests at Dulles the vehicles were accelerated using five motors energized in sequence at intervals of about 0.6 seconds. As the vehicle approached the desired cruising speed the motors were turned off in sequence. During cruise, one motor was on intermittently. The percentage of time with the motor on varies with grade and headwind conditions. For braking the motors are plugged, producing a reverse thrust. At Dulles, four motors were used in braking. They were applied in sequence to obtain the desired level of deceleration, then turned off in sequence as zero speed was approached. A short reverse burst with two motors was used just prior to the final stop.

From the available data it cannot be determined which motors were used. The data clearly shows the steps in power as motors are switched. When two or more motors are energized, the motors were assumed to provide equal thrust and demand equal power.

Figure 5-4 shows the performance of each motor energized during the acceleration, cruise at 27 ft/s and braking. The power used by each motor was determined by dividing total propulsion power by the number of motors operating.

The values of motor thrust shown in Figure 5-4 were calculated by application of Newton's law to the vehicle to determine total thrust produced by all motors; this value was then divided by the number of motors operating.

While cruising at 27 ft/second southbound and at 27 ft/second northbound the vehicle coasted at the same stretch of guideway. Friction drag was assumed to be the same in both directions, and always opposes the direction of motion. The forces caused by grade and headwinds act in the same direction regardless of the direction of vehicle motion. Thus southbound total retarding force is drag plus (grade and wind) while northbound the total retarding force is drag minus (grade and wind). From the recorded deceleration rates during coasting in the two directions the effect of drag and the effect of grade and wind can be calculated, permitting total motor thrust to be calculated. Both drag and grade were found to be small compared to the thrust necessary to accelerate the vehicle when motors were operating.

This type of calculation was made at several vehicle speeds to obtain a curve of motor thrust vs. speed.

## 5.4 PROPULSION SYSTEM POWER REQUIREMENTS

Figure 5-5 shows the total propulsion power requirements during acceleration, cruise at 27 ft/second, and braking. The step changes in power correspond to changes in the number of motors energized. During cruise there are periods of about one second during which the vehicle coasts and requires no propulsion power; the proportion of coasting and power would vary with grade and headwind. Where a three-phase system has two or more balanced loads, the total real power used is the arithmetic sum of the real powers of the individual loads. The total reactive power used is the algebraic sum of the reactive powers of the individual loads

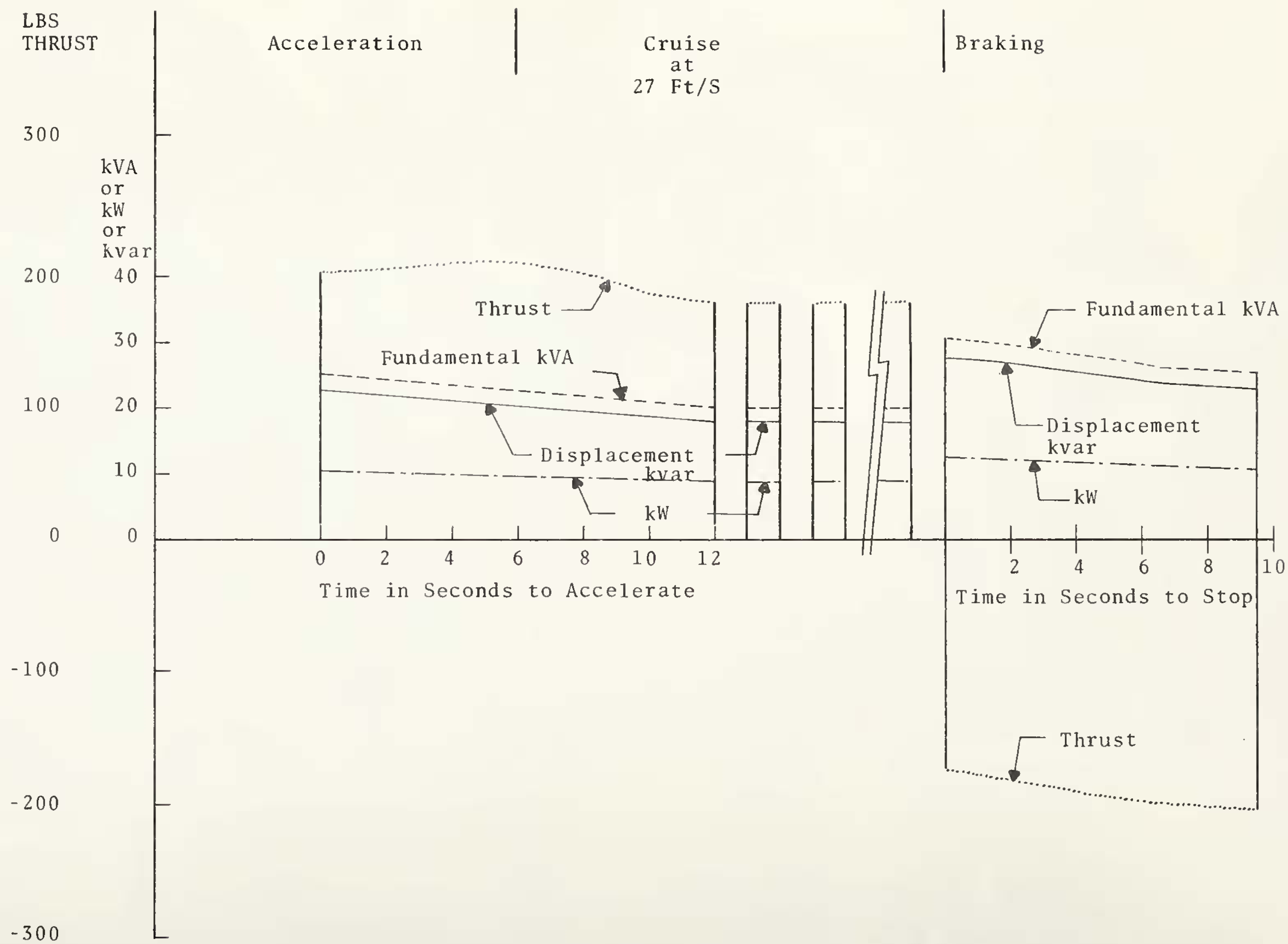


Figure 5-4 TTI Vehicle -- Performance of One Motor During Acceleration, Cruise at 27 ft/s and Braking; Vehicle Weight 9,400 lbs; Level Rail; No Wind; 480 V L-L on Rails

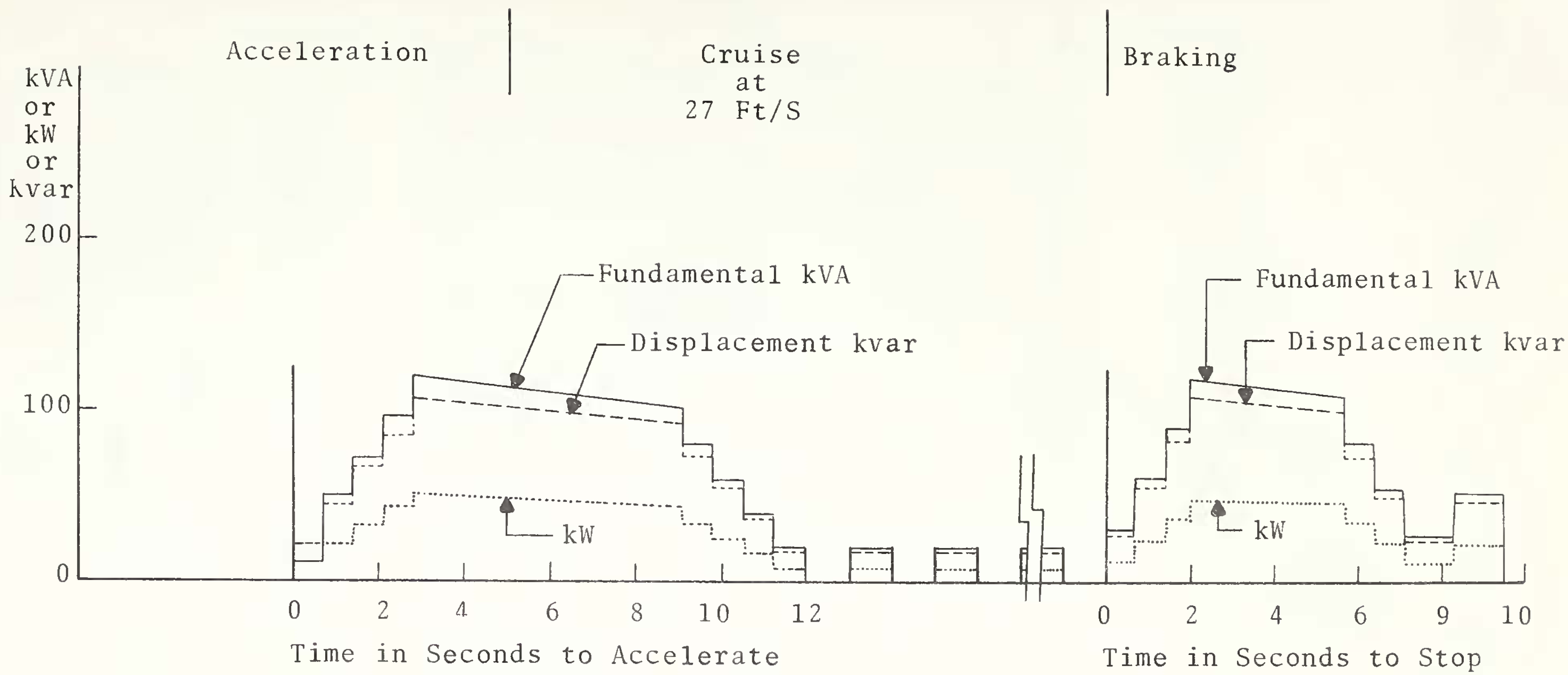


Figure 5-5 TTI Vehicle -- Propulsion Power for Acceleration, Cruise at 27 ft/s and Braking; Vehicle Weight 9,400 lbs; Level Rail; No Wind; 480 V L-L on Rails

since reactive power may have either a leading or lagging power factor. For any load the complex power may be determined using the relationship:

$$kVA = \sqrt{(kW)^2 + (kvar)^2}$$

These equations were used to subtract levitation power from the total of levitation and propulsion power and to calculate propulsion complex power.

## 5.5 PROPULSION SYSTEM PLUS LEVITATION SYSTEM POWER REQUIREMENTS

The vehicle cannot move until it has been supported on an air cushion created by fans driven by rotary induction motors. Total power required for levitation and propulsion is shown in Figure 5-6. The power for levitation is applied while the vehicle is in the dock where passengers may board. The levitation fans draw a heavy starting current lasting about 0.7 seconds. Typically the levitation power was applied 10 seconds before propulsion power. During that 10 seconds the vehicle is moved sideways by the docking mechanism. Power for docking and undocking is provided by separate motors built into the dock. This power is not shown in Figure 5-6.

The values of propulsion and levitation power were calculated by subtracting auxiliary power from input power to the vehicle using the three-phase power relationships described above.

## 5.6 VEHICLE POWER REQUIREMENTS

The power required by the vehicle was determined by using the following equations:

$$\text{Fundamental complex power} = \frac{\sqrt{3}}{1000} E_{LL} I_{L1}$$

$$\text{Fundamental real power} = \frac{\sqrt{3}}{1000} E_{LL} I_{L1} \cos \phi$$

$$\text{Displacement reactive power} = \frac{\sqrt{3}}{1000} E_{LL} I_{L1} \sin \phi$$

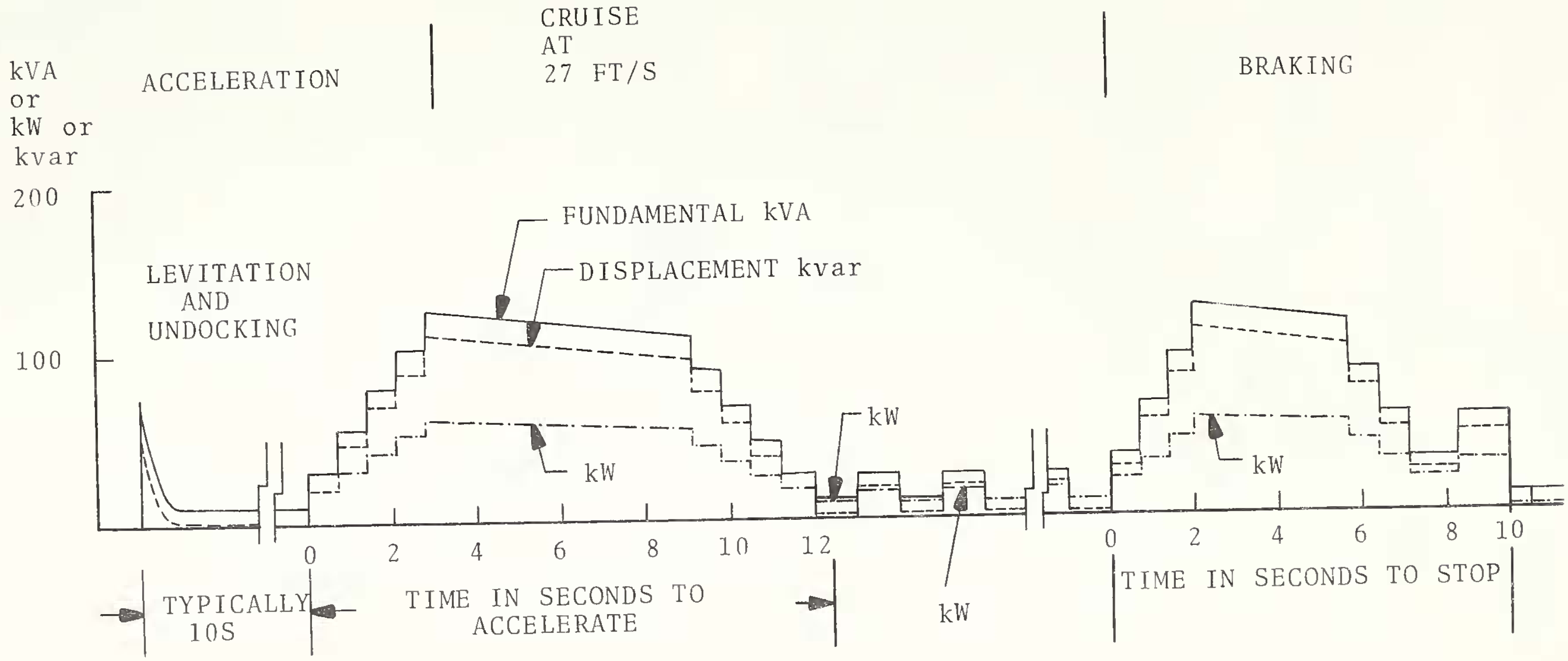


Figure 5-6 TTI Vehicle -- Propulsion and Levitation Power for Acceleration, Cruise at 27 ft/s and Braking; Vehicle Weight 9,400 lbs; Level Rail; No Wind; 480 V L-L on Rails

where

$E_{LL}$ = line-to-line voltage

$I_{L1}$ = fundamental rms current per phase

and

$\phi$ = the phase angle between fundamental voltage and fundamental current

The values of $E_{LL}$, $I_{L1}$ and $\phi$ were taken from the recordings of wayside data made during the tests.

When the vehicle was stationary there was a short period of time during which only the auxiliary equipment was operating. This provided a measured value of power required by the auxiliary equipment. There were periods with the vehicle stationary and with the vehicle coasting when auxiliary equipment and levitation equipment were operating with no propulsion motors energized. This provided measured values of auxiliary plus levitation power which were found to be independent of vehicle speed. Levitation power was calculated by subtracting auxiliary power from the sum of auxiliary and levitation power.

Figure 5-7 shows the power demands of the vehicle through a typical run of acceleration, cruise at 27 ft/second and braking.

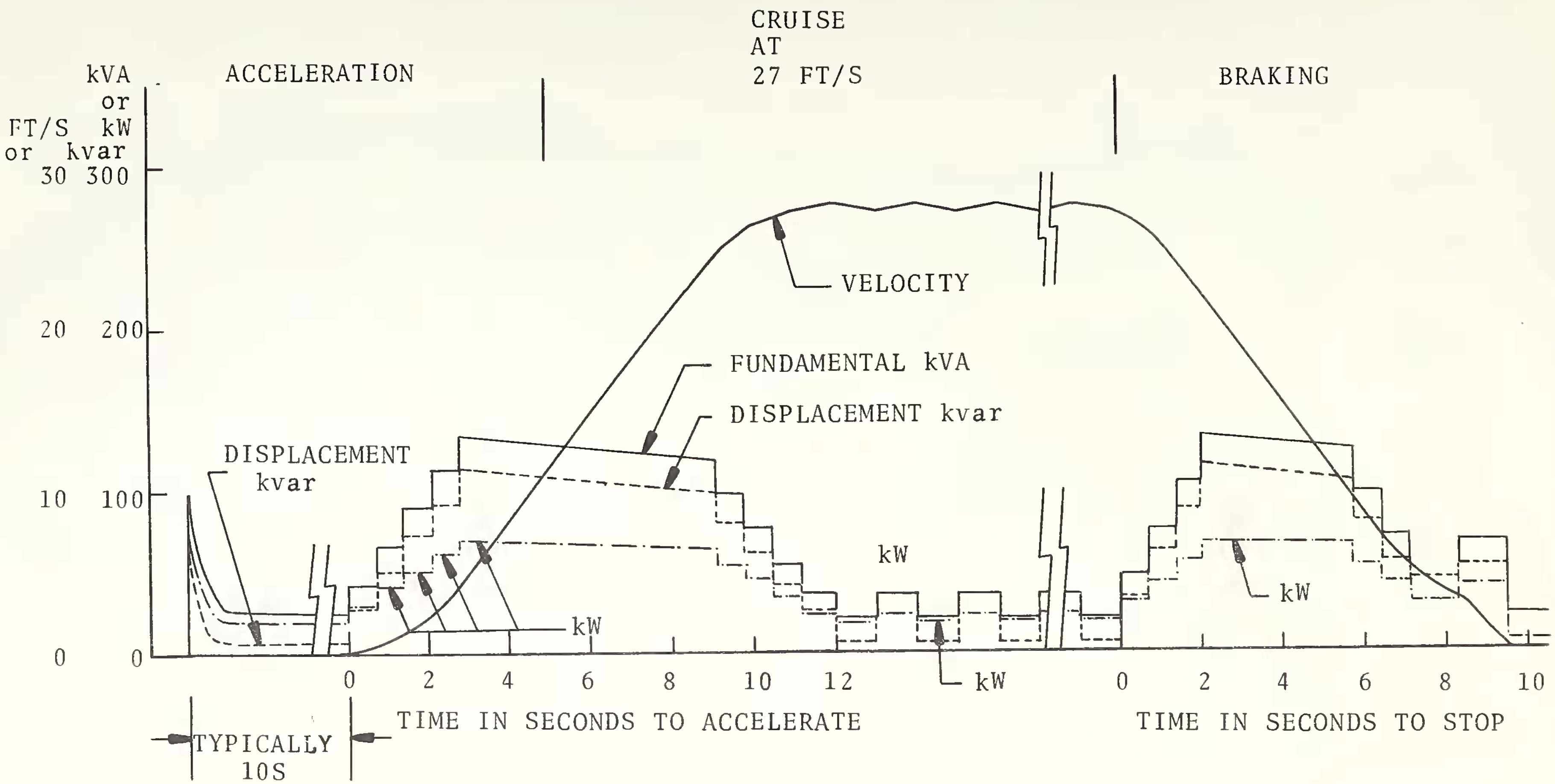


Figure 5-7 TTI Vehicle -- Vehicle Power During Acceleration, Cruise at 27 ft/s and Braking; Vehicle Weight 9,400 lbs; Level Rail; No Wind; 480 V L-L on Rails

# 6. COMPARATIVE ANALYSIS

This section contains selected areas of propulsion power and vehicle power characteristics to enable some comparative analysis of the Dulles Transpo® '72 PRT vehicles. The areas chosen for analysis have taken into consideration that the vehicles were designed to cruise with different velocities and payloads, with the vehicles using different propulsion and suspension systems. Because of the above differences, the comparative analysis performed in this report does not attempt to identify that vehicle having the most satisfactory characteristics. Rather, the analysis performed herein has as its objective the identification of those performance features necessary to adequately describe the power and propulsion characteristics of the vehicles.

For the analysis that follows, all vehicles are operated at a speed of 18 MPH, with maximum gross vehicle weight and are operated on level grades with zero headwinds.

## 6.1 PROPULSION POWER CHARACTERISTICS

The propulsion power characteristics selected for analysis are; acceleration energy, cruise energy, propulsion real power per gross vehicle weight, propulsion real power per tractive effort, and propulsion complex power per tractive effort and per gross vehicle weight.

### 6.1.1 Acceleration and Cruise Energy

The acceleration energy and cruise energy are shown in Figure 6-1. The acceleration energy shown has been normalized for two factors, the kilowatt-seconds per passenger, and the watt-seconds per pound of gross vehicle weight. For the kilowatt-second to passenger ratio, the data shows that this ratio is proportional to the number of passengers carried by each of the vehicles; however, this ratio is not linear, when the four vehicles are considered as a single group. However, if the vehicles are

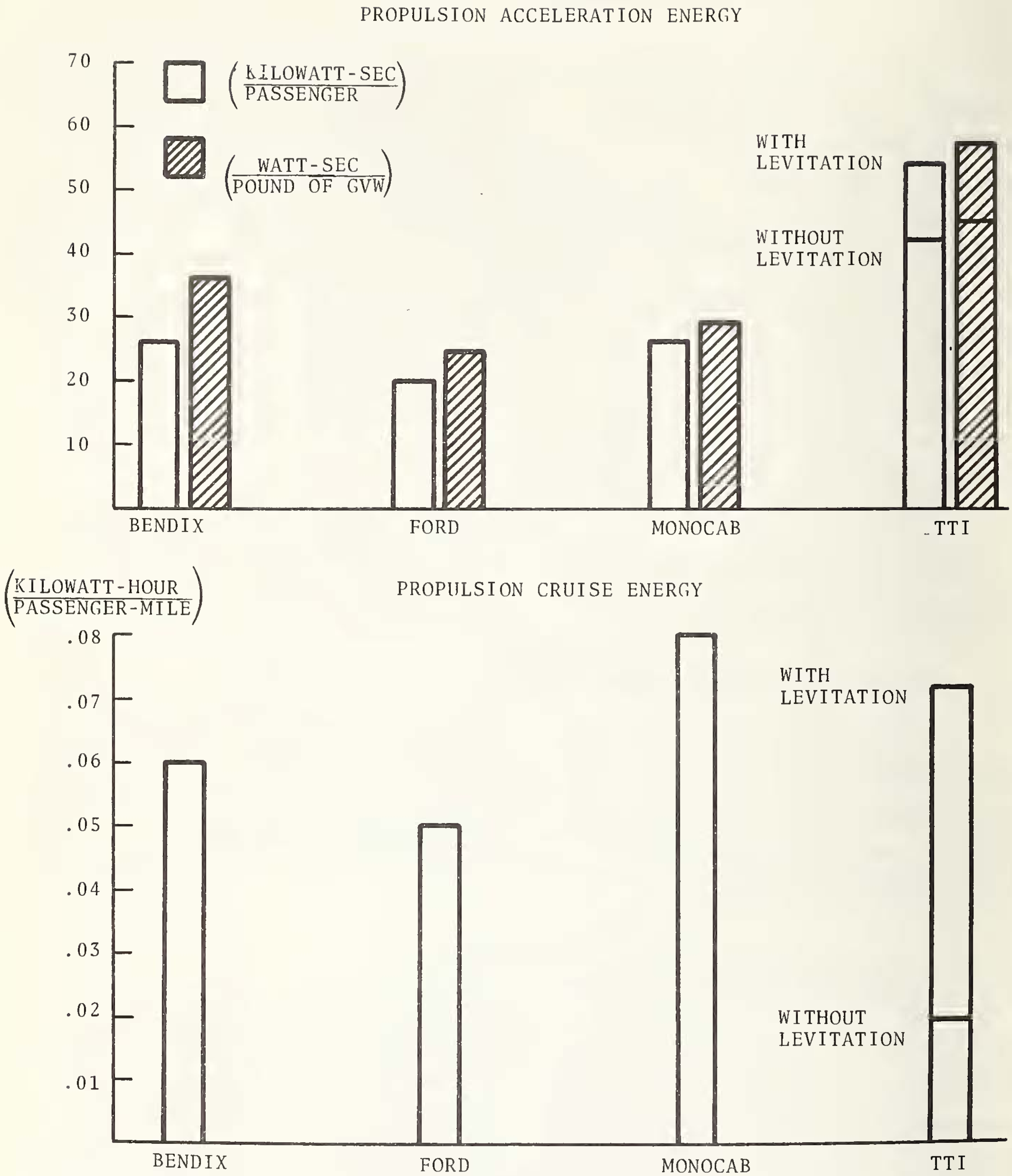


Figure 6-1 Acceleration Energy and Cruise Energy

divided into two groups, with one group consisting of the two larger vehicles and the other group consisting of the two smaller vehicles, we then obtain approximate linear ratios. For the watt-seconds to the vehicle gross weight ratio, the data shows this ratio is proportional to vehicle gross weight only if we again pair the vehicles as described above.

All vehicles except for TTI utilize phase control within the propulsion system to achieve non-dissipative power control. For these systems the electrical energy into the vehicle closely follows the energy requirements of the vehicle, the difference between the two being the efficiency of the propulsion system. The TTI vehicle control approach of stepping in linear induction motors (LIMs) at full voltage and frequency forces the LIMs to operate at large slip velocities where it has been shown that the losses in the reaction rail are very large compared to the output power being developed (Reference 7). This results in poor energy utilization during acceleration.

The propulsion cruise energy shown has been normalized to kilowatt-hours per passenger mile. This data clearly shows that the larger vehicles are more cruise energy efficient when compared to the smaller vehicles; this appears to be a result of the larger vehicles being designed to accomodate standees. The levitation power requirements of the TTI vehicle significantly impact its energy requirements; if the levitation power were to be excluded from this analysis, the TTI vehicle would be the most energy efficient for the cruise conditions analyzed herein. The implication of the above is that tracked levitated vehicles potentially are the most cruise energy efficient, if a levitation system can be used which requires minimum energy. For example, if the levitation system were to require 1/3 of the TTI system analyzed in this report, then the total propulsion and levitation cruise energy requirements of the tracked levitated vehicle would be 75 percent of the best rubber tired vehicle tested at Post-Transpo® '72.

### 6.1.2 Propulsion Real Power

The propulsion real power characteristics are shown in Figure 6-2. The cruise propulsion real power has been normalized for two factors; gross vehicle weight, and tractive effort. The real power to gross vehicle weight ratio does not follow any particular pattern, except that the lowest ratio occurs with the Ford ACT vehicle, one of the heaviest; and, the highest ratio occurs with the Monocab vehicle, the lightest of the four vehicles. A modification to the real power to gross vehicle weight ratios can be made by considering payload weight; the following ratios are then obtained:

| | | |
|---|---|---|
| BENDIX | 6.3 | watts/pound of payload |
| FORD | 4.9 | |
| MONOCAB | 8.4 | |
| TTI | 7.2 | with levitation |
| | 2.4 | without levitation |

These ratios generally follow the pairing of the vehicles as previously described. Again, the Ford ACT vehicle has the lowest ratio and the Monocab vehicle has the highest ratio. The levitation power requirement of the TTI vehicle significantly impacts both power ratios for this vehicle.

The cruise propulsion power to tractive effort ratio (P/F) is a measure of the overall efficiency of the propulsion system in that it can be used to compare the real input power to the propulsion system, to the tractive effort being developed by the vehicle. At 18 MPH the theoretical vehicle $P_o/F$ ratio can be shown to be 35.8 watts output per pound of tractive effort being developed. Using this value the following propulsion system efficiencies are obtained:

| | | |
|---|---|---|
| Bendix | 70% | |
| Ford | 85% | |
| Monocab | 70% | |
| TTI | 29% | with levitation |
| | 87% | without levitation |

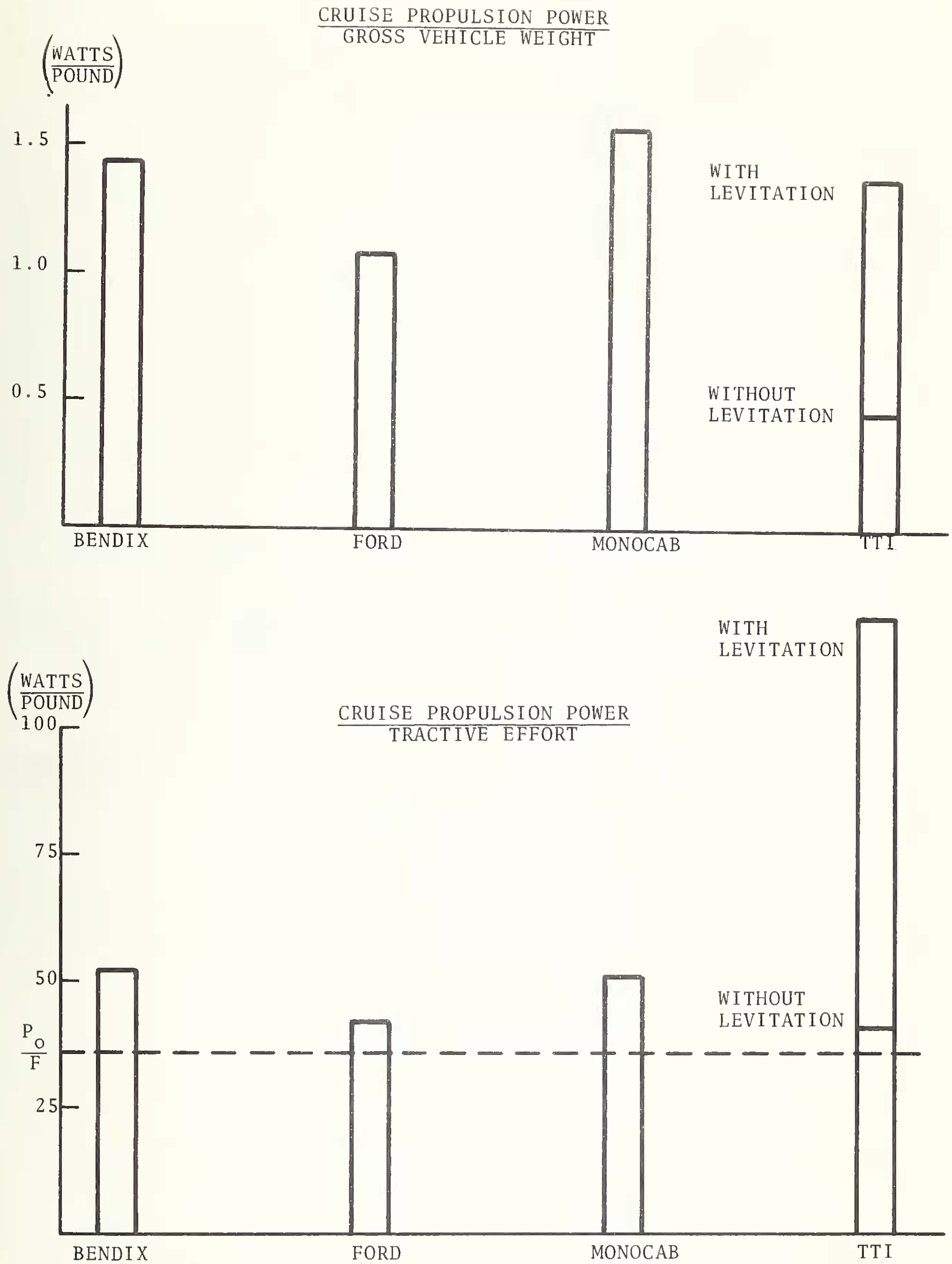


Figure 6-2 Propulsion Real Power Characteristics

### 6.1.3 Cruise Complex Power

The complex power of a system is the product of the voltage across the system and the current demand of the system. The complex power of a system is equal to the real power consumption of the system only when the voltage and current are in phase; for all other cases, the complex power demand exceeds the real power consumption. Rectifier systems produce phase angles between voltage and current as a result of their control characteristics.

The cruise complex power is shown in Figure 6-3, and has been normalized for two factors; gross vehicle weight, and tractive effort. The complex power to gross vehicle weight ratio shown is influenced by two factors, namely, the phase angle control of the rectifiers and the real power to gross vehicle weight ratio shown in the previous figure. The TTI vehicle has the lowest ratio, and this is a direct result of this system not using any phase angle control. The Monocab vehicle has the highest ratio and is a result of both the phase angle control and the high cruise real power to gross vehicle weight ratio shown in the previous figure.

The cruise complex power to tractive effort ratios follow closely the real power to tractive effort ratios of the previous figure except for the TTI vehicle. Again, this is a result of the TTI vehicle not using any phase angle control.

A measure of the system power utilization can be obtained by using the above data to determine the complex power input to the system compared to the real power output of the system ($V\text{-}A_{IN}/W_{OUT}$), and is:

| | | |
|---|---|---|
| Bendix | 4.2 | $V\text{-}A_{IN}/W_{OUT}$ |
| Ford | 3.0 | |
| Monocab | 4.2 | |
| TTI | 4.5 | with levitation |
| | 2.7 | without levitation |

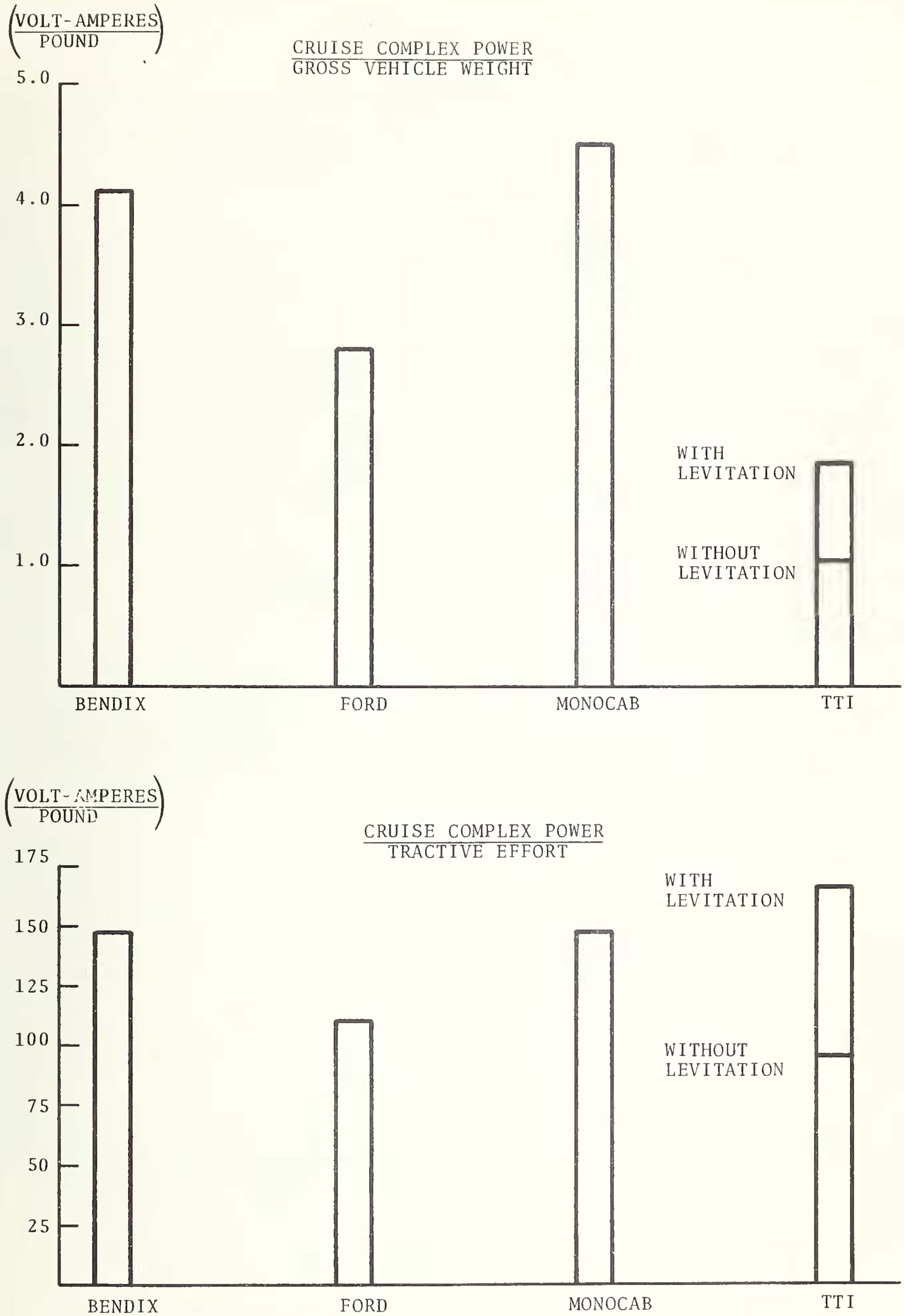


Figure 6-3. Propulsion Complex Power Characteristics

## 6.2 VEHICLE POWER CHARACTERISTICS

The vehicle power characteristics selected for analysis are the system power factor and the vehicle complex power.

### 6.2.1 System Power Factor

The system power factor is shown in Figure 6-4. The low power factors of the Bendix, Ford, and Monocab vehicles are a result of the use of thyristor rectifiers for propulsion system control. The displacement power factor shown is a result of phase angle control of the rectifiers, and the system power factor shown includes both the effect of phase angle control and distortion of the input currents. A more detailed discussion of system power factor is contained in Appendix A. For those systems designed to operate at speeds greater than the 18 MPH analyzed herein, a higher power factor would result when operating the vehicles at the higher speeds.

For the TTI vehicle, the displacement and system power factors shown are equivalent because of its propulsion system control of switched motors not introducing any controlled phase lag between the input voltage and current.

### 6.2.2 Vehicle Complex Power

The vehicle complex power is shown in Figures 6-5, and has been normalized to gross vehicle weight and tractive effort. This data is similar to the data shown in Figure 6-3, the propulsion complex power characteristics, the differences being the vehicle auxiliary power requirements. For the Bendix and Ford vehicles the auxiliary load requirement has only a slight impact on the vehicle power requirements. However, for the Monocab and TTI vehicles, the auxiliary load requirements increase the vehicle power requirements by more than 40 percent over the propulsion power requirements.

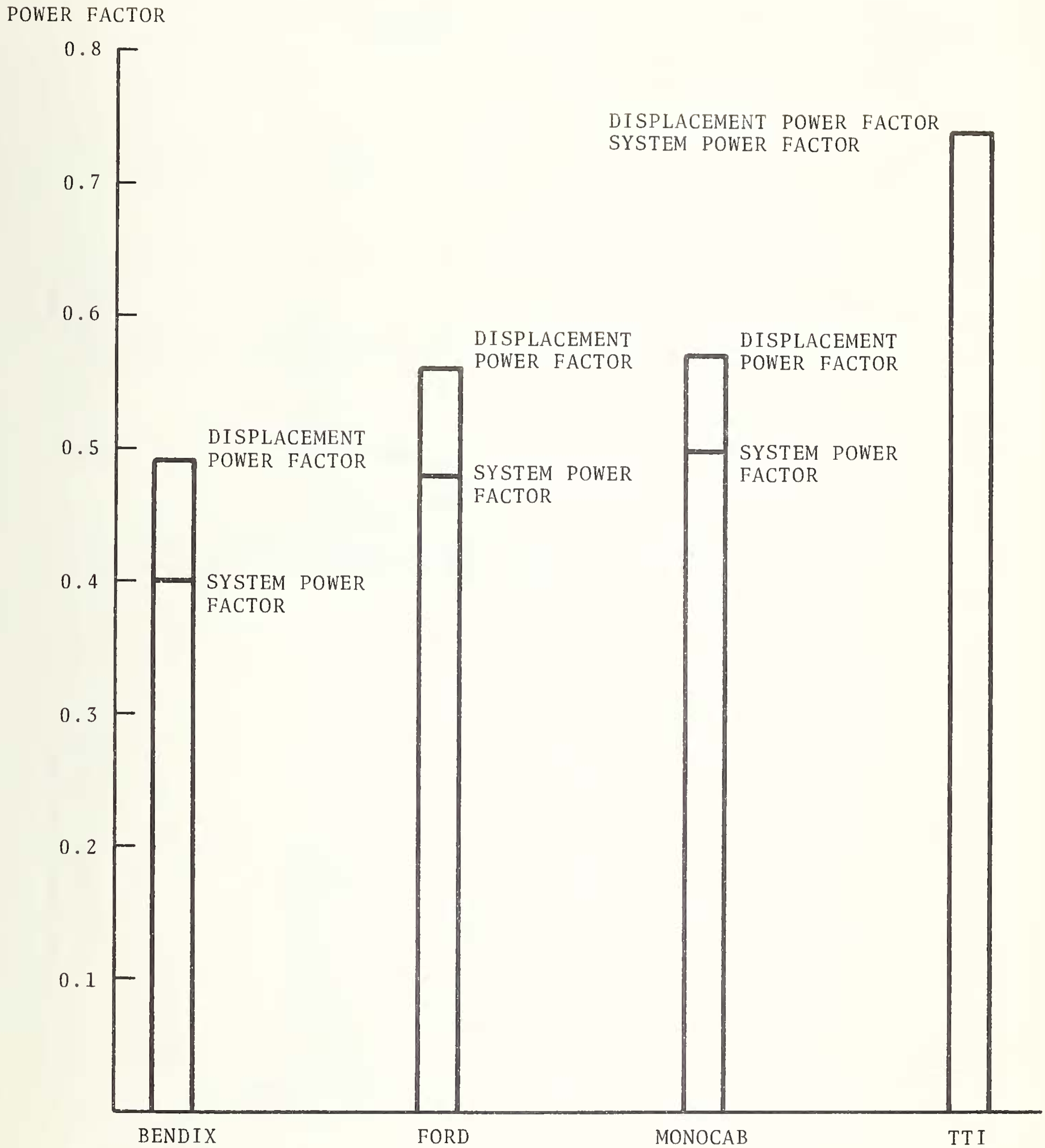


Figure 6-4. Vehicle Complex Power Characteristics

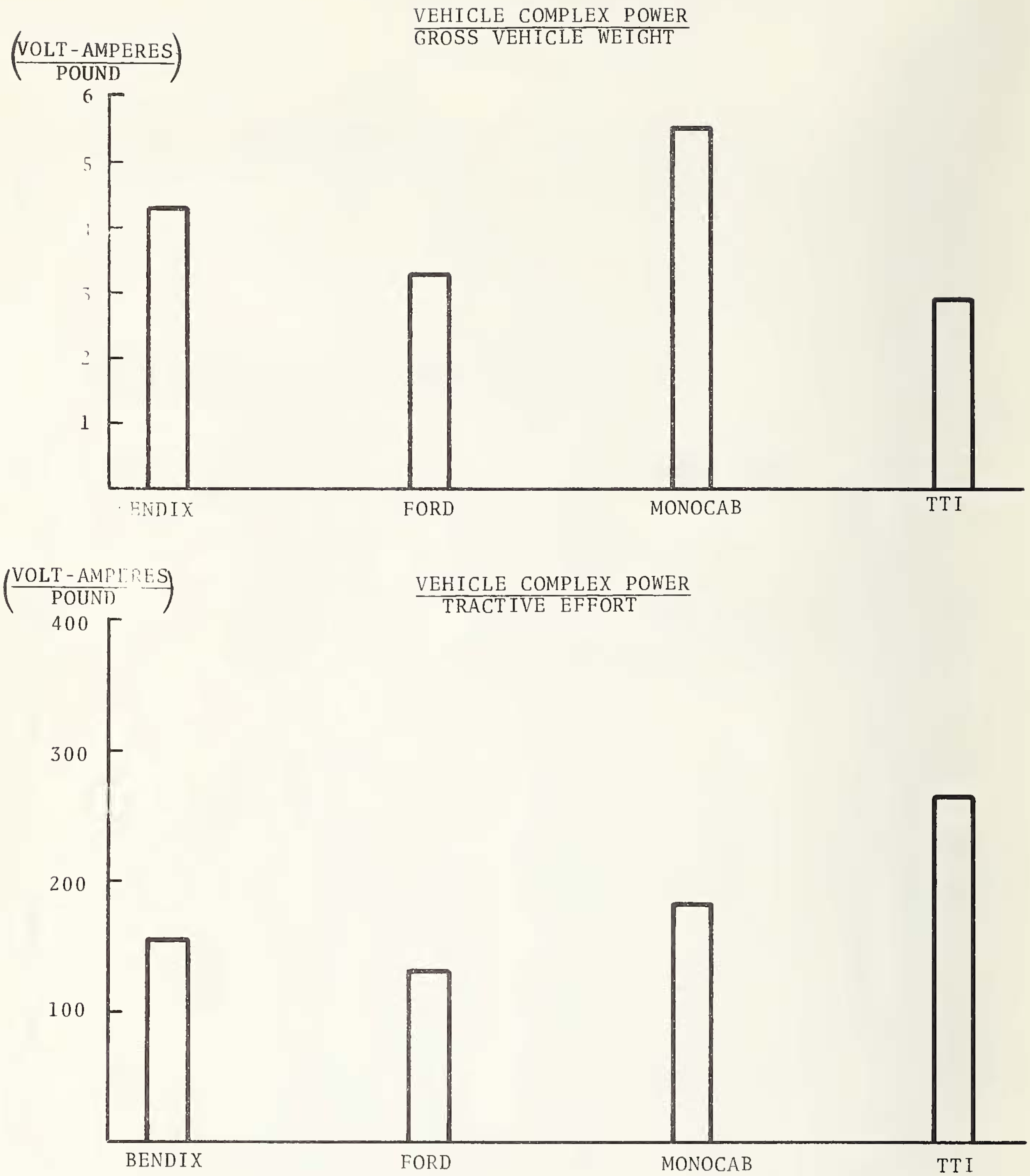


Figure 6-5. Vehicle Input Power Factor

# 7. REFERENCES


1. Johannes Schaefer, Rectifier Circuits: Theory and Design, John Wiley and Sons, Inc., New York, pp. 347, 1965.

2. Charles S. Siskind MSEE, Direct Current Machinery, McGraw-Hill Book Company, Inc., New York, pp. 319, 1952

3. Alexander Kusko, Solid-State DC Motor Drives, The MIT Press, Cambridge MA, pp. 126, 1969.

4. General Electric Motor - MD-606-AE, 25 HP (60', 75°C), 575 RPM, 230 volts, Series Wound Motor.

5. Raymond A. Wlodyka, Joseph D. Abbas, George Ploetz, Input Power Characteristics of a Three-Phase Thyristor Converter, Department of Transportation, Transportation Systems Center, Report No. FRA-ORD&D-74-20, October 1973.

6. E.R. Laithwaite, Induction Machines for Special Purposes, Chemical Publishing Company, New York, pp. 337, 1966.

7. J. Stickler, Effect of Frequency and Spatial-Harmonics on Rotary and Linear Induction Motor Characteristics, Department of Transportation, Transportation Systems Center, Report No. DOT-TSC-UMTA-72-7, March 1972.

# APPENDIX

# POWER CHARACTERISTICS OF A THREE-PHASE, SIX-PULSE RECTIFIER

In balanced three-phase systems, where the currents and voltages are sinusoidal and the same frequency, the power characteristics of the system can be completely determined using the two-wattmeter method. The individual wattmeter outputs can be used to determine the active power, reactive power, power factor and apparent power.

In rectifier systems, the line currents are abruptly switched, or chopped, and contain harmonic distortion components of current, voltage or both. For these systems, significant measurement errors result if only wattmeters are used to determine the power characteristics of the system. To characterize these systems, the following data are required: real power, complex power, displacement reactive power, distortion reactive power, and system power factor. Some of these characteristics are available through direct measurement; the remaining characteristics can be determined only through indirect measurement. A more detailed discussion of power measurements in rectifier systems follows.

There is a power factor associated with a rectifier or chopper system which is the result of either or both of two phenomena.

a. The delay of thyristor turn-on in phase delayed rectifier systems results in a phase displacement of the current and voltage waveforms and hence a displacement component of power factor.

b. The chopping action of rectifier systems generates harmonic currents which distort the waveforms and produce a distortion component of power factor.

The current and voltage can be expressed in terms of the fundamental, its harmonics and displacement angles,

$$v(t) = \sum_{m=1}^{\infty} E_{pm} \sin(m\omega t)$$

$$i(t) = \sum_{n=1}^{\infty} I_{pn} \sin(n\omega t+\psi)$$

and the integral for average power can be rewritten

$$W = \frac{1}{T} \int_{o}^{T} \sum_{\substack{n=1 \\ m=1}}^{\infty} E_{pm} \sin(m\omega t) \cdot I_{pn} \sin(n\omega t+\psi)\ d\omega t$$

This integral has a non-zero solution only for the cases where m=n.

Figure A-1 is a phasor diagram of the power components which can be constructed from data taken with two wattmeters. It does not completely describe the power characteristics of the system with harmonics. All of the components in Figure A-1 result from currents and voltages of the same frequencies. The complex power, $S_p$, associated with these quantities can be resolved into its components: the real power, P, and a reactive power component, $Q_p$, which results from the phase displacement of the currents and voltages. The angle, $\phi$, is the displacement or phase angle between the active power and $S_p$.

For the case where the input voltage waveform contains only the fundamental frequency and no harmonics, the angle $\phi$ is the angle between the active power of the fundamental and the apparent power of the fundamental. It is also the displacement angle between the fundamental voltage and the fundamental current. The cosine of this angle is the displacement power factor which is measured by watt-hour and var-hour meters.

The displacement angle varies with the delay interval in phase delay rectifiers. Addition of inducive filtering to a rectifier output increases the current phase lag and results in a lower displacement power factor.

The presence of harmonics in the line current must also be considered in characterizing a power system. Since the harmonics do not contribute to active power, and since they do contribute to apparent power, the harmonic or distortion component of power must be considered as a component of reactive power. Note that the displacement power factor is the same as the system power factor only for sinusoidal conditions.

The RMS quantities which are used to calculate total apparent power contain both fundamental and harmonic components. These components combine vectorially to produce the RMS line currents and voltages; e.g.,

$$I_L = \sqrt{\sum_{n=1}^{\infty} I_n^2}$$

where $I_L$ = RMS line current

$n$ = order of harmonic

$I_n$ = RMS value of nth harmonic

Since the harmonic distortion components contribute to the total RMS value vectorially, the distortion components also contribute to total reactive power vectorially. This is illustrated in Figure A-2 which is a phasor diagram of the displacement and distortion components of reactive power.

A pictorial presentation of the power components and how they combine is presented in Figure A-3. The total system apparent power consists of three mutually orthogonal components: real power, phase displacement reactive power and distortion reactive power. All three components must be known to completely characterize the system.

## MEASUREMENT OF POWER SYSTEM COMPONENTS

In a three-phase system, two wattmeters can be used to measure the active power for all conditions of load balance and waveform distortion. The total system apparent power can be determined from the true RMS current and true RMS voltage measurements.

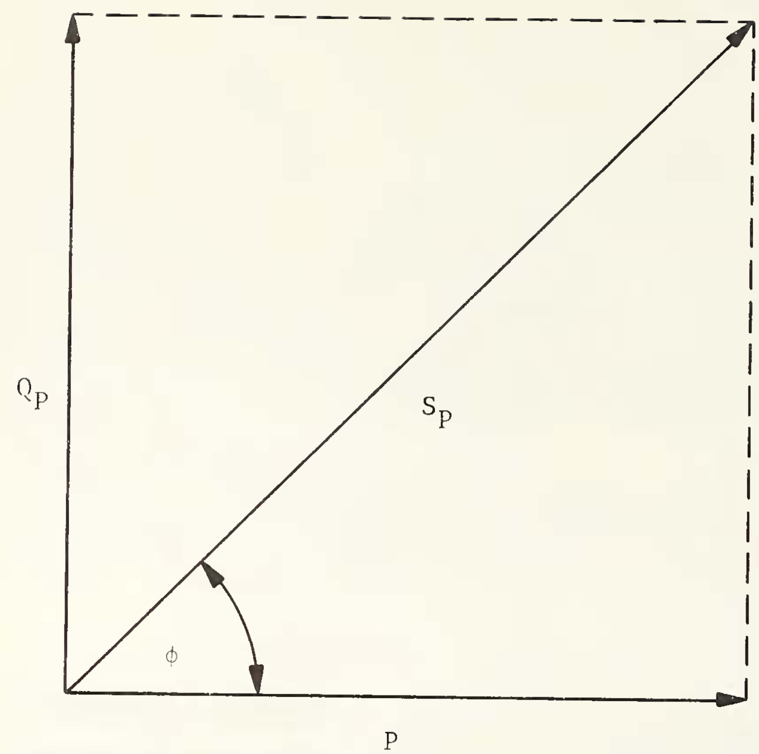


Figure A-1. Phasor Diagram of Power Components from Two-Wattmeter Measurements

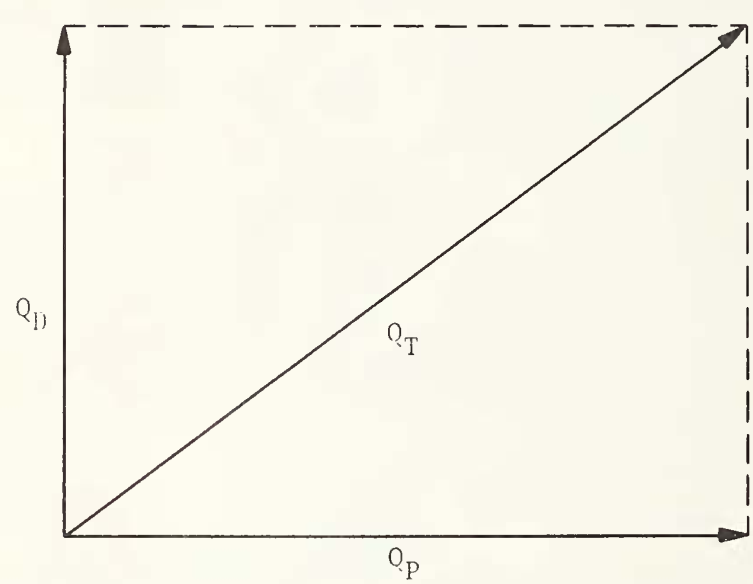


Figure A-2. Phasor Diagram of Reactive Power Components

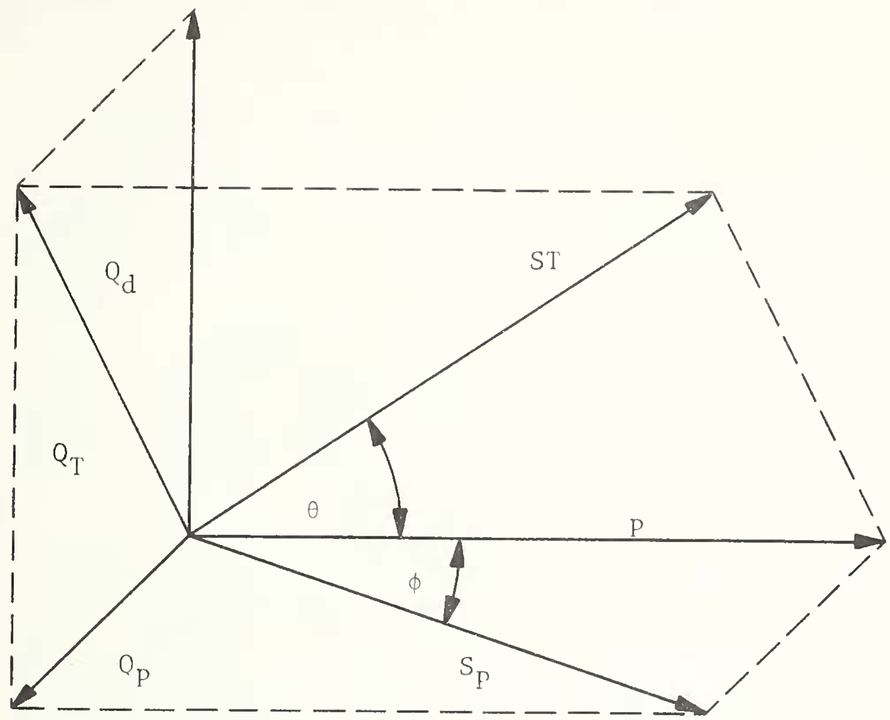


Figure A-3. Phasor Diagrams of Total System Power Components

The total real power and the total complex power requirements can be used to determine the system power factor and total reactive power

$$pf = \frac{W_1 + W_2}{\sqrt{3}\, V_L\, I_L} = \cos\theta$$

$$Q_T = \sqrt{3}\, V_L\, I_L \sin\theta$$

The two-wattmeter readings can also be used to determine displacement reactive power

$$Q_p = \sqrt{3}\,(W_1 - W_2)$$

The distortion reactive power can then be calculated from

$$Q_d = \sqrt{Q_T^2 - Q_p^2}$$

It can also be shown that

$$Q_d = V_L \sqrt{I_D{}^2}$$

where

$$I_D{}^2 = I_L{}^2 - I_1{}^2$$

The fundamental component as well as the harmonic components of the line current have been measured in the laboratory for a six-pulse, three-phase rectifier system. The magnitudes of the fundamental current and its harmonics vary with phase control, and do not follow a simple $\frac{1}{n}$ relationship. Values of the harmonic current ratio versus delay angle are shown in Figure A-4, for resistive loading.

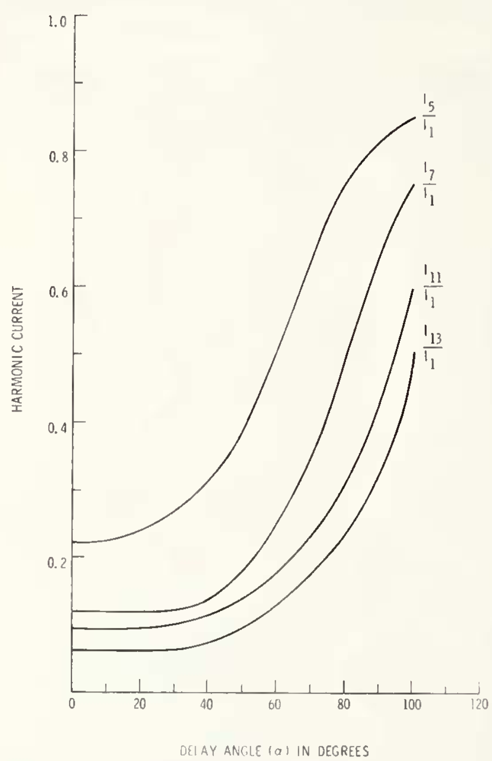


Figure A-4. Harmonic Current vs. Delay Angle

The total line current can be rewritten as

$$I_L = \sqrt{I_1{}^2 + I_D{}^2}$$

Normalizing with respect to $I_1$ and expanding $I_D$ gives

$$\frac{I_L}{I_1} = \sqrt{1 + \left(\frac{I_5}{I_1}\right)^2 + \left(\frac{I_7}{I_1}\right)^2 + \left(\frac{I_{11}}{I_1}\right)^2 + \ldots\ldots + \left(\frac{I_n}{I_1}\right)^2}$$

and

$$I_L = MI_1$$

The M factor can be used to determine the total apparent power requirements if the fundamental component of current is known. Using the data given in Figure A-4, the M factor as a function of delay angle, is given in Figure A-5 as the L = 0 curve. For any firing angle condition, the total complex power requirement can be determined as

$$V_L I_L = V_L MI_1$$

The above relationships assume that the harmonics of the applied voltage are negligible.

Rectifier systems that assume an infinite value of output inductance have the M factor independent of phase angle control and equal to a constant. For this condition, the input current waveform has the characteristic shown in Figure A-6.

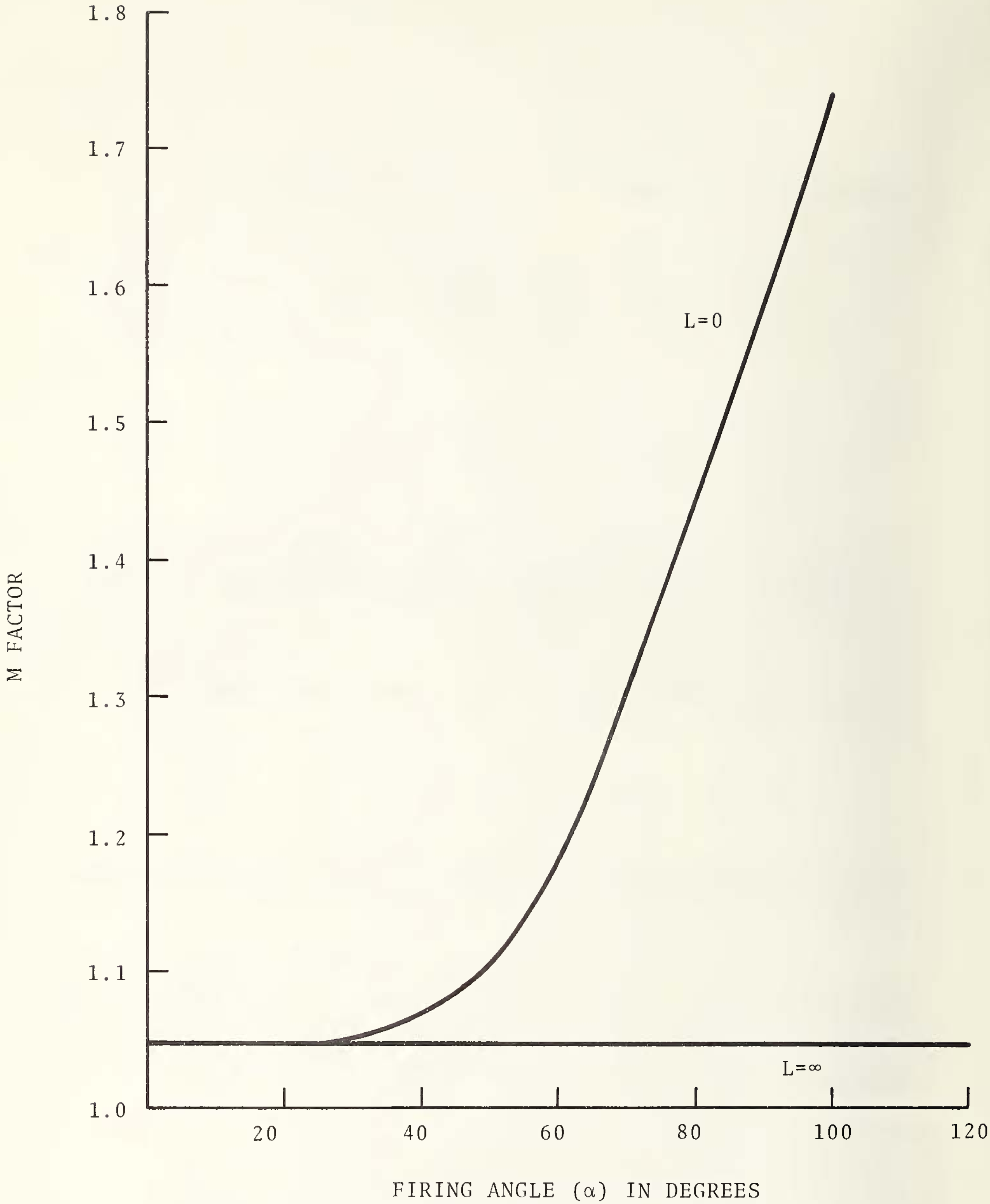


Figure A-5. M Factor as a Function of Firing Angle

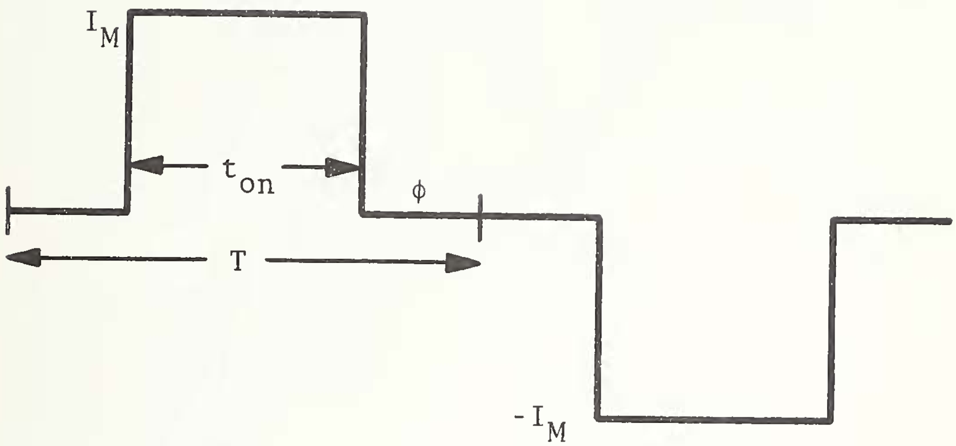


Figure A-6. Input Current for Infinite Inductance Case

From the previous relations relationship of

$$M = \frac{I_L}{I_1}$$

it can be shown that

$$M = \frac{I_m \sqrt{\frac{t_{on}}{T}}}{\left(\frac{\sqrt{2}}{2}\right) \frac{4 \; I_m}{\pi} \cos \phi}$$

For the case of six-pulse, three-phase rectifier system,

$$\phi = 30^{\circ}$$

and

$$M = 1.05$$

This is plotted in Figure A-5 as the $L = \infty$ curve.